12-15-2016

Immune mechanisms of influenza vaccine adjuvants and respiratory syncytial viral vaccines

Eunju Ko

IMMUNE MECHANISMS OF INFLUENZA VACCINE ADJUVANTS AND RESPIRATORY SYNCYTIAL VIRAL VACCINES

by

Eunju Ko

Under the Direction of Sang-Moo Kang, PhD

ABSTRACT

Adjuvants have been used for enhancing vaccine-specific immune responses, but the mechanisms of adjuvants and the roles of CD4 in adjuvant effects have been poorly understood. In a conventional model of vaccine adjuvant action mechanism, $CD4^+$ T helper cells are known to play a critical role for adjuvants in improving vaccine efficacy. In this study, both licensed MF59 and monophosphoryl lipid (MPL)+Alum adjuvants were found to mediate IgG isotype-switched antibodies, memory responses, and protection against influenza virus in CD4 knockout (CD4KO) mice, which were comparable to those in wild type (WT) mice. Licensed oil-in-water emulsion MF59 adjuvanted influenza split vaccination was able to induce protective $CD8^+$ T cells and long-lived IgG antibody-secreting cells in CD4KO mice. MF59 adjuvant mechanisms in CD4KO mice might be associated with uric acid, inflammatory cytokines, and recruitment of multiple immune

cells at the injection site. Another licensed platform of MPL+ Alum adjuvant was also found to be effective in inducing IgG antibodies and protection, which appeared to be mediated by recruiting monocytes, neutrophils, dendritic cells in CD4KO mice. Additional studies in CD4-depleted WT mice and MHCIIKO mice suggest that $MHCII^+$ antigen presenting cells contribute to providing alternative B cell help in CD4 deficient condition in the context of MPL+Alum adjuvanted vaccination. These findings suggest a new paradigm of CD4-independent adjuvant mechanisms, providing the rationales to improve vaccine efficacy in infants, elderly, and immune-compromised patients as well as in healthy adults.

Respiratory syncytial virus (RSV) is an important human pathogen, but there is no licensed RSV vaccine. RSV virus-like particle (VLP) vaccine conferred protection against RSV. RSV F and G VLP mixed with F-DNA (FdFG VLP) immunization induced low infiltrating cellularity, T helper type-1 immune responses, and no sign of eosinophilia in bronchoalveolar lavages upon RSV challenge, whereas alum adjuvanted formalin-inactivated RSV (FI-RSV) vaccination caused vaccine-enhanced eosinophilia. This study provides evidence that combination of recombinant RSV VLP and plasmid DNA vaccines may have a potential anti-RSV prophylactic vaccine inducing balanced innate and adaptive immune responses.

INDEX WORDS: Vaccine adjuvants, $CD4^+$ T cells, Influenza virus, Respiratory syncytial virus

IMMUNE MECHANISMS OF INFLUENZA VACCINE ADJUVANTS AND RESPIRATORY SYNCYTIAL VIRAL VACCINES

by

Eunju Ko

A Dissertation Submitted in Partial Fulfillment of the Requirements for the Degree of

Doctor of Philosophy

in the College of Arts and Sciences

Georgia State University

2016

IMMUNE MECHANISMS OF INFLUENZA VACCINE ADJUVANTS AND RESPIRATORY SYNCYTIAL VIRAL VACCINES

by

Eunju Ko

Committee Chair: Sang-Moo Kang

Committee: Andrew Gewirtz

Timothy Denning

Electronic Version Approved:

Office of Graduate Studies

College of Arts and Sciences

Georgia State University

December 2016

DEDICATION

To my family and all of my friends

ACKNOWLEDGEMENTS

I wish to express my sincere gratitude to my mentor, Dr. Sang-Moo Kang, for his guidance and encouragement in carrying out all projects and completing my PhD degree.

I also thank my committee members, Dr. Andrew Gewirtz and Dr. Timothy Denning, for the abundant help and advice to guide my projects to right way.

I would like to gratefully acknowledge the outstanding help and contributions of my lab mates. Without their support, I would not have been able to achieve my degree.

My family have been truly supportive and encouraging during my PhD studies, and even before that. I thank them for their endless love, sacrifices, and trust.

I appreciate all those who have been directly or indirectly related to my projects.

TABLE OF CONTENTS

LIST OF TABLES

LIST OF FIGURES

1 INTRODUCTION

1.1 Influenza virus

Influenza virus is the cause of seasonal and pandemic flu. It causes approximately 200,000 hospitalizations and approximately 49,000 deaths in US annually[1, 2]. It belongs to *Orthomyxoviridae* family, and there are 3 *genera*, A, B, and C, based on the expression of matrix protein (M1), membrane protein (M2) and nucleoprotein (NP). Influenza B and C mainly infect humans, but influenza A virus shows wide range of host including humans, birds, pigs and other mammals. Usually, the virus outbreak is epidemic and seasonal, but sometimes it causes pandemic outbreak and shows severe symptoms and relative high mortality[3, 4]. Most recently, H1N1 swine flu was pandemic outbreak in 2009 and caused around 20,000 deaths worldwide. The pandemic influenza outbreaks occur when a new influenza strain emerges and gets transmission ability to human[3].

Influenza virus is single-stranded RNA virus. It contains 7 (*genera* C) or 8 (*genera* A and B) segmented negative-sense RNA and each RNA encodes 1 or 2 genes. It is enveloped, spherical shape and the approximate diameter of the virus is 80 to 120 nm[5].

The subtypes of influenza A virus are based on the surface expression of major glycoproteins, hemagglutinin (HA) and neuraminidase (NA). Currently, 18 subtypes of HA and 9 subtypes of NA have been found. HA is a lectin and plays a critical roles in binding and entry of the virus to host cells. On the other hand, NA activity is critical for release of virus from the infected cells[6, 7, 8].

Influenza virus can be transmitted by direct contact and airborne droplet dissemination. Generally it takes 1 to 3 days for incubation periods, and headache, runny nose, sore throat, fever, cough, and chills are common symptoms. In case of severe flu, joint swelling and vomiting can be

followed. In healthy population, the flu symptoms are mild and recovered within 7 to 10 days, but children, the elderly and immune-compromised patients show more severe symptoms and higher mortality[9, 10, 11, 12]. This is because of $CD4^+$ T cell-mediated adaptive immune responses are not fully developed or reduced in those populations and fail to develop strong innate and adaptive immune responses.

Reassortment of influenza genes from different strains causes genetic shift and make completely new influenza strains. The new strain results pandemic influenza outbreaks and causes severe symptoms, high hospitalization rates and mortality because the most population does not have the pre-existing immune responses. Minor mutations in the HA or NA genes (genetic drift) cause virus antigenicity alteration. The genetic drift of influenza virus is responsible for the outbreaks of severe seasonal flu. Because of the antigenic diversity of the influenza virus and antigenic specificity of HA and NA, world health organization (WHO) predicts seasonal flu strains and recommends vaccination annually[5, 13].

Currently, trivalent (2 influenza A and 1 influenza B strains) or quadrivalent (2 influenza A and 2 influenza B strains) inactivated whole influenza virus vaccines are approved to wide age range of populations. In addition, live attenuated influenza virus vaccines are used in a population between 2-49 years old[5].

1.2 Vaccines

Vaccination has been used to induce adaptive immune responses against specific pathogens and prepare to protect host from the pathogen invasion[14, 15, 16]. Since the first attempt of cowpox immunization by Edward Jenner, many types of vaccines have been tried and tested experimentally

and clinically. Successful vaccinations can elicit antigen-specific isotype-switching antibody production and long-term cellular memory responses[17].

Inactivated form of pathogens is the most widely used vaccine platform. Pathogens are amplified and inactivated by chemicals, heat or radiation. Whole inactivated pathogen has strong immunogenicity and cost-effective compared to other vaccine platforms. However, it sometimes has adverse effects such as inflammation at the site of injection[18].

Live attenuated pathogens are used in measles, mumps, and chicken pox vaccines. The pathogens are attenuated via passages in foreign hosts or gene modification. Thus, the attenuated pathogens are still live, but have reduced virulence in the host. These vaccines can elicit strong cellular and antibody responses because of alive characteristics. However, there is a possibility of reversion to the virulent form and causing diseases. In addition, this type of vaccine is high-cost because refrigeration is required to preserve potency of the living organisms[19].

Recently, many subunit vaccines were developed to reduce the potential adverse effects of the whole pathogen-derived vaccines and elicit an appropriate type of immune responses. The subunit vaccines include only antigenic epitopes. This type of vaccine is now used in human hepatitis B virus vaccine. These subunit vaccines are considered safer than other types of vaccines, on the other hand, show lower immunogenicity than that of the whole pathogen-derived vaccines[20, 21, 22].

1.3 Adjuvants

To increase immune responses and efficacy of the vaccination, vaccine adjuvants have been developed and used with the subunit vaccines[20, 23]. Generally, the adjuvants are known to stimulate innate immune cells at the site of injection, induce rapid response to pathogens, amplify

the immune responses, modulate T helper cell responses and finally enhance long-lasting B and T cell immunity. Moreover, vaccine adjuvants can reduce the number of immunization and vaccine dose[24]. Strong innate immune responses are expected to generate better antigen-specific adaptive immune responses.

1.3.1 Alum

Alum is one of the most popular adjuvants. It has used more than 70 years for veterinary and human vaccines. It adsorbs the vaccine antigens and makes antigen depot at the site of injection. The antigen depots can release vaccine antigen slowly, so the immune system is stimulated by the antigen for a longer time. Also, the alum can stimulate innate immune cells like neutrophils and macrophages through NLRP3 inflammasome signaling pathway. The inflammasome-activated immune cells secret pro-inflammatory cytokines such as IL-1beta and IL-18[25, 26, 27]. Alum has relatively weak adjuvant effects compared to other adjuvants, but it is the only approved adjuvant for human use in the USA because of its high safety record[20].

1.3.2 MF59

MF59 is an oil in water emulsion type of adjuvants. It is used in influenza vaccine (Fluad™) and pandemic flu vaccine. It stimulates stronger antibody responses and spares antigen dose. MF59 makes cells in injection sites express various genes which encode chemokines and cytokines. These chemokines and cytokines recruit innate immune cells and antigen-presenting cells. They uptake antigen as well as MF59 and migrate to draining lymph nodes and induce stronger immune responses[28, 29].

1.3.3 Toll-like receptor (TLR) agonist

Toll-like receptor (TLR) signaling pathway induces innate immune cell activation. TLRs are expressed on immune cells as well as non-immune cells. Distinct pathogen patterns are recognized by specific types of TLRs. For example, peptidoglycan of gram positive bacteria is recognized by TLR2 and DNA of virus and bacteria activates TLR9. TLR agonists activate downstream TLR signaling molecules and make the cells to produce pro-inflammatory cytokines, chemokines and increase the cell surface activation molecules expression[30]. Thus, the TLR agonists have been developed as adjuvants and many adjuvant candidates containing TLR agonists are under pre-clinical and clinical trials[20]. AS04 is composed of monophosphoryl lipid A (MPLA), a TLR4 agonist, and alum. It was approved for human vaccine adjuvant in Europe recently, and used in human papilloma virus vaccine and hepatitis B virus vaccine[20, 24, 31, 32]. Flagellin, a TLR5 agonist, is a component of bacterial motor system. Many researches have tried to make a form of flagellin-antigen fusion proteins to increase vaccine and adjuvant efficacy[33, 34]. The flagellin can be recognized by TLR5 and activate TLR signaling, and, at the same time, the antigen can be uptaken by immune cells[20, 24].

1.4 Possible adjuvant action mechanisms

Many adjuvants are known to increase the vaccine efficacy by stimulation of the innate immune system, especially, antigen presenting cells (APCs). The APCs include DCs and macrophages. The adjuvants help the APC activation when the APCs uptake antigens. The activated APCs migrate to the secondary lymphoid organs, present the antigenic information to the immune cells and initiate antigen-specific immune responses. To increase efficacy of antigen-specific antibodies, isotype-switching and somatic hypermutation of immunoglobulin genes in B

cells are required. These antibody maturation processes are known to be a germinal center (GC) reaction, because the reaction is occurred in the GC of the secondary lymphoid organs. GCs are formed as a result of cognate interactions of $CD4^+$ T cells and B cells as well as the cytokines produced by activated $CD4^+$ T cells. Therefore, $CD4^+$ T cells have been considered to be a critical cell type for adjuvants to induce strong antigen-specific immune responses[23, 35].

$CD4^+$ T cells are required for antibody maturation. Nonetheless, few studies have reported that isotype-switched antibodies were produced without $CD4^+$ T cell help but at lower levels. For example, Sha et al. immunized CD4-deficency mice with inactivated whole viral vaccines. The immunized mice showed antigen-specific IgG and IgA production at a low level[36]. Whole-pathogen derived vaccines are likely to be a strong innate immune system stimulator. DCs can be activated by whole inactivated virus and produce pro-inflammatory cytokines such as IL-6, TNF-alpha and IL-12[37, 38, 39]. In addition, the activated DCs interact with B cells directly, stimulate B cells and provide survival signals to the B cells[40]. Thus, it is suggested that strong innate immune stimulation by vaccine adjuvants may be able to overcome the $CD4^+$ T cell deficiency and elicit antigen-specific immune responses without $CD4^+$ T cell help.

1.5 Aims and hypothesis of influenza vaccine adjuvant study

Previous studies reported that immunization with inactivated virus[36, 41, 42] or virus-like particles (VLPs)[43] induced antigen-specific antibody production even in the deficiency of $CD4^+$ T helper cells. However, the roles of $CD4^+$ T cells in exhibiting adjuvant effects on enhancing vaccine immunogenicity, inducing long-lived isotype-switched IgG antibody responses, duration of B cells, and protective immunity remain largely unknown. I proposed a hypothesis that certain adjuvants would overcome a deficiency of $CD4^+$ T cell help in inducing IgG isotype-switched

antibodies and protective immunity. Main goals in my PhD projects of vaccine adjuvants parts are as follows: 1) To determine whether the most commonly used current influenza vaccine platform of inactivated, detergent split virus would be CD4-dependent, 2) To determine whether the effects of licensed vaccine adjuvants (alum, MF59, MPL+Alum) would be dependent on $CD4^+$ T cell help, 3) To address whether certain adjuvants would overcome a deficiency of $CD4^+$ T cells in inducing IgG isotype-switching and protective immunity, and 4) to determine whether adjuvant effects in a condition of CD4 deficiency would be correlated with strength and safety of vaccine adjuvants. Finally, additional studies were carried out to better understand the action mechanisms of adjuvants in a $CD4^+$ T cell deficient condition by using novel in vivo mice and in vitro cell models.

1.6 Respiratory syncytial virus (RSV)

Respiratory syncytial virus (RSV) is an enveloped virus with a single-stranded negative-sense RNA genome, belonging to the family of Paramyxoviridae [44]. RSV is a major cause of viral respiratory disease in infants, young children, elderly, and immune-compromised patients [2, 45, 46]. The World Health Organization estimates that RSV causes 64 millions of infection and 160,000 deaths globally [47].

In the 1960s, a formalin-inactivated RSV vaccine (FI-RSV) induced exacerbated disease during the next winter season, resulting in 80% hospitalizations of FI-RSV recipients and two deaths [48, 49]. Despite the extensive endeavor to develop RSV vaccines, there is no licensed vaccine available. RSV fusion (F) or attachment (G) glycoprotein subunit and recombinant vectored RSV vaccines are also known to cause enhanced RSV disease (ERD) [50, 51, 52, 53]. Live RSV may induce short-term immunity [50, 54, 55]. Reinfection is common throughout life, indicating that natural RSV

infection fails to establish long-lasting sterilizing immunity [56, 57, 58]. Therefore, it is a formidable challenge to develop an effective and safe RSV vaccine.

1.7 RSV VLP as a vaccine candidate

Despite the extensive endeavor to develop RSV vaccines, there is no licensed vaccine. RSV reinfection is common throughout life, indicating that natural RSV infection fails to establish long-lasting immunity[59, 60]. Virus-like nanoparticles (VLP) can be generated through the assembly of structural proteins and lipid bilayer membranes, and are morphologically similar to the virus[61, 62]. Recent studies reported that recombinant baculovirus-derived VLP vaccines containing the full-length of RSV F or G in a membrane-anchored form were shown to induce immune responses contributing to clearing lung viral loads[63].

1.8 Aims and hypothesis of RSV vaccine study

FI-RSV induces Th2-biased immune responses after immunization, and then elicits severe lung inflammation including eosinophil infiltration when the hosts are infected with RSV in next winter season[64, 65]. RSV glycoprotein (F and G) expressing virus-like particles (VLPs) were suggested as new RSV vaccine candidates and proved their immunogenicity and protective efficacy in mice model[63]. RSV VLPs are considered to be able to guide immune system to protective immune responses against RSV. However, the cellular action mechanisms of the RSV VLPs are not fully understood. In this study, mice were immunized with F and G RSV VLPs to investigate the cellular mechanisms of the vaccine. As for comparative groups, FI-RSV was included as a failed vaccine causing disease and RSV as live virus infection-induced immunity to better understand balanced immune responses contributing to protection.

2 EXPERIMENTAL METHODS

2.1 Animals and reagents

Female and male 6 to 8-week old Balb/c, C57BL/6, CD4 knock out (CD4KO, B6.129S6-$Cd4^{tm1Mak}$/J), and major histocompatibility complex class II (MHCII) KO (I-$A\beta^{-/-}$) mice were purchased and maintained in the animal facility at Georgia State University (GSU). All mouse experiments followed the approved GSU IACUC protocol (A14025). Commercial human monomeric influenza vaccine (inactivated and detergent split virus), derived from the 2009 pandemic strain of A/California/07/2009 H1N1 virus, was kindly provided by Green Cross (South Korea), a WHO-approved vaccine manufacturing company. Monophosphoryl lipid A (MPL) and aluminium hydroxide (Alum) were purchased from Sigma-Aldrich. 3-(4,5-Dimethylthiazol-2-yl)-2,5-Diphenyltetrazolium Bromide (MTT) was obtained from Sigma for cell death analysis. MF59® provided as a gift from Novartis Vaccines and Diagnostics, Inc. (Cambridge, MA).

2.2 Preparation of RSV VLPs, RSV F encoding DNA, and FI-RSV

Spodoptera frugiperda SF9 insect cells (ATCC, CRL-1711) were maintained in SF900-II serum free medium (Invitrogen, Carlsbad, CA) and used for production of Nanoparticle VLP consisting of an influenza virus matrix (M1) protein core and RSV glycoproteins F (RSV F VLP) or G (RSV G VLP) on the surface. SF9 insect cells were infected with recombinant baculoviruses expressing M1 and RSV F or RSV G proteins, and RSV VLP nanoparticles released into cell culture media were purified by ultracentrifugation [63]. The plasmid DNA encoding RSV F protein (RSV F DNA) was previously described [66] and amplified in E. coli cells and purified using endotoxin-free kits (Qiagen). HEp-2 cells obtained from the ATCC were maintained in Dulbecco modified Eagle medium (DMEM) media (GIBCO-BRL). RSV A2 strain was used for the

preparation of FI-RSV, live RSV infection and challenge [63]. An expression plasmid encoding human codon bias-optimized RSV A2 F was previously described [66]. RSV A2 stocks were grown and titrated in HEp-2 cells [63]. RSV, grown in HEp-2 cells, was harvested from infected cell cultures, and inactivated with formalin (1:4000 vol/vol) for 3 days at 37^{o}C, and then purified using ultracentrifugation [63, 67]. Inactivation was confirmed by an immune-plaque assay [63]. The FI-RSV vaccine adsorbed to aluminium hydroxide adjuvant (alum, 4 mg/ml) was used for immunization.

2.3 Immunization and virus infection

To investigate the vaccine adjuvant effects in CD4-deficiency, C57BL/6 wild-type (WT), CD4KO, CD4-depleted WT, and MHCIIKO mice were immunized intramuscularly with influenza vaccine alone or adjuvanted with MF59 (50% vol/vol as recommended by manufacturer), 5 μg of MPL, 50 μg of Alum, or 5 μg of MPL plus 50 μg of Alum (MPL+Alum). For antigen adsorption of Alum or MPL+Alum adjuvant, influenza vaccine was incubated with adjuvant in 37°C for 30 minutes before immunization. The immunizations were performed twice (prime and boost) in WT, CD4KO, and MHCII KO mice with an interval of 4 weeks and immune sera collected at 3 weeks after each immunization (Fig. 4.1A). For $CD4^+$ T cell acute depletion in WT mice, naïve WT mice were injected with anti-mouse CD4 monoclonal antibody (200 μg /mouse, clone GK1.5) intraperitoneally 2 days before each prime and boost immunization. To maintain CD4 depletion status, the mice were injected CD4-depleting antibodies every 7 days. At 20 weeks after boost, naïve and immunized mice were challenged with 17 × lethal dose 50% (LD_{50}) of A/California/04/2009 (H1N1) virus. The challenged mice were monitored to determine survival rates and body weight changes for 14 days. Kaplan Meier analysis and log rank were applied for the survival graphs. Additional sets of challenged mice were sacrificed at day 5 post infection to

determine protective efficacy. After sacrifice, bronchoalveolar lavages fluids (BALF), lung, bone marrow, and spleens were harvested for further analysis.

For cellular mechanisms of RSV vaccines, female BALB/c mice aged 6 to 8 weeks (Charles River) were immunized intramuscularly with RSV vaccines or infected intranasally with live RSV A2. Groups of mice (n=15) were intramuscularly immunized with RSV vaccines at week 0 and 4. For FI-RSV immunization, 2 μg and 1 μg of FI-RSV were used for prime and boost, respectively. A mixed RSV vaccine designated as FdFG VLP contained RSV F DNA, RSV F VLP and RSV G VLP. The priming dose of FdFG VLP was composed of 10 μg F VLP/10 μg G VLP/50 μg F DNA and the boosting dose was half of each component (5 μg F VLP/5 μg G VLP/25 μg F DNA). For a control group, mice (n=15) were intranasally infected with live RSV A2 strain (1×10^6 plaque forming units (PFU) for prime, 0.5×10^6 PFU for boost) at weeks 0 and 4. Serum samples were collected at 3 weeks after prime and boost immunization. At 26 weeks after boost immunization, naïve, immunized, and infected mice were challenged with RSV (1×10^6 PFU/mouse).

2.4 Enzyme linked immunosorbent assay (ELISA)

Immune sera were collected 3 weeks after each immunization and used to determine IgG antibody levels by ELISA. Briefly, serially diluted immune sera were applied to the ELISA plates coated with inactivated virus (2 μg/ml), FI-RSV (4 μg/ml), RSV F protein (100 ng/ml, BEI, NIH) or RSV G protein (200 ng/ml, Sino biological Inc.) as an antigen. After washing, horseradish peroxidase-labeled secondary anti-mouse antibody reagents were used to detect antigen-specific IgG, IgG1 and IgG2c antibodies. Tetramethylbenzidine (TMB) was used as a substrate and optical density (OD) was measured at 450 nm by an ELISA reader (Bio-Rad). For analysis of long-lived

antibody secreting cell responses, bone marrow cells and spleen cells were harvested from mice at day 5 post virus infection and incubated in influenza virus-coated cell culture plates for 1 or 5 days. Antibodies secreted *in vitro* were measured by ELISA. Cytokines and chemokines in BALF, lung extract, peritoneal exudates, sera and cell culture supernatants were measured by using ELISA kits from eBiosciences and R&D systems.

2.5 Hemagglutination inhibition (HAI) assay

Immune sera were incubated with receptor destroying enzymes (Sigma Aldrich) at 37ºC for 18 hours and then at 56ºC for 30 minutes for complement inactivation. Inactivated sera were serially diluted and incubated with 8 HA units of A/California/4/2009 (H1N1) virus in V-bottom microplates. After 30 minutes, 0.5% chicken red blood cells were treated to the wells and the hemmagglutination was determined after 40 minutes. The detection limit of HAI titer was 2 of Log2.

2.6 *In vivo* protection assay of immune sera

Naïve and immune sera were incubated at 56ºC for 30 minutes for inactivation of complements and diluted to 4 times with phosphate-buffer saline (PBS). Diluted sera were mixed with a lethal dose ($7.5\times LD_{50}$) of A/California/4/2009 (H1N1) virus and incubated for 30 minutes. A mixture of sera and virus was used to infect naïve WT mice intranasally. Body weight changes of the infected mice were daily monitored for 14 days.

2.7 Neutralizing antibody assay

RSV-specific neutralizing antibody titers in mouse sera were measured using the red fluorescent monomeric Katushka 2 protein expressing RSV A2 strain (A2-K-line19F) [68, 69]. Heat-inactivated naïve and immunized mice sera were serially diluted and mixed with 1000 PFU of A2-K-line19F virus. After 1 hour culture at 37°C, the sera and virus mixtures were added to confluent monolayers of HEp-2 cells in a separated 96-well culture plate. After 2 hours infection, the remaining virus was removed and the infected HEp-2 cells were incubated at 37°C, 5% CO_2 for 22 hours. The plates were washed and fluorescent intensity as a result of replication of A2-K-line19F virus was read (588 nm excitation, 635nm emission) by using an Synergy H1 hybrid Reader (BioTek Instruments,Inc, Winooski, VT). For lung RSV titers, at 26 weeks after boost immunization, the mice were intranasally challenged with RSV (1 x 10^6 PFU/mouse) and lung tissues were collected day 5 post challenge (n=15). RSV titers were measured by using a plaque assay and presented as numbers of plaques per gram lung tissues.

2.8 Lung virus titration

Lung extracts were prepared for viral titers using a mechanical tissue grinder with 1.5 ml of PBS per each lung. For influenza virus titer, embryonated chicken eggs were inoculated with diluted lung extracts and incubated at 37ºC for 3 days. The allantoic fluids of eggs were collected and hemagglutination assay was performed to determine viral titers. Virus titers as 50% egg infection dose (EID_{50})/ml were evaluated according to the Reed and Muench method [70]. The detection limit of EID_{50} was 1.7 (Log50). An immunoplaque assay was used to determine RSV titer in lung extracts as described.

2.9 Histology

Intact lungs from immunized mice were harvested at day 5 post virus infection and treated with formalin for fixation. The fixed lung tissues were processed, sectioned, and stained with hematoxylin and eosin as described (21). Photographs were acquired by a microscope (Zeiss Axiovert 100) with an attached camera at 100x magnification (Canon 30D).

2.10 $CD8^+$ cell depletion

The MF59 adjuvanted CD4KO mice at 5 months after boost immunization were treated with anti-mouse CD8α monoclonal antibodies (150 μg/mouse, clone 53-6.7) intraperitoneally on days –2, +1 relative to the day of challenge. The mice were challenged with a lethal dose of A/California/04/2009 (H1N1) virus and sacrificed at day 5 post infection to determine the roles of CD8+ T cells in protection against the virus infection.

2.11 Intraperitoneal injection of adjuvants

WT and CD4KO mice were injected with 200 μl of phosphate buffered saline (PBS), MF59 (100 μl in 200μl), MPL (5 μg) + Alum (50 μg), MPL (5 μg), or Alum (50 μg) intraperitoneally. Sera were collected at 1.5, 6 and 24 hours post injection for detection of cytokines and chemokines. Peritoneal exudates were harvested at 24 hours post injection by PBS flushing. Peritoneal cells were used to determine phenotypes and cellularity of infiltrating cells by flow cytometry and peritoneal exudates were used for detection of cytokines and chemokines.

2.12 Flow cytometry

Cells harvested after IP injection were treated with Fc receptor blocker, anti-CD16/32, and then stained with fluorescence-labeled CD11b (clone M1/70), CD11c (clone N418), F4/80 (clone BM8), MHC class II (clone M5/114.15.2), Ly6c (clone HK1.4), B220 (clone RA3-6B2), SiglecF (clone E50-2440), CD3 (clone 17A2), CD4 (clone GK1.5), CD8 (clone 53-6.7) and pan-natural killer (NK) cell marker (clone DX5) antibodies. Macrophages ($CD11b^{+}F4/80^{+}$), $MHCII^{high}$ macrophages ($CD11b^{+}F4/80^{+}MHCII^{high}$), monocytes ($CD11b^{+}Ly6c^{high}F4/80^{+}$), neutrophils ($CD11b^{+}Ly6c^{+}F4/80^{-}$), eosinophils ($CD11b^{+}SiglecF^{+}$), plasmacytoid pDCs ($CD11c^{+}B220^{+}MHCII^{high}$), $CD11b^{high}$ DCs ($CD11c^{+}CD11b^{high}MHCII^{high}$), $CD11b^{low}$ DCs ($CD11c^{+}CD11b^{low}MHCII^{high}$), $CD4^{+}$ T cells ($CD3^{+}CD4^{+}$), $CD8^{+}$ T cells ($CD3^{+}CD8^{+}$), NKT cells ($CD49b^{+}CD3^{+}$), NK cells ($CD49b^{+}CD3^{-}$) were gated by flow cytometry.

For cell phenotype analysis after RSV infection, the harvested BAL cells from BALF samples (n=5, pooled) were stained with fluorophore-labeled surface markers. Anti-mouse CD16/32 (clone 93) was used as a Fc receptor blocker and then, an antibody cocktail which contained anti-mouse CD45-PerCP (clone 30-F11), CD11b-APC (clone M1/70), CD11c-PE-Cy7 (clone N418), CD3-Pacific Blue (clone 17A2), CD8-APC eFluor780 (clone 53-6.7) and SiglecF-PE (clone E50-2440) was used to treat the cells. For intracellular interferon-gamma (IFN- γ) staining, Cytofix/Cytoperm™ Fixation/Permeabilization Solution Kit with BD GolgiStop™ was used as manufacturer's protocol.

Adjuvants-treated BMDCs were harvested and stained with fluorescence-labeled anti-mouse CD40, CD80, CD86 and MHCII antibodies after blocking Fc receptors (anti-mouse CD16/32).

The stained cells were acquired by BD Fortessa (BD Biosciences, Mountain View, CA, USA) and analyzed by FlowJo (Tree Star Inc., Ashland, OR, USA).

2.13 *In vitro* cell cultures

Bone marrow (BM) derived dendritic cells (BMDCs) and BM derived macrophages (BMMs) were generated from BM cells. Briefly, bone marrow cells were cultured with mouse granulocyte-macrophage colony stimulating factor (10 ng/ml) for 6 days to enrich BMDCs or macrophage-colony stimulating factor (25 ng/ml) for 7 days to enrich BMMs.

Cell viability was determined using the [3-(4,5-dimethylthiazol-2-yl)-2,5-diphenyltetrazolium] bromide (MTT) assay measuring the activity of mitochondrial dehydrogenase. DC 2.4 cells kindly provided by Dr. Martin D'Souza were seeded at the concentration of $5x10^5$ cells/well in 12-well plates. Alum (50 μg) or MF59 (50%) were treated for 24 hours and the cells were harvested. The cells were stained with annexin V and propidium iodide (PI) kit (BD Pharmigen) followed by manufacturer's protocol and analyzed by flow cytometry.

The generated BMDCs were treated with MPL (5 μg) + Alum (50 μg), MPL (5 μg), or Alum (50 μg) to determine pro-inflammatory cytokine production, DC activation marker expression and cell death by adjuvants. For measuring *in vitro* IgG production by adjuvant-stimulated BMDCs, vaccine (Vac, 3 μg) + MPL (5 μg) + Alum (50 μg) combination was used to pre-treat BMDCs for 2 days for preparation of mature DCs (mDCs). Spleen cells from naïve CD4KO mice were cultured with MPL+ Alum, mDCs, or mDCs + mDC culture supernatant for 7 days. IgG levels in culture supernatants were determined by ELISA. To determine proliferated double negative (DN) T cells, spleen cells were harvested from Vac+MPL+Alum-immunized CD4KO mice and stained with carboxyfluorescein succinimidyl ester (CFSE). The CFSE-labeled

cells were co-cultured with immature DCs (imDCs), mDCs or mDC plus anti-mouse MHCII monoclonal antibodies (1 μg/ml, clone M5/114.15.2) for 5 days. The percentages of DN T cell proliferation were measured by flow cytometry.

To determine the immunostimulatory effects of RSV vaccines, the generated BMDCs were seeded at the concentration of 5×10^4 cells/well in 96-well cell culture plates and treated with 10 μg/ml of FI-RSV, F VLP, G VLP and live RSV. 2×10^5 cells/well of the harvested splenocytes in 96-well cell culture plates were treated with 10 μg/ml of FI-RSV, F VLP and G VLP. After 2 days culture, the cell culture supernatants were harvested and cytokine production were measured. BMDC and splenocyte culture supernatants were used to determine cytokine levels.

2.14 Uric acid assay

Peritoneal exudates were harvested from PBS, MF59, or alum-injected WT or CD4KO mice at 24 hours post injection. The uric acid levels in peritoneal exudates were measured by uric acid assay kit (Bioassay system) followed by manufacturer's protocol.

2.15 Statistical analysis

Experimental data were presented as means ± SEM (standard error of mean). The statistical significance was determined by 1-way ANOVA and followed Tukey's multiple comparison test or by 2-way ANOVA and followed Bonferroni post-test. $p<0.05$ was considered as significance. We analyzed all data with statistical Prism Software (GraphPad Software Inc, San Diego, CA).

3 CHAPTER 1. MF59 ADJUVANT EFFECTS ON INDUCING ISOTYPE-SWITCHED IGG ANTIBODIES AND PROTECTION AFTER IMMUNIZATION WITH T-DEPENDENT INFLUENZA VIRUS VACCINE IN THE ABSENCE OF $CD4^+$ T CELLS

3.1 Summary

$CD4^+$ T cells play a central role in orchestrating adaptive immunity. To better understand the roles of $CD4^+$ T cells in the adjuvant effects, we investigated the efficacy of T-dependent influenza virus split vaccine with MF59® or alum in CD4-knockout (CD4KO) and wild-type (WT) mice. $CD4^+$ T cells were required for the induction of IgG antibody responses to split vaccine and alum adjuvant effects. In contrast, MF59® was found to be highly effective in raising isotype-switched IgG antibodies to T-dependent influenza split vaccine in CD4KO mice or CD4-depleted WT mice, equivalent to those in intact WT mice, thus overcoming the deficiency of $CD4^+$ T cells in helping B cells and inducing immunity against influenza virus. MF59-adjuvanted influenza split vaccination was able to induce protective $CD8^+$ T cells and long-lived antibody-secreting cells in CD4KO mice. MF59 adjuvant effects in CD4KO mice might be associated with uric acid, inflammatory cytokines, and recruitment of multiple immune cells at the injection site, but their cellularity and phenotypes were different from those in WT mice. These findings suggest a new paradigm of CD4-independent adjuvant mechanisms, providing the rationales to improve vaccine efficacy in infants, elderly, and immune-compromised patients as well as in healthy adults.

3.2 Results

3.2.1 MF59 is effective in generating influenza vaccine-specific isotype-switched IgG antibodies in CD4-deficient mice.

To determine the roles of $CD4^+$ T cells in the adjuvant effects on generating vaccine-specific isotype-switched antibodies, WT and CD4KO mice were intramuscularly immunized with influenza split vaccine only, or in combination with MF59 or alum adjuvant. Split vaccine only immunization induced IgG1 dominant antibody responses at low levels in WT mice but no antibody responses in CD4KO mice (Fig. 3.1), indicating that antibody responses to split vaccine require $CD4^+$ T cell help. Similarly, the alum group showed significantly lower levels of IgG and IgG1 antibodies in CD4KO mice compared to those in WT mice (Fig. 3.1), suggesting the $CD4^+$ T cell dependency of alum adjuvant effects. The MF59 group could generate vaccine-specific IgG, IgG1, and IgG2c antibodies at a substantial level after priming of CD4KO mice, which is significantly higher than those in WT mice immunized with split alone (Fig. 3.1A). Split alone and split plus alum vaccination in WT mice induced IgG1 dominant antibodies indicating T helper type 2 (Th2) immune responses. Whereas split plus MF59 vaccination of CD4KO mice induced both IgG1 and IgG2c isotypes similar to those in WT mice, eliciting Th1 and Th2 type immune responses regardless of $CD4^+$ T cells. In addition, MF59-adjuvanted CD4KO mice induced IgG and IgG1 antibodies specific for vaccine at significantly higher levels than those in WT mice immunized with split alone and split plus alum after boost (Fig. 3.1B). In general, $CD4^+$ T cells are required for long-lived antibody and memory responses. Surprisingly, the antibody levels of split plus MF59 immunized CD4KO mice were maintained 5 months after boost immunization (Fig. 3.1C), suggesting the induction of long-lived IgG isotype-switched antibodies in the absence of conventional $CD4^+$ T cells. The levels of IgG, IgG1 and IgG2c in split plus MF59 immune

CD4KO mice were comparable to those in the WT MF59 group (Fig. 3.1). Hemagglutination inhibition (HAI) assays were performed to determine whether protective antibodies would be induced in immune sera (Fig. 3.1D). Split vaccine alone or with alum induced low HAI titers in WT mice and no HAI titers in CD4KO mice. The MF59 group exhibited high levels of HAI titers in CD4KO mice, which are comparable to those in WT mice, indicating that MF59 adjuvant vaccination induces protective HAI antibodies in the absence of $CD4^+$ T cells. In addition, CD4-independent induction of isotype-switched IgG antibodies were similarly observed in CD4-depleted WT mice with MF59 split vaccination (Fig. 3.2). These results of adjuvant effects in CD4KO mice suggest that MF59 can overcome $CD4^+$ T cell deficiency in raising IgG, IgG1, IgG2a isotype-switched and functional (HAI) antibodies specific for split vaccine, a T-dependent antigen.

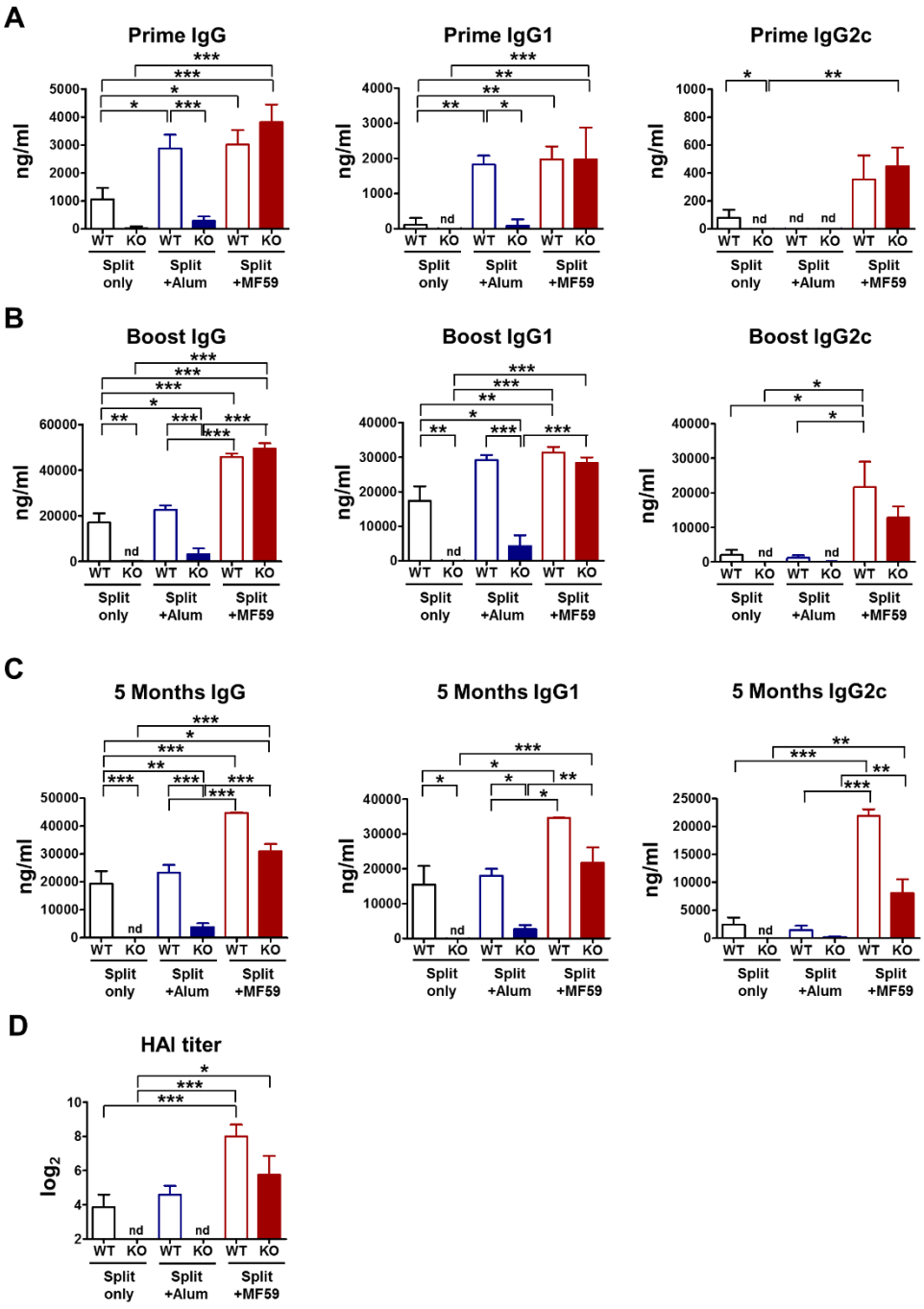

Figure 3.1 CD4KO mice with MF59 are more effective in inducing IgG isotype antibodies than WT mice with split vaccine alone or plus alum.

Immune sera were taken 3 weeks after each immunization from WT and CD4KO mice (n=10 per group) intramuscularly immunized with split vaccine ± alum or MF59 adjuvant. Inactivated A/California/04/2009 H1N1 virus (iCal)-specific IgG and isotype-switched IgG antibody levels in immune sera were determined by ELISA. Antibody levels after prime (A), boost (B) and 5 months after boost (C) immunizations are presented in mean ± standard error (SEM). (D) HAI titers were determined in immune sera from split vaccine ± alum or MF59 adjuvant immunized WT and CD4KO mice. WT: C57BL/6 wild type mice (n=10), KO: CD4 knockout mice (n=10). A representative of duplicate experiments was shown. Statistical significances were calculated by 1-way ANOVA and Tukey's multiple comparison tests. *; $p<0.05$, **; $p<0.01$, and ***; $p<0.001$ as indicated.

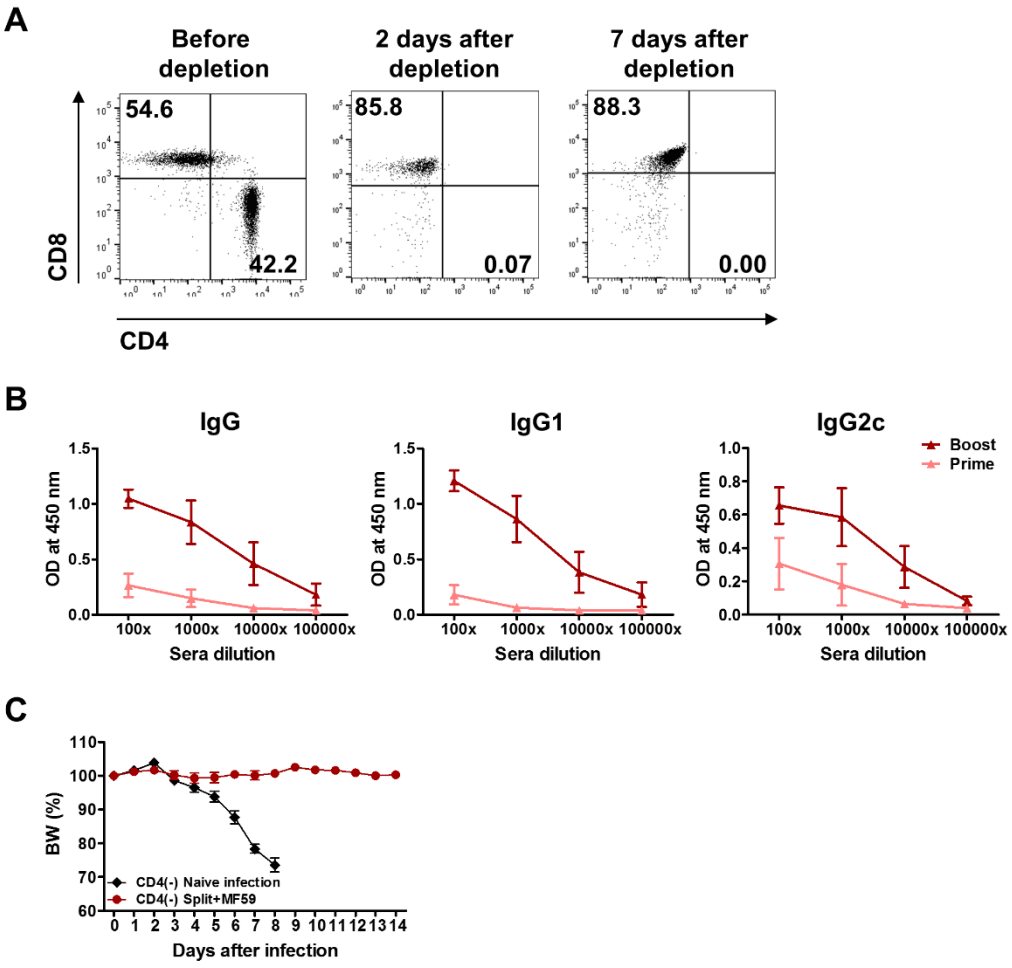

Figure 3.2 Induction of protective isotype-switched antibodies by MF59 adjuvanted split vaccination of CD4-depleted B6 WT mice.

(A) C57BL/6 wild-type mice were injected with anti-CD4 monoclonal antibody (200 µg/mouse, clone: GK1.5) to deplete $CD4^+$ T cells. Cells were harvested from blood of CD4-depleted mice to determine CD4-depletion. CD4 and CD8 marker profiles are shown from $CD3^+$ gated T cells. (B) CD4-depleted WT mice were immunized 2 times (prime and boost) with split vaccine plus MF59. The CD4-depletion was maintained by additional weekly treatments with CD4-depleting antibodies during the immunization. After 2 weeks from each immunization, immune sera were collected to determine virus-specific IgG and isotype-switched IgG antibodies by ELISA. (C) Naïve and the immune mice were infected with the lethal dose of virus 4 weeks after boost immunization. Body weight changes were monitored for 14 days.

3.2.2 MF59 but not alum split vaccination induces equivalent protection in CD4KO and WT mice.

To investigate the adjuvant effects on conferring protection, at 5 months after boost vaccination, immunized WT and CD4KO mice were intranasally challenged with a lethal dose of A/California/04/2009 H1N1 virus. WT mice with split vaccine alone were severely sick as shown by over 18% weight loss and 60% survival rates, indicating low efficacy of protection. CD4KO mice with split vaccine were not protected (Fig. 3.3A and B). Alum adjuvant effects were evident in WT mice with moderate weight loss of approximately 8% but ineffective in CD4KO mice displaying over 18% weight loss and 40% survival rates (Fig. 3.3A and B). MF59 adjuvant effects on conferring 100% protection without weight loss in CD4KO mice were similar to those in WT mice (Fig. 3.3A and B). Consistent with protective effects of MF59 in CD4KO mice, we observed 100 % protection without weight loss against lethal infection in CD4-depleted WT B6 mice (Fig. 3.2C). To better assess the protective efficacy, lung viral titers were determined at day 5 post virus infection (Fig. 3.3C). The split vaccine and alum adjuvant groups showed high levels of lung viral loads in both CD4KO and WT mice. The MF59 group showed lowest levels of lung viral titers in both CD4KO and WT mice. These results suggest that MF59 but not alum adjuvant was effective in conferring protection independent of $CD4^+$ T cell help even after 5 months of vaccination in a mouse model.

In addition, we determined the protective roles of immune sera from CD4KO mice that were immunized with split vaccine plus MF59 (Fig. 3.3D). Naïve mice were intranasally infected with a mixture of lethal dose of A/California/04/2009 H1N1 virus and immune sera or naïve sera, and daily monitored (Fig. 3.3D). All mice that were infected with virus and naïve sera died of infection by day 7. Whereas mice infected with virus and CD4KO mouse immune sera of split and

MF59 vaccination did not show any weight loss and 100% survived (Fig. 3.3D). Therefore, antibodies induced by split plus MF59 vaccination of CD4KO mice can confer protection to naïve mice.

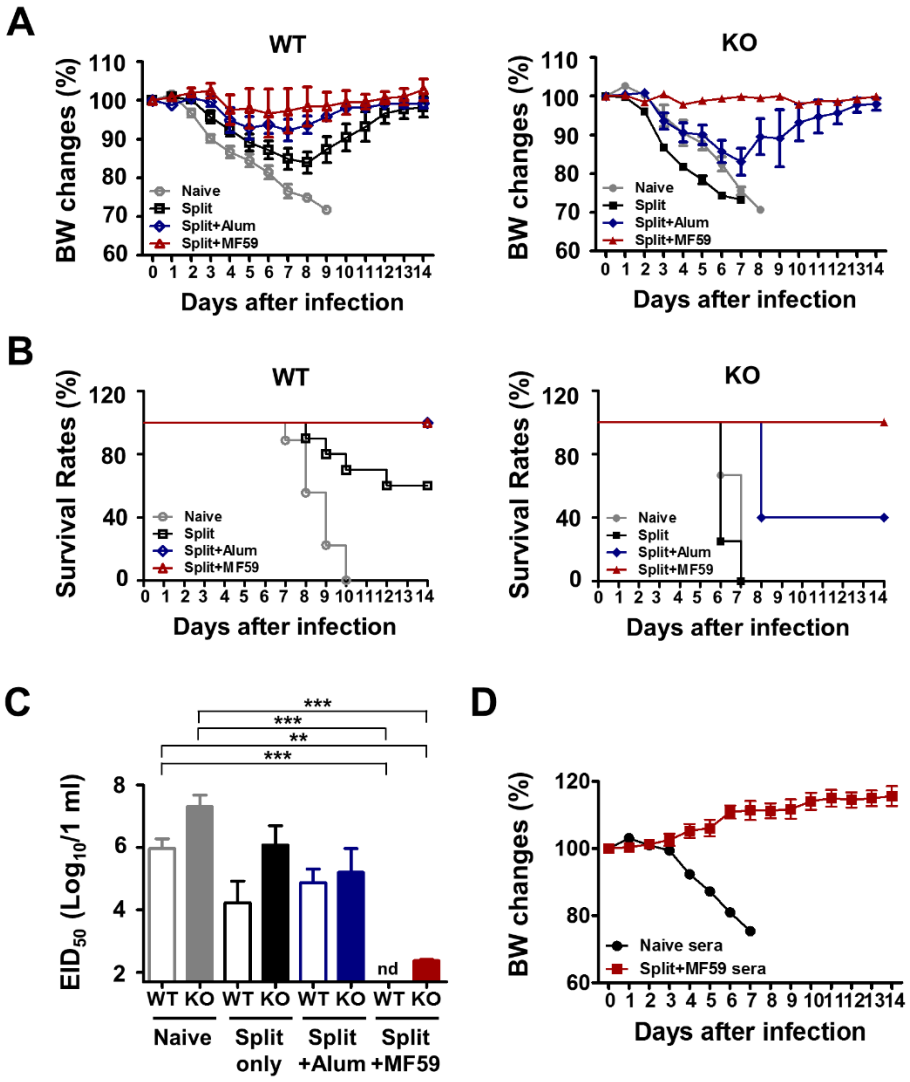

Figure 3.3 MF59 split vaccination confers equal protection in CD4KO and WT mice.
(A) Body weight (BW) changes and (B) survival rates after lethal dose of A/California/2009 H1N1 influenza virus challenge after 5 months of vaccination. (C) Lung virus titers in embryonated chicken eggs at day 5 post infection by an egg infection dose 50 (EID50). The detection limit of EID50 was 1.7 (Log10). (D) *In vivo* protective effects of immune sera. Naïve mice were intranasally infected with a lethal dose ($7.5\times LD_{50}$) of virus (A/California/04/2009 H1N1) mixed with naïve or split-MF59 immune sera from CD4KO mice. WT: C57BL/6 wild type mice (n=10), KO: CD4 knockout mice (n=10). Statistical significances were calculated by 1-way ANOVA and Tukey's multiple comparison test. **; $p<0.01$, and ***; $p<0.001$ as indicated among the groups. nd; not detected.

3.2.3 MF59 but not alum is effective in generating antibody secreting long-lived cells in both CD4KO and WT mice.

Antibody secretion at the infection site plays a role in blocking virus invasion and replication. WT mice with split vaccine with or without adjuvants showed IgG antibodies in bronchoalveolar lavage fluids (BALF) (Fig. 3.4A) and lung extracts (Fig. 3.4B) at day 5 after infection. However, split vaccine only CD4KO mice did not display IgG antibodies in BALF and lungs collected at day 5 after infection (Fig. 3.4A and B). $CD4^+$ T cell-independent antibody responses are characterized to be short-lived within 30 days and deficient of long-lived plasma cells in the bone marrow (BM) [71, 72]. To determine whether MF59 would contribute to the generation of long-lived plasma cells and memory type B cells, *in vitro* antibody production was determined using cells of BM and spleens collected from immune mice after 5 months of vaccination and then virus infection (Fig. 3.4C and D). The split only and split plus alum immune WT mice groups showed low levels of antibodies from 1-day BM or 5-day spleen cell cultures (Fig. 3.4C and D). Surprisingly, MF59 CD4KO mice showed significantly high levels of antibodies in cultures of BM and spleen cells, which are comparable to those in MF59 WT mice (Fig. 3.4C and D). These results suggest that MF59 adjuvant contributes to the generation of long-lived antibody secreting cell responses even without the help from $CD4^+$ T cells.

3.2.4 MF59 plus split vaccination protects against pulmonary inflammation in immune CD4KO and WT mice.

Pathogenic influenza virus infection inflames lung tissues by inducing excessive pro-inflammatory cytokines and/or recruiting immune cells. High levels of IL-6 were observed in BALF and lungs from the groups of WT naïve and split only, and CD4KO alum mice at day 5

after challenge (Fig. 3.4E and F). In contrast, low levels of IL-6 in BALF and lungs were detected in the MF59-CD4KO and WT groups (Fig. 3.4E and F). Histopathological changes in the lung were analyzed to better evaluate the protective efficacy of adjuvants after challenge of WT and CD4KO mice (Fig. 3.4G). Both WT and CD4KO naïve mice showed severe lung inflammation upon influenza virus infection as shown by extensive infiltrates around the airways, blood vessels, and interstitial spaces (Fig. 3.4G). Split vaccine only and split plus alum immune WT and CD4KO mice showed moderate to high levels of immune cell infiltration, and CD4KO mice displayed a tendency of being more severe inflammation compared to corresponding WT mice (Fig. 3.4G). Importantly, MF59 adjuvanted WT and CD4KO mice showed lowest or no overt pulmonary inflammation, which is consistent with effective protection in the MF59 adjuvanted WT and CD4KO groups. These data suggest that MF59 adjuvant vaccination effectively protects against lung inflammation due to viral infection even in the absence of $CD4^+$ T cell help.

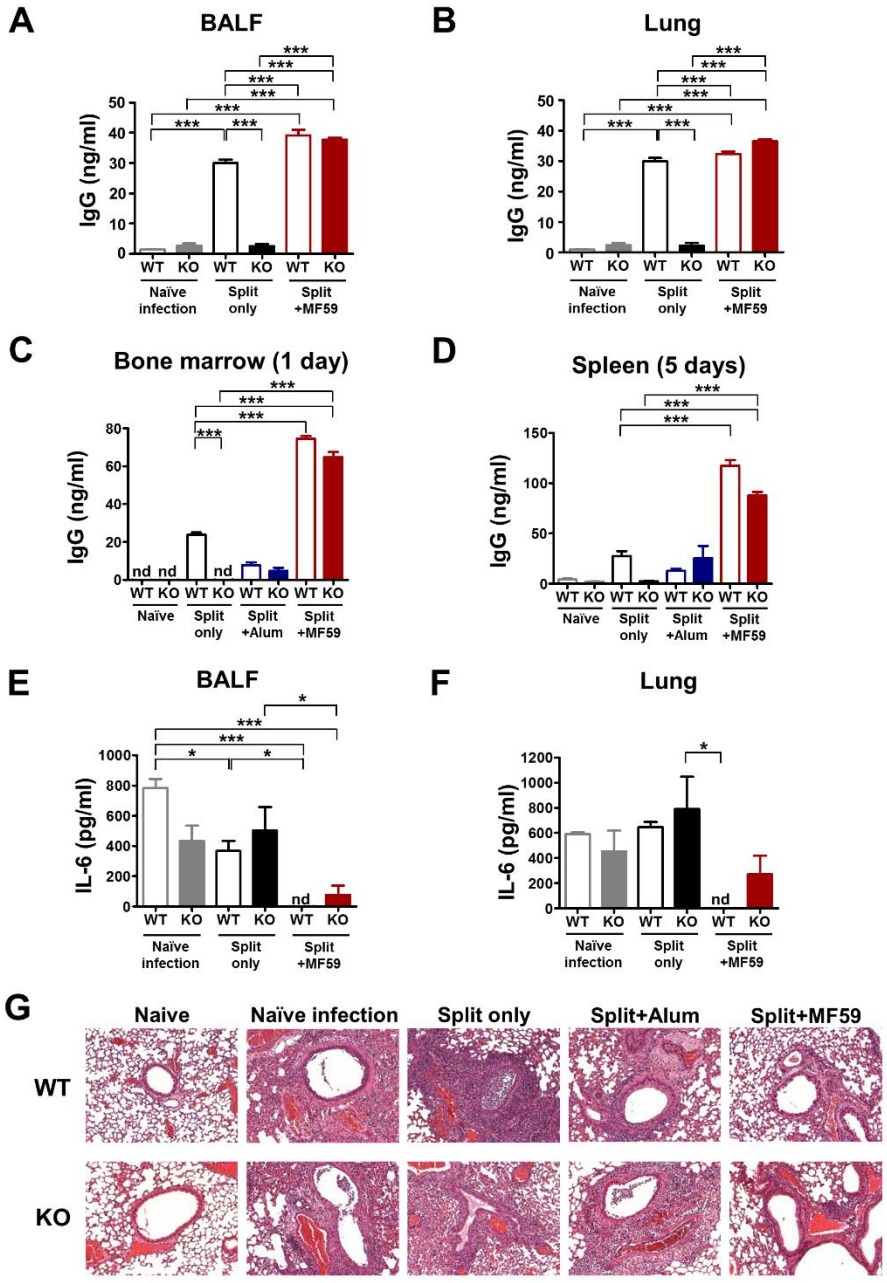

Figure 3.4 MF59 split vaccination of CD4KO mice induces mucosal antibodies, long-lived plasma and memory B cell responses, and protects against lung inflammation after virus challenge.
(A) IgG levels in BALF. (B) IgG levels in lung extracts. (C and D) BM and spleen cells were harvested day 5 post infection after 5 months of vaccination. BM cells (C) and spleen cells (D) were cultured in the plates coated with virus antigen for 1 day or 5 days, respectively, and IgG levels were detected by ELISA. (E) IL-6 inflammatory cytokine in BALF. (F) IL-6 inflammatory cytokine in lung extracts. BALF and lung samples (n=5) were collected at 5 days after lethal challenge. (G) Lung histopathology of mice (n=5) after virus challenge. Lung tissues at day 5 post challenge were stained with hematoxylin and eosin. Statistical significances were calculated by 1-way ANOVA and Tukey's multiple comparison test. *; $p<0.05$, and ***; $p<0.001$ as indicated among the groups. nd; not detected.

3.2.5 CD4KO mice with MF59 plus split vaccination induce protective CD8$^+$ T cells.

Since CD4$^+$ T cells play an essential role in generating functionally effective CD8$^+$ T cells, we determined whether MF59 would contribute to the generation of protective CD8$^+$ T cells in CD4KO mice. We applied a CD8-depletion approach to the MF59 adjuvanted group prior to virus challenge (Fig. 3.5A). The MF59 CD4KO group with CD8-depletion displayed approximately 20% weight loss compared to the control MF59 CD4KO group with 4-5% weight loss after lethal virus infection (Fig. 3.5B). In addition, CD8$^+$ T cell depletion in the split plus MF59 immunized CD4KO mice led to 1000-fold higher egg infectious titers compared to those in the CD8-competent CD4KO group (Fig. 3.5C). In terms of lung inflammation, CD8-depleted CD4KO mice showed more severe pulmonary inflammation as examined for histopathology (Fig. 3.5D) and pro-inflammatory cytokine production in both BALF and lung extracts (Fig. 3.5E). These results suggest that MF59 adjuvant contributes to the generation of protective CD8$^+$ T cells in the absence of CD4$^+$ T cells.

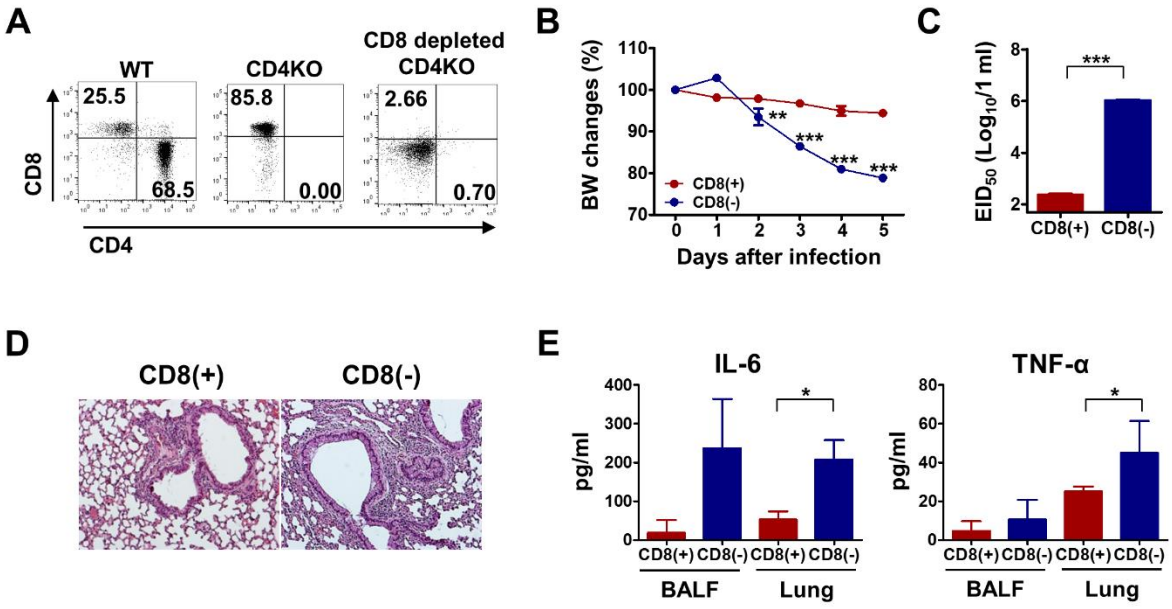

Figure 3.5 MF59 adjuvanted CD4KO mice induce protective CD8$^+$ T cell responses.
(A) Split plus MF59 immunized CD4KO mice were injected with anti-CD8 monoclonal antibody (150 µg/mouse, clone: clone 53-6.7) to deplete CD8$^+$ T cells before virus challenge. Cells were harvested from blood of CD8-depleted mice 2 days after injection to determine CD8-depletion. CD4 and CD8 marker profiles are shown from CD3$^+$ gated T cells. (B) Body weight changes of CD8-depleted CD4KO mice after virus infection. (C) Lung virus titers in embryonated chicken eggs at day 5 after infection. (D) Lung histopathology of CD8-depleted CD4KO mice day 5 post infection. (E) Inflammatory IL-6 and TNF-α cytokine in BALF and lung extracts day 5 post infection. Statistical significances were calculated by 1-way ANOVA and Tukey's multiple comparison test. *; $p<0.05$, **; $p<0.01$, ***; $p<0.001$ between CD8-depleted and CD8-undepleted CD4KO mouse groups (n=5).

3.2.6 MF59 induces in vivo inflammatory cytokines and chemokine in CD4KO and WT mice.

Certain adjuvants recruit innate immune cells resulting in immunocompetent microenvironment. To investigate underlying CD4$^+$ T cell-independent adjuvant mechanisms of MF59, we injected alum and MF59 intraperitoneally to WT and CD4KO mice. Sera at 1.5, 6, and 24 hours (h), and peritoneal exudates at 24 h were harvested after injection. Cytokines and chemokines in peritoneal exudates and sera were detected by ELISA (Fig. 3.6A and B). MF59 induced high levels of pro-inflammatory cytokines (IL-5, IL-6 and TNF-α) and chemokines (MCP-1 and RANTES) in peritoneal exudates whereas alum induced low levels of IL-6 and MCP-1 only (Fig. 3.6A). Interestingly, MF59-injected CD4KO mice showed higher levels of IL-6, TNF-α and

RANTES and similar levels of IL-5 and MCP-1 compared to WT mice (Fig. 3.6A). These results indicate that MF59 injection could induce more inflammatory environment in CD4KO mice than that in WT mice. In addition to the local responses, systemic cytokine/chemokine levels were also higher in MF59 injected mice than those of PBS or alum injected mice (Fig. 3.6B). IL-6 in sera was rapidly increased at the early time point (1.5 h), but IL-5 was induced at high levels at late time points in sera from MF59-treated WT mice (6 h) and CD4KO mice (24 h), and maintained at high levels for a while. MCP-1, a chemokine to recruit monocytes and DCs, was transiently increased in both MF59 injected WT and CD4KO mice.

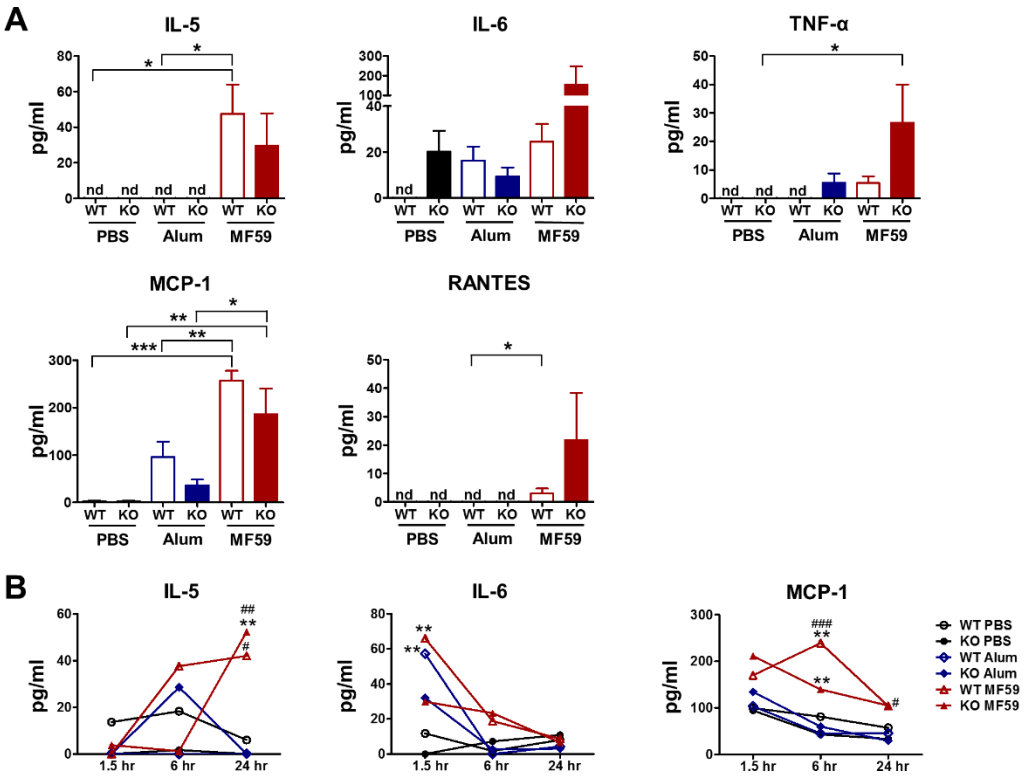

Figure 3.6 MF59 induces acute production of cytokines and chemokines at higher levels than alum.
WT and CD4KO mice (n=5) were intraperitoneally injected with PBS, alum, or MF59. (A) Cytokines and chemokines in peritoneal exudates at 24 h after injection. Statistical significances were calculated by 1-way ANOVA and Tukey's multiple comparison test. *; $p<0.05$, **; $p<0.01$, and ***; $p<0.001$ as indicated among the groups. (B) Kinetics of cytokines and chemokine levels in sera from adjuvant injected mice (n=5 mice per group). Statistical significances were calculated by 2-way ANOVA and Bonferroni post-tests. **; $p<0.01$ compared to PBS-treated group and $^{\#}$; $p<0.05$, $^{\#\#}$; $p<0.01$, and $^{\#\#\#}$; $p<0.001$ compared to alum treated group. nd; not detected.

3.2.7 MF59 recruits multiple innate immune cells and dendritic cells in CD4KO mice.

To analyze the cellular phenotypes at the injection site, the peritoneal cells were harvested at 24 h after adjuvant injection. Most of macrophages were disappeared (or depleted) in alum and MF59 treated WT mice whereas some levels of macrophages were maintained in CD4KO mice with MF59 (Fig. 3.7). In contrast, monocytes, neutrophils and natural killer (NK) cells were significantly increased to higher levels in MF59 adjuvant treated CD4KO and WT mice than those in alum-treated mice. Surprisingly CD4KO mice with MF59 showed higher cellularity of macrophages, eosinophils, and natural killer T (NKT) cells as well as DC populations including plasmacytoid DCs (pDCs), $CD11b^{high}$ DCs, and $CD11b^{low}$ DCs compared to WT mice with MF59 (Fig. 3.7). These results suggest that differential cellularity and patterns of immune cell recruitment after MF59 treatment of WT mice and CD4KO mice may explain CD4-independent and CD4-dependent MF59 adjuvant effects and superior adjuvanticity of MF59 over alum.

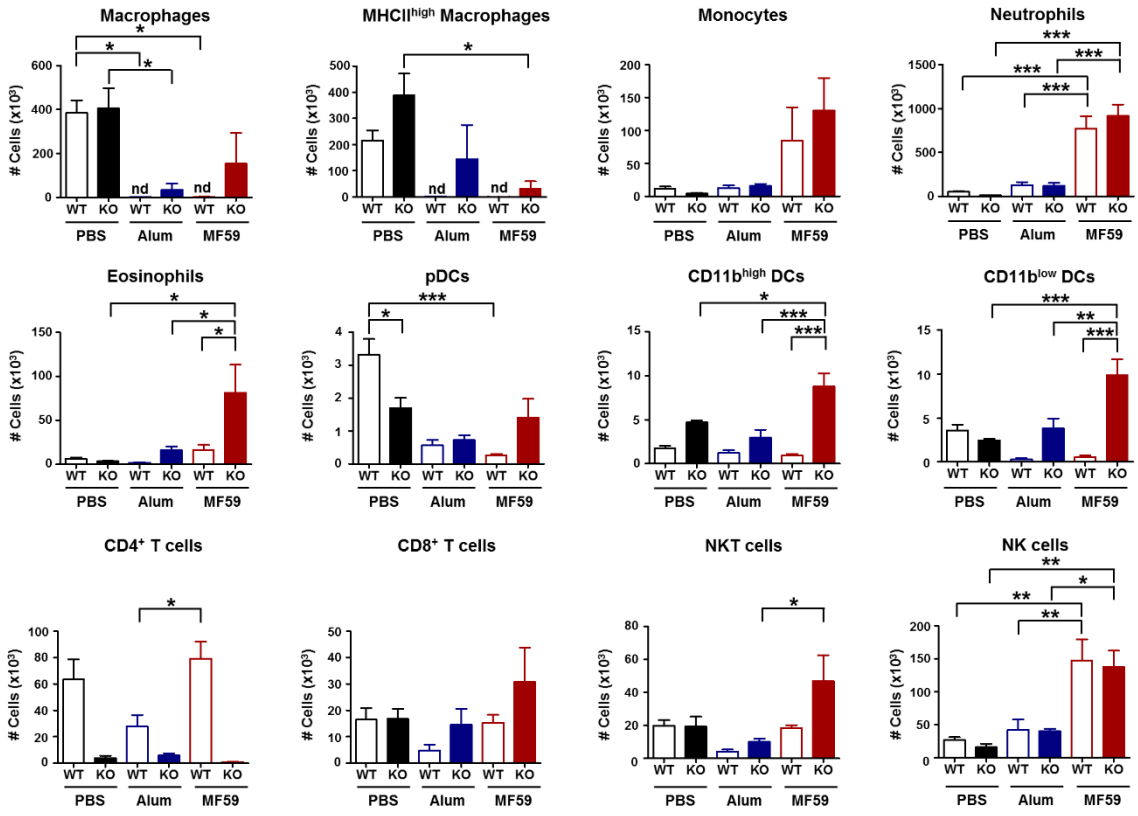

Figure 3.7 MF59 injection of CD4KO mice acutely recruits multiple innate and dendritic cells.
Cells in peritoneal exudates were collected at 24 hours after adjuvant injection and their phenotypes and cellularity determined using flow cytometry (n=5 mice per group). Macrophages; $CD11b^{+}F4/80^{+}$, $MHCII^{high}$ macrophages; $CD11b^{+}F4/80^{+}MHCII^{high}$, Monocytes: $CD11b^{+}Ly6c^{high}F4/80^{+}$, Neutrophils; $CD11b^{+}Ly6c^{+}F4/80^{-}$, Eosinophils; $CD11b^{+}SiglecF^{+}$, pDCs; $CD11c^{+}B220^{+}MHCII^{high}$, $CD11b^{high}$ DCs; $CD11c^{+}CD11b^{high}MHCII^{high}$, $CD11b^{low}$ DCs; $CD11c^{+}CD11b^{low}MHCII^{high}$, $CD4^{+}$T cells; $CD3^{+}CD4^{+}$, $CD8^{+}$ T cells; $CD3^{+}CD8^{+}$, NKT cells; $CD49b^{+}CD3^{+}$, NK cells; $CD49b^{+}CD3^{-}$. Statistical significances were calculated by 1-way ANOVA and Tukey's multiple comparison test. *; $p<0.05$, **; $p<0.01$, and ***; $p<0.001$ as indicated among the groups. nd; not detected.

3.2.8 MF59 as well as alum adjuvant induces in vitro cell death and uric acid production

Induction of cell death or tissue damage can be a mechanism for alum adjuvant effects [73, 74, 75]. To investigate whether alum or MF59 adjuvant would induce cell death, BM-derived DCs (BMDC) and macrophages (BMM) were *in vitro* cultured in the presence of adjuvant for 48 h and cell viability was determined (Fig. 3.8A and B). BMM showed approximately 20% and 30% cell viability in the presence of alum and MF59 adjuvant respectively (Fig. 3.8A). BMDCs treated with

alum or MF59 resulted in 50% cell death (Fig. 3.8B). Alum- and MF59-treated DC2.4 cells showed approximately 25% and 15% necrotic cell death, respectively (Fig. 3.8C and D). MF59-treated cells also displayed substantial cell death via apoptosis. Consistent with *in vitro* cell death results, high levels of uric acid, a danger signal in response to cell death [76], were observed in the peritoneal exudates at 24 h after injection of WT and CD4KO mice with MF59 (Fig. 3.8E). These *in vitro* results appear to be consistent with *in vivo* lower cellularity of macrophages and DC populations at the site of alum or MF59 adjuvant injection.

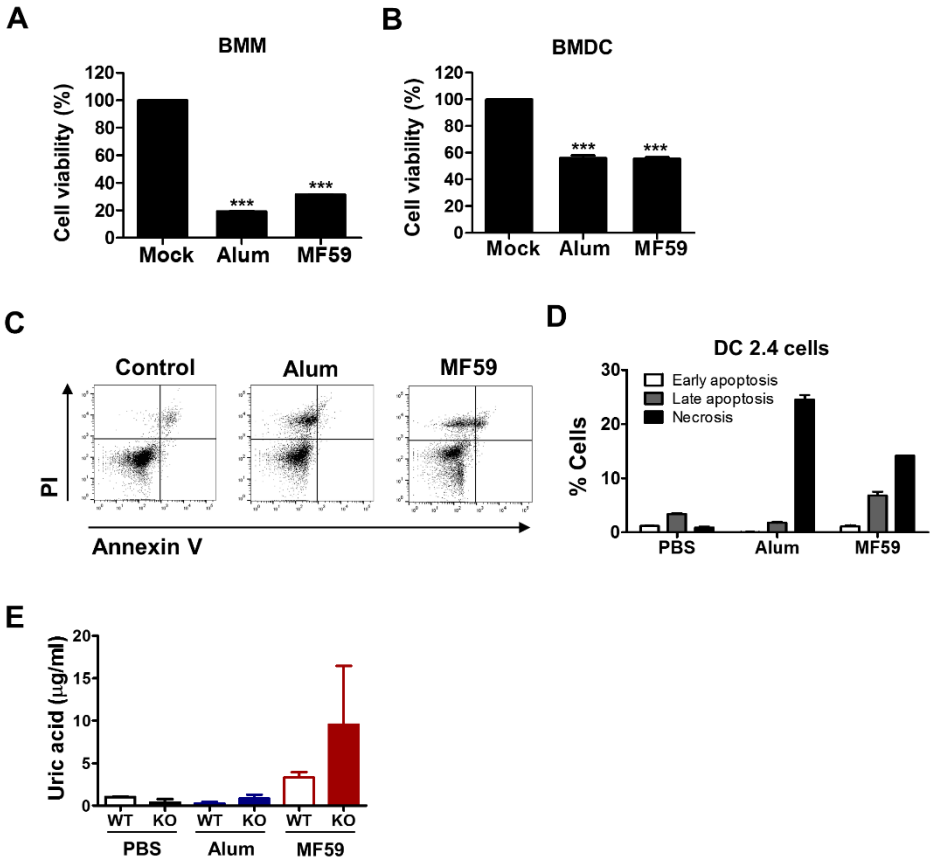

Figure 3.8 Alum and MF59 adjuvants induce in vitro cell death and uric acid production.
(A, B) Cell viability of BMMs (A) and BMDCs (B) after in vitro culture with alum or MF59. Primary BMMs and BMDCs from C57BL/6 mice were cultured in the presence of alum (100 μg/ml) or MF59 (20%) for 48 h and cell viability was determined by an MTT assay. Statistical significances were calculated by 1-way ANOVA and Tukey's multiple comparison test. ***; $p<0.01$ compared to mock control group. (C) Flow cytometry profile and (D) apoptotic or necrotic cell death percentages of dendritic cell line DC 2.4 cells. DC 2.4 cells were treated with adjuvants for 24 h, and then stained with annexin V and PI. Necrotic cell death: $PI^+AnnexinV^-$, Late apoptosis: $PI^+AnnexinV^+$, Early apoptosis: $PI^-AnnexinV^+$. (E) WT and CD4KO mice were intraperitoneally injected with PBS, alum, or MF59. Peritoneal exudates were collected 24 hours post adjuvant injection and uric acid levels were measured.

3.3 Discussion

It is a conventional mechanism that most adjuvants activate components of the innate immune system, mediating the effective presentation of antigens via APCs, which subsequently determines a pattern of T helper cell immune responses (Th1, Th2, Th17, follicular T cells, regulatory T cells). Activation of T helper cells via adjuvants and APCs provide a differential and critical role in controlling specific B cells to produce isotype-switched IgG antibodies. As expected, $CD4^+$ T cells were found to be critical for inducing isotype-switched IgG antibodies by split vaccination and for alum adjuvant effects. Nonetheless, the efficacy of alum was low as evidenced by ineffective lung viral clearance, lung inflammation, and weight loss in immune competent WT mice after virus challenge.

Different from a conventional dogma of the critical roles of $CD4^+$ T cells in generating adaptive immunity, $CD4^+$ T cells appear to be differentially required for inducing protective immunity, depending on the IgG isotypes, and the types of adjuvants. Here, unexpectedly, we found that MF59 adjuvant could overcome a deficiency of $CD4^+$ T cells in generating isotype-switched IgG antibodies and conferring effective protection even after 5 months of vaccination. CD4-independent IgG antibody responses induced by sublethal virus infection were shown to be short-lived within 30 days, to wane rapidly, and no antibody-secreting plasma cells [71, 72]. IgG antibody responses in CD4KO mice with MF59 conferred protective immunity, high virus-specific serum antibodies, and long-lived antibody secreting plasma cells in BM even after 5 months. Also, the induction of protective humoral antibody and cellular $CD8^+$ T cell responses was evident in CD4KO mice with MF59 adjuvant split vaccination. Adaptive immune responses and efficacy of protection against influenza virus were significantly higher in CD4KO mice with MF59 compared to those in WT mice with split vaccine alone or with alum. These results provide convincing clues

that MF59 adjuvant may replace the roles of conventional $CD4^+$ T cells in conferring protective immunity after T-dependent split vaccine immunization. This study suggests an alternative pathway between innate and adaptive immune systems via certain adjuvants such as MF59, which can be either CD4-independent or CD4-dependent mechanism.

CD4KO mice were reported to develop MHC class II-restricted $CD8^+$ T cells and double negative T cells which might contribute to providing $CD4^+$ T cell-like help in CD4KO mice [41, 77]. T cell receptor αβ-deficient mice were shown to have a severe defect in inducing IgG antibodies after vaccination [41]. Nonetheless, an alternative approach of acute CD4 depletion in this study provides further evidence that MF59 can induce IgG isotype-switched antibodies in the absence of $CD4^+$ T cells by eliminating the potential contribution of compensatory immune cells that might have developed in CD4KO mice. The possible roles of double negative and/or γδ T cells in generating IgG antibodies in CD4KO mice remain to be determined.

Although it is not clear how MF59 works in a CD4-independent manner, possible mechanisms of MF59 adjuvant effects were previously reported. Alum and MF59 did not exhibit any *in vitro* stimulatory effects on DCs [26, 28]. Intriguingly adjuvanticity of alum and MF59 required MyD88 *in vivo*, a common signaling adaptor for most Toll-like receptors, using a MyD88 mutant mouse model with recombinant bacterial protein vaccines or ovalbumin model antigens [26, 78]. MF59 was shown to create an immunocompetent micro-environment at the injection site by inducing chemokines and cytokines as well as recruiting neutrophils, eosinophils, and later DCs and macrophages [79]. Previous studies on MF59 suggest that immunocompetent micro-environment with activated innate and APCs leads to the induction of effector $CD4^+$ T cells eventually helping B cells to differentiate IgG antibody secreting plasma cells [28, 29, 80, 81]. Using microarray and immunofluorescence analysis, MF59 was a strong inducer of cytokines, cytokine receptors,

adhesion molecules, antigen presenting genes, and a rapid influx of $CD11b^+$ blood cells [82]. In this study, MF59 was more effective in inducing acute production of IL-5 and MCP-1 than alum. Compared to alum, MF59 was more effective in attracting innate immune cells (monocytes, neutrophils, eosinophils) and APCs ($CD11b^{hi/low}$ DCs), NK, and NKT cells, which is consistent with a previous study [79]. Interestingly, antibody-mediated neutrophil ablation did not alter MF59 adjuvanticity [79]. MF59 induced more production of IL-6, TNF-α, and RANTES in CD4KO mice than those in WT mice. Thus, MF59 may work in a different mechanism in CD4KO from the one in WT mice. Higher levels of DC populations including pDC and $CD11b^{hi/low}$ DCs, NKT, and $CD8^+$ T cells were recruited in CD4KO mice than those in WT mice after MF59 treatment. Therefore, in the absence of $CD4^+$ T cells, CD4KO mice might have differentially responded in their innate immune cells and cytokines to MF59 adjuvant, suggesting an alternative immune activation pathway in CD4KO mice.

Cell death sends danger signals such as uric acid and creates local inflammatory microenvironment triggering the innate immune system [76, 83]. Necrotic sterile cell death or injury induces the generation of uric acid as an adjuvant, promoting adaptive immune responses [76, 84], and could be a powerful mediator of a Th2-associated adjuvant effects [85]. Most interestingly, we discovered that alum and MF59 injection resulted in significant depletion of macrophages ($F4/80^+CD11b^+MHCII^{low/high}$) and pDCs in the peritoneal cavity in WT mice, possibly causing cell death of these particular cell types. In line with these results, substantial levels of uric acid were detected at the injection site of WT and particularly CD4KO mice (Fig. 8E). High levels of uric acid might be correlated with inflammatory micro-environment producing IL-6, TNF-α, and RANTES in CD4KO-MF59 mice.

In vitro cultures of primary BM derived cells (BMMs, BMDCs), and DC2.4 DC cell lines with alum or MF59 displayed significant cell death. MF59 induced both apoptotic and necrotic cell death of DC2.4 whereas alum displayed mostly necrotic cell death of DC2.4 cell line. Compared to WT mice, MF59 IP injection of CD4KO mice maintained substantial levels of macrophages and pDCs together with increased cellularity of $CD11b^{hi/low}$ DCs, which might be contributing to MF59 adjuvant effects in CD4KO mice. These multiple mechanisms by MF59, which are different from alum quantitatively and qualitatively, appear to contribute to inducing IgG isotype antibodies in CD4KO mice to comparable levels as observed in WT mice.

The efficacy of influenza vaccines is low in young children and the elderly who may have some defects in $CD4^+$ T helper cells due to the immature immune system or aging. MF59-adjuvanted influenza vaccine was effective in infants and young children [86]. Our present data are relevant to these clinical studies and have significant clinical applications in providing rationales to improve vaccine efficacy in young infants, elderly, and CD4-deficient immunocompromised patients. Emerflu (an alum adjuvanted, inactivated, split H5 hemagglutinin) is a symbolic failure of alum-adjuvanted influenza vaccines in adults [87], requiring more effective adjuvants. Another implication is that adjuvant studies using CD4KO mice may provide a model to search for effective adjuvants such as MF59. WT mice are likely to over-respond to experimental adjuvants and vaccines, which may not represent the efficacies expected in humans [88].

4 CHAPTER 2. ROLES OF ALUM AND MONOPHOSPHORYL LIPID A ADJUVANTS IN OVERCOMING CD4+ T CELL DEFICIENCY TO INDUCE ISOTYPE-SWITCHED IGG ANTIBODY RESPONSES AND PROTECTION BY T-DEPENDENT INFLUENZA VIRUS VACCINE

4.1 Summary

Vaccine adjuvant effects in CD4 deficient condition largely remain unknown. We investigated the roles of combined monophosphoryl lipid A (MPL) and Alum adjuvant (MPL+Alum) in inducing immunity after immunization of CD4-knockout (CD4KO) and wild-type (WT) mice with T-dependent influenza vaccine. MPL+Alum adjuvant mediated IgG isotype-switched antibodies, IgG secreting cell responses, and protection in CD4KO mice, which were comparable to those in WT mice. In contrast, Alum adjuvant effects were dependent on $CD4^+$ T cells. MPL+Alum adjuvant was effective in recruiting monocytes and neutrophils as well as in protecting macrophages from alum-mediated cell loss at the injection site in CD4KO mice. MPL+Alum appeared to attenuate MPL-induced inflammatory responses in WT mice, likely improving the safety. Additional studies in CD4-depleted WT mice and MHCII KO mice suggest that MHCII positive antigen presenting cells contribute to providing alternative B cell help in CD4 deficient condition in the context of MPL+Alum adjuvanted vaccination.

4.2 Results

4.2.1 MPL+Alum and MPL adjuvanted influenza vaccines induce isotype-switched IgG antibodies in CD4KO mice

To determine whether adjuvanted vaccination would overcome a defect in $CD4^+$ T cells for inducing isotype-switched IgG antibodies, WT and CD4KO mice were intramuscularly immunized with influenza vaccine or in the presence of MPL+Alum, MPL or Alum adjuvant

(n=10). At 3 weeks after prime, the influenza vaccine (WT-Vac) and Alum (WT-Alum) groups of WT mice showed low levels of virus-specific IgG antibodies (Fig. 4.1B). CD4KO mice with vaccine (KO-Vac) only or alum-adjuvanted (KO-Alum) vaccination did not induce virus-specific IgG antibodies after prime (Fig. 4.1B), suggesting that vaccine is a T-dependent antigen and that Alum adjuvant effects are dependent on $CD4^+$ T cells. Surprisingly the MPL+Alum and MPL adjuvant groups induced IgG antibodies in CD4KO (KO Vac-MPL+Alum, KO Vac -MPL) mice at high levels comparable to the corresponding WT groups (WT Vac -MPL+Alum, WT Vac-MPL) after prime immunization (Fig. 4.1B). Therefore, MPL+Alum combination and MPL adjuvants can overcome a defect of $CD4^+$ T cells in priming IgG antibodies to T-dependent influenza vaccine in CD4KO mice.

When we determined IgG antibodies in boost vaccinated WT and CD4KO mice (Fig. 4.1C), the vaccine alone KO group did not induce IgG antibodies whereas the WT-Vac group showed substantial levels of IgG with dominant IgG1 (Th2 type) isotype (Fig. 4.1D, E). Also, the KO Vac+Alum group showed significantly lower level of IgG and IgG1 antibodies compared to those in WT-Alum mice (Fig. 4.1C, D), indicating that $CD4^+$ T cells are required for Alum adjuvant effects. The KO-MPL+Alum group exhibited high levels of IgG and IgG1 isotype antibodies, which are comparable to those in WT-MPL+Alum mice and higher than the KO-MPL group (Fig. 4.1C, D). The KO Vac+MPL group displayed boost IgG antibodies comparable to those in WT mice (Fig. 4.1C) but a trend of lower levels of IgG1 antibodies compared to those in WT mice (Fig. 4.1D). Induction of low IgG2c (Th1 type) levels was observed in the WT Vac and WT Vac+Alum but not the corresponding KO groups (Fig. 4.1E). The KO Vac+MPL+Alum group induced IgG2c antibodies at substantial but lower levels compared to those in the corresponding WT mice (Fig. 4.1E). The KO Vac+MPL group was effective in inducing IgG2c isotype antibodies

to an equivalent level as observed in the corresponding WT mice (Fig. 4.1E). We observed that IgG antibody levels in KO-MPL and particularly in KO-MPL+Alum mice kept increasing when determined at 3 months after boost vaccination (Table 4.1), which were still maintained for over 9 months (data not shown). It is important to note that MPL+Alum and MPL adjuvanted vaccination of CD4KO mice induced IgG antibodies to comparable levels in the corresponding WT mouse vaccination.

Serum HAI titers are used as a measure of functional antibodies predicting the efficacy of protection against influenza virus. The WT-Vac and WT-Alum groups showed a trend of lower levels of HAI titers compared to those in the WT-MPL+Alum and WT-MPL groups. Vaccine only and vaccine plus Alum immunized CD4KO mice did not induce detectable levels of HAI titers (Fig. 4.1F). In contrast, the KO-MPL+Alum and KO-MPL groups showed high levels of HAI titers similar to those in WT-MPL+Alum and WT-MPL immune mice, and there were no statistical significances in the corresponding WT and KO groups (Fig. 4.1F). Thus, MPL+Alum or MPL adjuvant in influenza vaccination can induce protective antibodies in CD4KO mice at comparable levels as observed in corresponding WT-adjuvant immune mice.

To determine adjuvant effects of MPL+Alum in primed mice, we primed wild-type mice with vaccine only, and then boosted the mice with vaccine only or vaccine+MPL+Alum. The boosted mice with MPL+Alum showed significantly higher levels of IgG antibody responses (Fig. 4.1G, Vac+MPL+Alum boost; 13.6±2.47 μg/ml) compared to the vaccine only primed and boosted mice (Fig. 1G, Vac boost; 3.71±0.48 μg/ml).

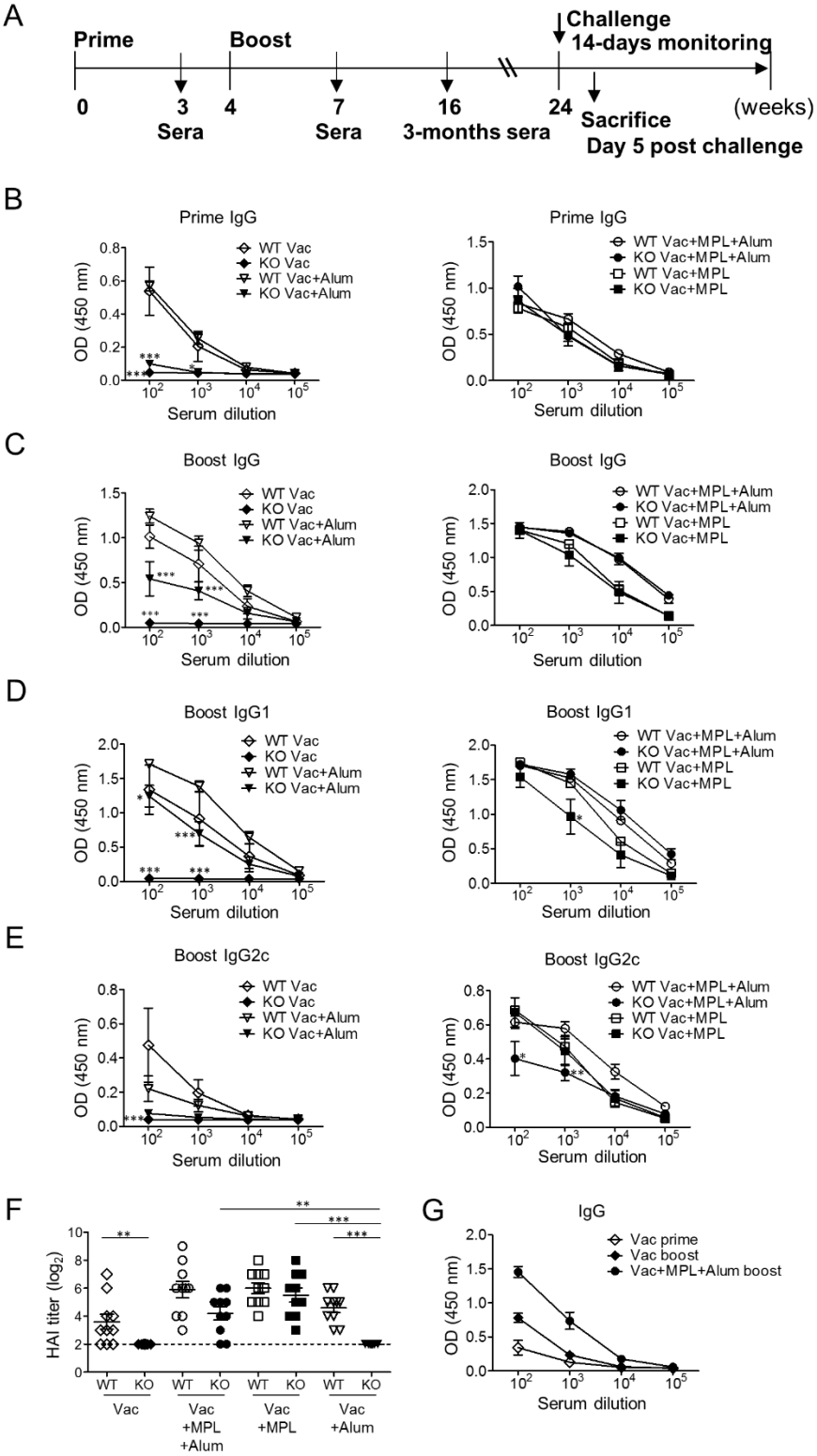
A
Prime
Boost
Challenge
14-days monitoring
0
3
Sera
4
7
Sera
16
3-months sera
24
Sacrifice
Day 5 post challenge
(weeks)
B
Prime IgG
WT Vac
KO Vac
WT Vac+Alum
KO Vac+Alum
WT Vac+MPL+Alum
KO Vac+MPL+Alum
WT Vac+MPL
KO Vac+MPL
OD (450 nm)
Serum dilution
C
Boost IgG
D
Boost IgG1
E
Boost IgG2c
F
HAI titer (log2)
WT
KO
Vac
Vac +MPL +Alum
Vac +MPL
Vac +Alum
G
IgG
Vac prime
Vac boost
Vac+MPL+Alum boost

Figure 4.1 MPL+Alum-adjuvanted vaccination induces isotype-switched IgG antibodies regardless of $CD4^+$ T cells.

(**A**) A schematic diagram of vaccination schedule and assessment of protective efficacy. WT: C57BL/6 wild type mice, KO: CD4 knockout mice, Vac; Inactivated influenza virus split vaccine (Vac) only immunized group, Vac+Alum; influenza split vaccine + aluminum hydroxide (Alum) immunized group, Vac+MPL; influenza split vaccine + MPL immunized group, Vac+MPL+Alum; influenza split vaccine + MPL + Alum immunized group. (**B**) Prime IgG antibody levels of immunized WT and CD4KO mice. (**C**) Boost IgG antibody levels of immunized WT and CD4KO mice. (**D**) Boost IgG1 isotype antibody levels of immunized WT and CD4KO mice. (**E**) Boost IgG2c isotype antibody levels of WT and CD4KO mice. Immune sera were collected 3 weeks after prime and boost immunization from WT and CD4KO mice (n=10 per group). Inactivated virus specific-IgG antibody levels were determined by ELISA and shown as mean ± SEM of optical density (OD). Statistical significances were calculated by 2-way ANOVA and Bonferroni post-tests. *; $p<0.05$, **; $p<0.01$, and ***; $p<0.001$ compared between each corresponding WT and CD4KO groups. (**F**) Hemagglutination inhibition (HAI) titers were determined from immune sera of vaccine ± MPL+Alum, MPL or Alum adjuvant immunized WT and CD4KO mice. The detection limit of HAI titer was 2. Statistical significances were calculated by 1-way ANOVA and followed Tukey's multiple comparison tests. **; $p<0.01$ and ***; $p<0.001$ as indicated among the groups. (**G**) IgG antibody levels of WT mice. All mice were primed with vaccine only, and then vaccine-primed mice were boosted with vaccine only or vaccine+MPL+Alum. Statistical significances were calculated by 2-way ANOVA and Bonferroni post-tests. **; $p<0.01$, and ***; $p<0.001$ compared to Vac boost group.

Table 4.1 Kinetics of IgG levels (μg/ml) in the immunized mice.

Immune sera were collected and performed ELISA to determine antigen-specific IgG levels. Data were shown in mean concentration (μg/ml) ± SEM. Statistical analysis was performed by one-way ANOVA and Tukey's multiple comparison test. n.d.; not detected, **; $p<0.01$ and ***; $p<0.001$ compared to the corresponding C57BL/6 wild-type IgG levels of each time points. ##; $p<0.01$ and ###; $p<0.001$ compared to the corresponding CD4KO mice IgG levels of each time points.

		3 weeks after prime	3 weeks after boost	3 months after boost
C57BL/6 wild-type	Vac	3.11 ± 1.82	13.10 ± 3.94	12.55 ± 2.46
	Vac+MPL+Alum	12.26 ± 1.16	26.44 ± 0.55	20.46 ± 3.50
	Vac+MPL	10.44 ± 0.86	22.83 ± 1.19	21.61 ± 1.52
	Vac+Alum	4.06 ± 0.69	17.73 ± 1.55	17.89 ± 1.53
CD4KO	Vac	n.d.	n.d.	0.22 ± 0.09**
	Vac+MPL+Alum	8.85 ± 0.86	26.00 ± 1.15	28.88 ± 3.23
	Vac+MPL	8.76 ± 2.26	19.63 ± 3.09	24.70 ± 5.34
	Vac+Alum	n.d.	7.13 ± 1.96**	2.45 ± 0.96***
CD4-depleted C57BL/6 wild-type	Vac+MPL+Alum	0.40 ± 0.44***, ###	2.66 ± 1.15***, ###	-
	Vac+MPL	2.15 ± 1.31***, ##	6.83 ± 2.29***, ###	-
MHCIIKO	Vac+MPL+Alum	0.06 ± 0.06***, ###	0.82 ± 0.30***, ###	-
	Vac+MPL	n.d.	0.61 ± 0.17***, ###	-

4.2.2 MPL+Alum or MPL-adjuvanted vaccination of CD4KO mice induces protection against influenza virus.

To determine adjuvant effects on improving the efficacy of protection, naïve and immunized WT and CD4KO mice were intranasally challenged with a lethal dose of A/California/04/2009 (H1N1) virus after 5 months of vaccination (Fig. 4.2). Both CD4KO and WT naïve mice all died by day 8 and 10 post infection, respectively. The WT-Vac group showed severe weight loss of approximately 18% resulting in 60% of survival rates whereas the KO-Vac group did not show any protection similar to naïve infection mice (Fig. 4.2A, B). The WT-Alum group displayed moderate weight loss of 9-10% and 100% survival rates. In contrast, KO-Alum immune mice were very sick as indicated by 18% weight loss at a peak point and thus resulted in only 40% survival rates. Both the WT-MPL+Alum and WT-MPL groups showed 100% protection without weight loss (Fig. 4.2A). Also, KO-MPL+Alum and KO-MPL mice were similarly well protected against the same lethal dose challenge as used in WT mice, although a transient weight loss was observed in these KO mice at 6-9 days after challenge probably due to the lack of $CD4^+$ T cells (Fig. 4.2A, B).

At day 5 post challenge, lung viral titers were measured to determine the efficacy of clearing lung viral loads (Fig. 4.2C). The naïve, vaccine only and vaccine plus alum groups showed high levels of viral loads in WT and particularly in CD4KO mice, which are consistent with low or no HAI titers, severe weight loss, and low survival rates in these groups. MPL+Alum and MPL adjuvant in the vaccination led to low lung viral titers, and there were no statistical differences in between WT and CD4KO mice although the MPL+Alum group showed a trend of increasing viral titers in CD4KO mice.

To further determine the protective roles of immune sera from CD4KO mice, we infected naïve mice with a mixture of lethal dose of A/California/04/2009 (H1N1) virus and immune sera or naïve sera. All naïve mice that were infected with virus plus naïve or vaccine only sera died at day 8 or 9 post infection (Fig. 4.2D). The naïve mice infected with virus and Alum adjuvanted vaccination sera shows 10% of body weight loss, but naïve mice that received MPL+Alum or MPL adjuvanted immune sera did not show any weight loss (Fig. 4.2D). Overall, these results provide evidence that MPL+Alum or MPL adjuvanted vaccination induces protective immunity against lethal infection in CD4KO mice at a comparable level observed in WT mice.

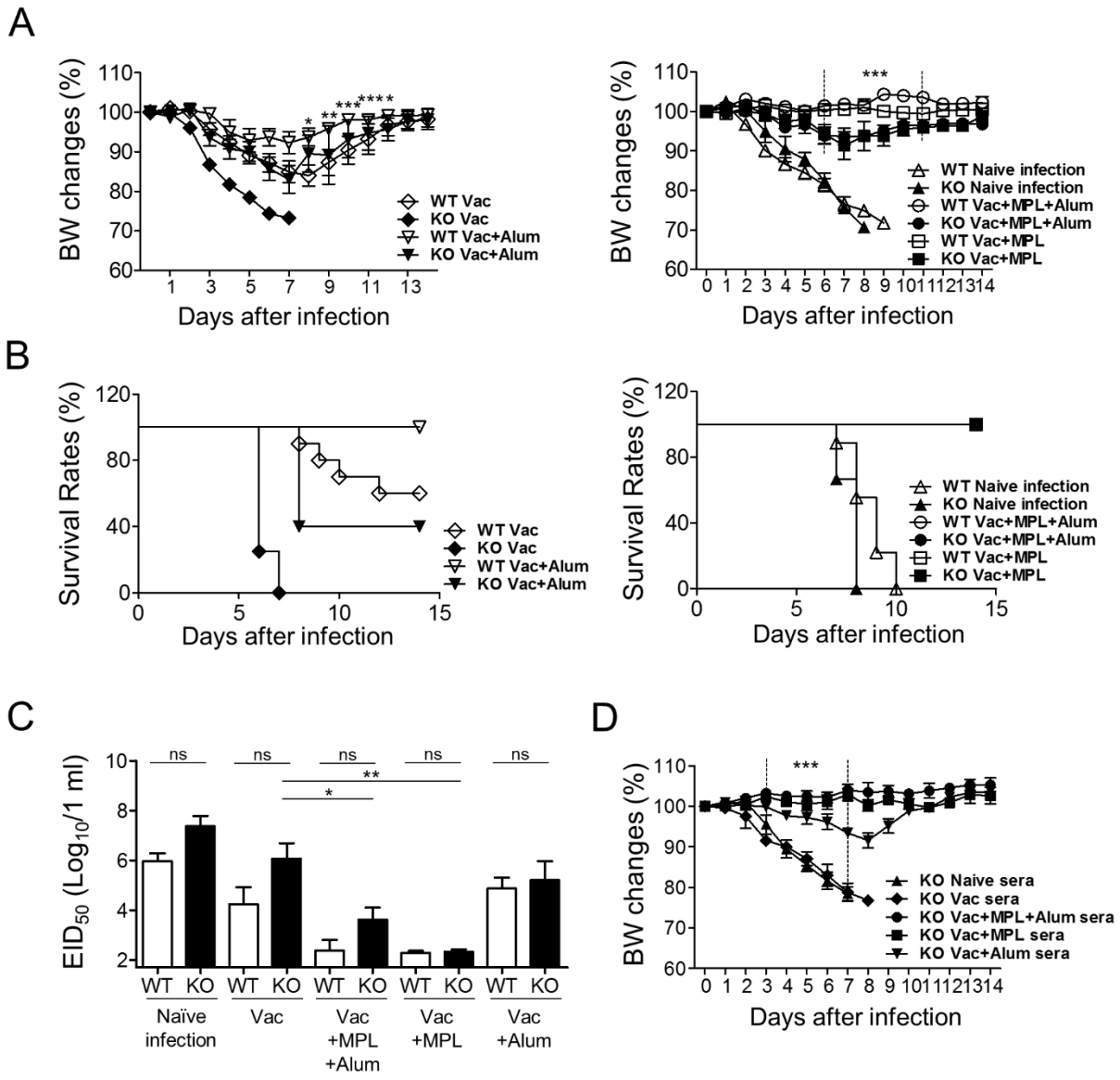

Figure 4.2 Protective efficacy of MPL+Alum or MPL-adjuvanted split vaccination against influenza virus in WT and CD4KO mice.

(A) Body weight changes. (B) Survival rates. Immune mice (n=10 per group) were challenged with a lethal dose of A/California/04/2009 virus 5 months after boost immunization. Statistical significances were calculated by 2-way ANOVA and followed by Bonferroni post-tests. *; $p<0.05$, **; $p<0.01$, and ***; $p<0.001$ compared to corresponding KO groups. (C) Lung virus titers. Lung viral titers were determined at day 5 post infection by an egg infection dose 50% (EID50). Data (n=10) were shown as mean ± SEM. The detection limit of EID50 was 1.7. (D) Protective roles of immune sera. Naïve and immune sera were incubated at 56ºC for 30 minutes for complement inactivation and mixed with a lethal dose of A/California/04/2009 (H1N1) virus. After 30 minutes, the mixture of sera (25 µl containing a range of 0– 24 HAI titers) and virus was used to infect naïve WT mice (n=5) intranasally. Body weight changes of the infected mice were daily monitored for 14 days. Statistical significances were calculated by 1-way ANOVA and followed Tukey's multiple comparison tests or by 2-way ANOVA and followed Bonferroni post-tests. *; $p<0.05$, **; $p<0.01$, and ***; $p<0.001$ compared to vaccine only group or as indicated among the groups. ns; not significant.

4.2.3 MPL+Alum adjuvanted influenza vaccination prevents lung disease due to viral infection of CD4KO mice

Influenza virus can cause severe lung inflammation leading to pneumonia and high mortality. To better assess the protective effects of adjuvant vaccination on alleviating disease symptoms, blood oxygen saturation (SpO_2) levels were measured in live animals at day 4 post influenza virus infection by using oximetry (Fig. 4.3A). In both WT and CD4KO mice, the naïve infection and vaccine only groups exhibited significantly lower SpO_2 levels of approximately 90% (Fig. 4.3A) compared to uninfected control mice. Low SpO_2 levels would indicate severe breath disorder caused by blocking the airways due to respiratory virus infection. In contrast, MPL+Alum adjuvanted vaccination resulted in maintaining normal SpO_2 levels over 98% in both WT and CD4KO mice.

Upon lethal influenza virus challenge, highest levels of inflammatory IL-6 and TNF-α cytokines were observed in WT-naïve mice (Fig. 4.3B, C). Also, substantially high levels of IL-6 and TNF-α were detected in BALF from WT-naïve, KO-naïve, WT-Vac, KO-Vac, and KO-Alum mice at day 5 post challenge. In contrast, IL-6 and TNF-α cytokines were undetected or detected at low levels in BALF of WT-MPL+Alum and KO-MPL+Alum mice (Fig. 4.3B, C). KO-MPL mice displayed IL-6 and TNF-α cytokines in BALF at moderate levels (Fig. 4.3B, C). Thus, these results suggest that MPL+Alum adjuvanted vaccination prevents the induction of pro-inflammatory cytokines even in CD4KO mice.

As for further evidence of lung inflammation, examination of lung histology showed that severe immune cell infiltration around the airways, alveolar septa, and interstitial spaces as well as narrowing or collapsing the airways were observed in WT and CD4KO naïve mice at day 5 after infection (Fig. 4.3D), which are consistent with low SpO_2 levels. Significant lung

histopathology was displayed in the WT-Vac, KO-Vac, and KO-Alum groups (Fig. 4.3D). Low to moderate histopathology including the thickening in the airway endothelial layers was revealed in the WT-Alum, WT-MPL, and KO-MPL groups (Fig. 4.3D). Both WT- MPL+Alum and KO-MPL+Alum mice did not exhibit an overt sign of lung histopathology, indicating protection from lung inflammation due to influenza viral infection (Fig. 4.3D).

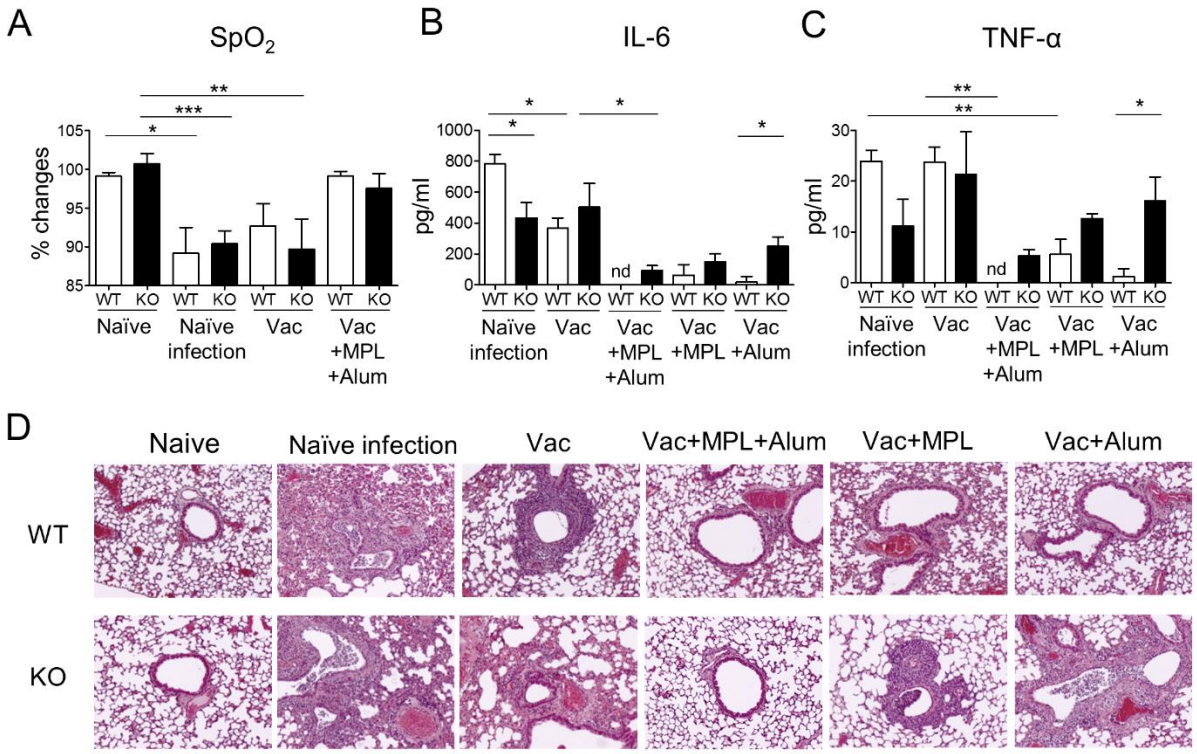

Figure 4.3 MPL+Alum-adjuvanted vaccination of CD4KO mice prevents lung inflammation after virus challenge.

Immune mice (n=10 per group) were challenged with a lethal dose of A/California/04/2009 virus. (**A**) At day 0 and 4 post virus infection, the SpO_2 values were measured by using oximetry. The changes of day 4 compared to those of day 0 were shown as percentages. (**B** and **C**) BALF samples were collected (n=5 mice per group) at 5 days after lethal dose of A/California/04/2009 H1N1 influenza virus infection and used to determine cytokine IL-6 (**B**) and TNF-α (**C**) levels. (**D**) Lung histopathology. Lung tissues from the infected mice (n=5 mice per group) at day 5 post challenge were stained with hematoxylin and eosin. WT: C57BL/6 wild type mice, KO: CD4 knockout mice. Statistical significance were calculated by 1-way ANOVA and Tukey's multiple comparison test. *; $p<0.05$, **; $p<0.01$ and **; $p<0.001$ as indicated among the groups. nd; not detected.

4.2.4 MPL+Alum adjuvanted influenza vaccination induces antibody secreting cell responses in WT and CD4KO mice.

A goal of vaccination is to induce long-lived antibody secreting cell (ASC) responses. Vaccinated mice were challenged after 5 months of vaccination, and then BM and spleen cells harvested at day 5 post challenge for analysis of IgG antibodies secreted from ASCs in *in vitro* culture supernatants using ELISA (Fig. 4.4) as described [89]. WT-Vac and WT-Alum mice showed only low levels of vaccine-specific IgG antibody production in BM cell cultures (Fig. 4.4A). BM cells from WT-MPL mice showed moderate levels of *in vitro* IgG antibody secretion whereas WT-MPL+Alum immune mouse BM cells produced significantly higher levels of IgG antibodies after 1 day *in vitro* culture (Fig. 4.4A). As a measure of memory B cells, spleen cells were cultured for 5 days in the presence of inactivated virus (A/California/04/2009 H1N1). Spleen cells from WT-Alum mice produced low levels of IgG antibodies. In contrast, WT-MPL+Alum groups of mice induced high levels of IgG antibody production in spleen cells (Fig. 4.4B).

$CD4^+$ T cells are required to induce long-lived isotype switched IgG ASCs in BM after viral infection [71, 90]. We determined whether certain adjuvants could mediate the *in vitro* production of IgG antibodies in BM and spleen cells from CD4KO mice after 5 months of vaccination at day 5 post challenge (Fig. 4.4). KO-Vac mice did not show *in vitro* IgG antibody production in BM and spleen cells. The KO-MPL+Alum and MPL groups showed high levels of *in vitro* IgG antibody production in BM cells, which are comparable to those in corresponding WT mice after 1 day *in vitro* culture (Fig. 4.4). MPL+Alum adjuvant was more effective in *in vitro* IgG protection in 5-day culture of CD4KO spleen cells compared to MPL. Consistent with *in vivo* IgG responses, MPL+Alum adjuvant may effectively mediate the generation of long-lived IgG antibody secreting cells in CD4KO mice comparable to those in WT mice.

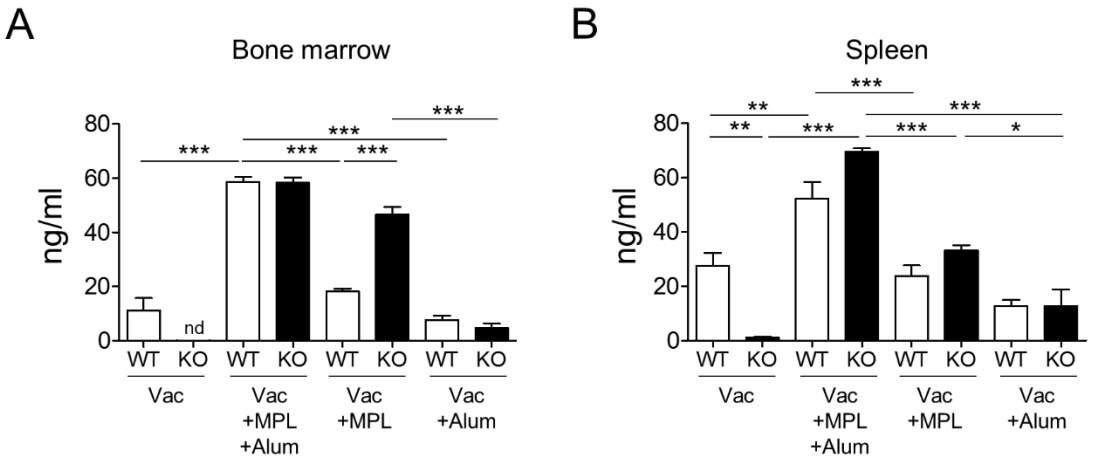

Figure 4.4 *In vitro* antibody secreting cell responses in BM and spleens.
(**A**) IgG production from bone marrow (BM) cells of immunized WT and CD4KO mice. (**B**) IgG production of spleen cells of immunized WT and CD4KO mice. BM and spleen cells were harvested day 5 post infection after 5 months of vaccination (n=5). BM cells of WT and CD4KO mice were cultured for 1 day, and spleen cells of WT mice and CD4KO mice were cultured for 5 days in presence of inactivated virus antigens. IgG levels were detected by ELISA. WT: C57BL/6 wild type mice, KO: CD4 knockout mice. Statistical significance were calculated by 1-way ANOVA and Tukey's multiple comparison test. *; $p<0.05$, **; $p<0.01$ and ***; $p<0.001$ as indicated among the groups.

4.2.5 Adjuvant effects on IgG antibodies in CD4 depleted WT and MHC II KO mice support a role of MHCII-expressing cells in the alternative B cell help

CD4KO mice might have developed compensatory immune components contributing to the alternative B cell help. To test this possibility, $CD4^+$ T cells in WT mice were acutely depleted up to over 99% by CD4-depleting antibody treatment before and during adjuvanted prime and boost vaccination (Fig. 4.5A). Approximately 3 fold lower levels of IgG (mostly IgG1 isotype) antibody responses were induced in acute CD4-depleted WT mice with MPL-adjuvanted vaccination compared to those in CD4KO mice with the same adjuvanted vaccination (Fig. 4.5B, Table 4.1). Also, acute CD4-depleted WT mice with MPL adjuvanted vaccination displayed weight loss of approximately 8-12 % (Fig. 4.5C), which is lower than those in CD4KO mice (Fig. 4.2A). CD4-depleted WT mice with MPL+Alum adjuvanted vaccination showed 10 fold lower levels of IgG antibodies compared to those in CD4KO mice (Table 4.1). MHCII KO mice deficient

in CD4$^+$ T cells in addition to a genetic defect in MHCII expression [91, 92] were used for adjuvanted influenza vaccination. The levels of IgG antibodies in MHCIIKO mice with MPL or MPL+Alum adjuvanted influenza vaccination were significantly lower by 32 folds compared to those in CD4KO mice (Table 4.1). These experimental data suggest that compensatory immune components particularly MHCII-expressing antigen presenting cells developed in CD4KO mice contribute to the generation of isotype-switched IgG antibodies, probably by providing an alternative form of T cell help.

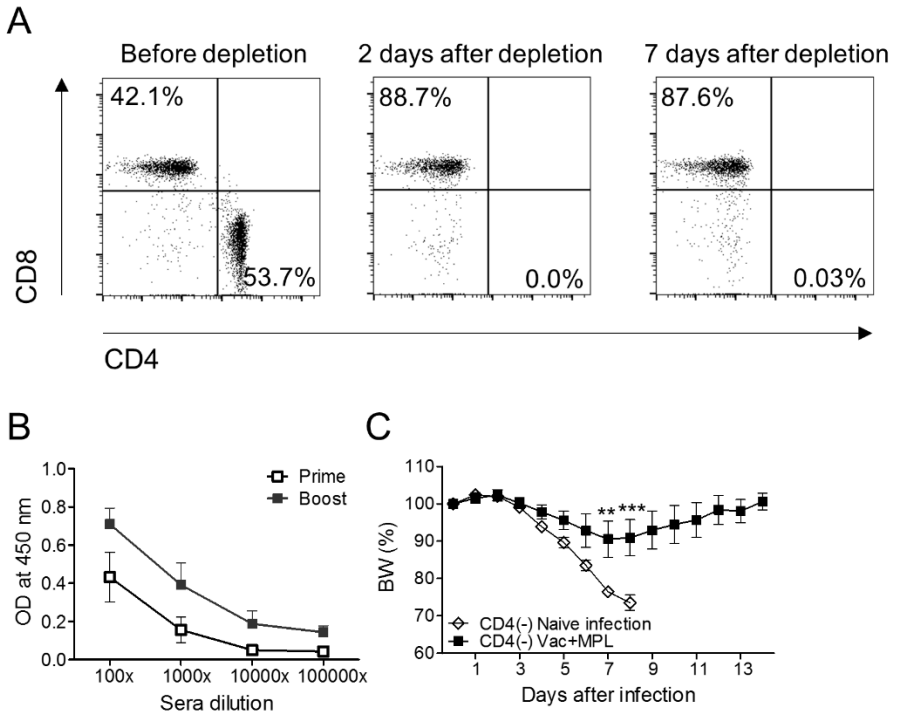

Figure 4.5 Antibody production and protective efficacy of MPL-adjuvanted vaccination against influenza virus in CD4-depleted C57BL/6 WT mice.

(**A**) C57BL/6 wild-type mice were injected with anti-CD4 monoclonal antibody (200 µg/mouse, clone: GK1.5) to deplete CD4$^+$ T cells. Blood cells from CD4-depleting antibody treated mice were used to determine the efficacy of CD4-depletion. CD4 and CD8 marker profiles are shown from CD3$^+$-gated T cells. (**B**) Virus-specific antibody levels of immunized CD4-depleted mice after prime and boost immunization. CD4-depleted WT mice were immunized intramuscularly with vaccine plus MPL. To maintain CD4 depletion status, the mice were injected CD4-depleting antibodies every 7 days. Immune sera (n=5 per group) were collected 2 weeks after each immunization. Inactivated virus-specific antibody levels were determined by ELISA and shown as mean ± SEM of optical density (OD). (**C**) Body weight changes of the CD4-depleted mice after lethal virus infection. Naïve and the immunized CD4-depleted mice were challenged with a lethal dose of A/California/07/2009 (H1N1) virus intranasally. Body weight changes of the infected mice were daily monitored for 14 days. Statistical significances were calculated by 2-way ANOVA and followed Bonferroni post-tests. **; $p<0.01$, and ***; $p<0.001$ compared to naïve infection group.

4.2.6 MPL+Alum attenuates MPL-induced serum inflammatory cytokines and chemokine in WT mice

To determine adjuvant effects on innate responses in CD4KO mice, we injected adjuvants (MPL+Alum, MPL, Alum) intraperitoneally (IP) to WT and CD4KO mice. Sera were taken at 1.5, 6 and 24 hours (h) after the injection and then the mice were sacrificed to collect peritoneal exudates. Cytokines and chemokines in peritoneal exudates and sera were determined by ELISA. MPL injection of WT mice acutely induced extreme high levels of pro-inflammatory cytokines (IL-6, TNF-α) and MCP-1 chemokine within 1.5 h systemically in blood, which were rapidly reduced within 6 h (Fig. 4.6A). In contrast, MPL+Alum did not acutely raise inflammatory cytokines and MCP-1 chemokine but induced a low level of TNF-α and MCP-1 at 6 h post-injection in sera of WT mice (Fig. 4.6A). Alum injection did not induce cytokines or chemokines. Therefore, these results suggest that Alum in the combination MPL+Alum adjuvant plays a role of attenuating acute inflammation due to MPL injection in WT mice.

A different pattern was observed after adjuvant injection in CD4KO mice (Fig. 4.6B). Serum IL-6 and TNF-α cytokines were induced to a moderate and low level respectively at 1.5 h and then lowered to a basal level within 6 h after MPL+Alum or MPL injection of CD4KO mice (Fig. 4.6B). MPL or MPL+Alum injection induced a high level of serum MCP-1 in CD4KO mice. These results indicate that MPL+Alum may have an effect on acutely inducing cytokines and MCP-1 chemokine in CD4KO mice, which is different from WT mice.

In contrast to acute cytokine levels in bloods, we observed a different profile of cytokines and chemokines at the injection site after 24 h (Fig. 4.6C). MPL injection of WT or CD4KO mice induced low levels of chemokines (MCP-1, RANTES) in the peritoneal cavity after 24 h (Fig. 4.6C). Interestingly, MPL+Alum injection of CD4KO mice induced moderate levels of IL-6, TNF-

α, MCP-1, and RANTES in the peritoneal cavity after 24 h, which are higher than those in MPL+Alum IP injection of WT mice (Fig. 4.6C).

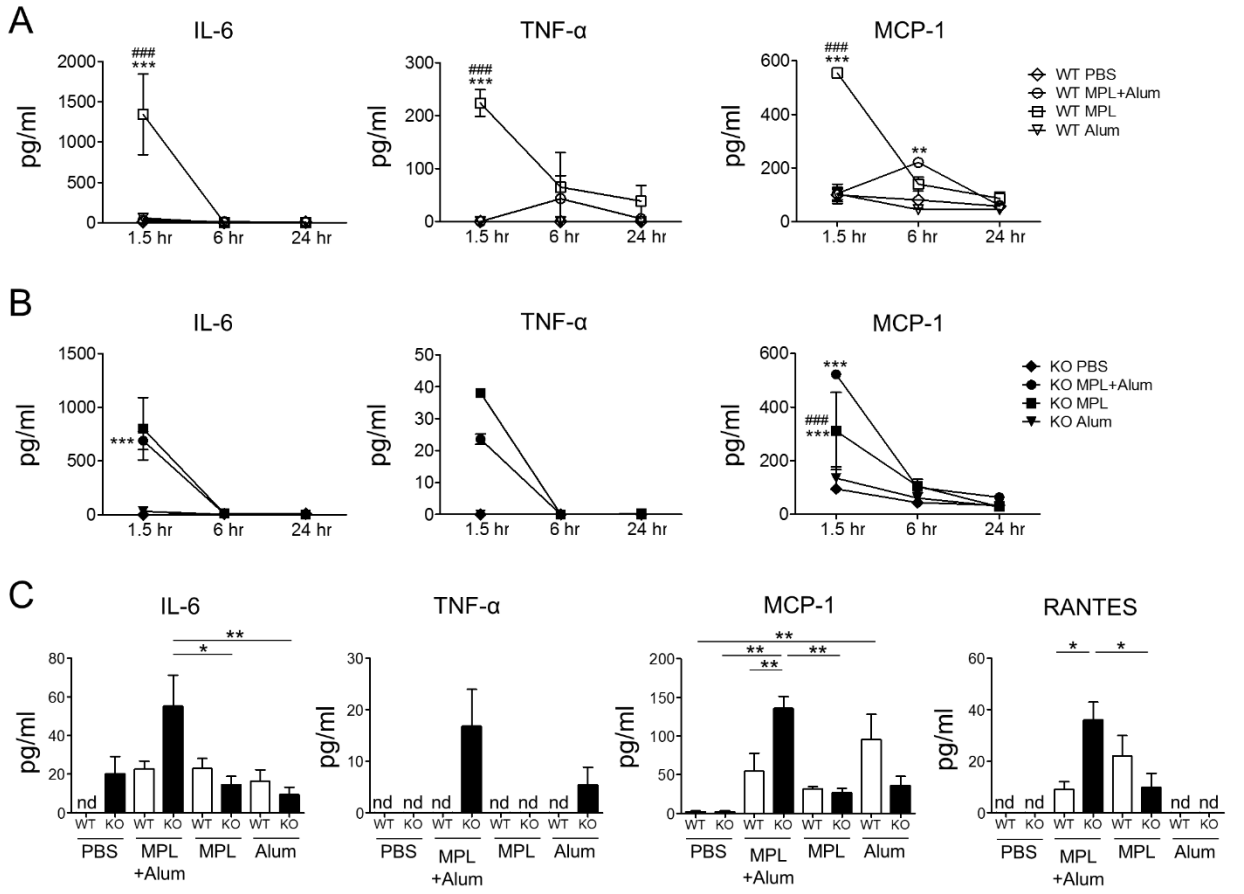

Figure 4.6 Levels of cytokines and chemokines in bloods and peritoneal exudates after injection of adjuvants. WT and CD4KO mice (n=5) were intraperitoneally injected with 200 μl of PBS, MPL+Alum, MPL, or alum. Kinetics of cytokines and chemokine levels in sera from adjuvant injected WT (**A**) and CD4KO (**B**) mice. Statistical significances were calculated by 2-way ANOVA and Bonferroni post-tests. ***; $p<0.001$ compared to PBS-treated group and ###; $p<0.001$ compared to MPL+Alum-treated group. (**C**) Cytokines and chemokines in peritoneal exudates at 24 hours after peritoneal adjuvant injection. Statistical significances were calculated by 1-way ANOVA and Tukey's multiple comparison test. *; $p<0.05$, **; $p<0.01$, and ***; $p<0.001$ as indicated among the groups. WT: C57BL/6 wild type mice, KO: CD4 knockout mice. nd; not detected.

4.2.7 MPL+Alum recruits a distinct pattern of innate immune cells at the injection site in CD4KO mice

Immune cell types and cellularity at the injection site might provide insight into mechanisms of adjuvant effects in CD4KO mice. We analyzed cell types recruited in the peritoneal cavity at 24 h after IP injection of mice with adjuvants. Naïve WT mice maintain high cellularity of macrophages in the peritoneal cavity (Fig. 4.7A, B). Interestingly, alum injection of WT mice resulted in almost complete depletion of macrophages (Fig. 4.7A, B), and lower cellularity of plasmacytoid DCs (pDCs, 17%, Fig. 4.7I) and $CD11b^{low}$ DCs (8%, Fig. 4.7H) in the peritoneal cavity whereas CD4KO Alum maintained $CD11b^{low/high}$ DC populations compared to PBS controls (Fig. 4.7G, H). In contrast, WT MPL+Alum mice low levels (20-30%) of macrophages ($CD11b^{+}F4/80^{+}$, $CD11b^{+}F4/80^{+}MHCII^{hi}$, Fig. 4.7A, B), pDCs (11%, Fig. 4.7I) and $CD11b^{low}$ DCs (10%, Fig. 4.7H) in the peritoneal cavity compared to those of PBS mock control mice (Fig. 4.7A, B, G-I). Different from a profile in WT mice, MPL+Alum injection of CD4KO mice maintained the cellularity of macrophages (100%, Fig. 4.7A, B) and resulted in increasing $CD11b^{low}$ DCs and $CD11b^{high}$ DCs (Fig. 4.7G, H). In addition, CD4KO MPL+Alum mice displayed significantly increased recruitment of neutrophils, monocytes, and NK cells by 76-, 23-, and 5-fold (Fig. 4.7D, C, F), respectively, which is a similar profile observed in WT-MPL+Alum mice. WT MPL and CD4KO MPL mice showed a similar pattern of cellular changes in macrophages (reduced to 25%, Fig. 4.7A, B), monocytes (4 fold up, Fig. 4.6C), neutrophils (8 fold up, Fig. .7D), NK cells (4 fold up, Fig. 4.7F). Uniquely, CD4KO MPL mice showed 2- to 4-fold increased levels of $CD11b^{high}$ DCs, $CD11b^{low}$ DCs, and pDCs compared to those in WT-MPL mice (Fig. 4.7G, H, I). KO-Alum mice recruited the highest level of eosinophils (4 folds) while reducing the levels of macrophages (<10%) and pDCs (<25%) in the peritoneal cavity compared to KO-PBS control mice (Fig. 4.7A,

B, I). In addition, CD4KO mice showed higher cellularity of double negative (DN) T cell ($CD3^{+}CD4^{-}CD8^{-}$) population and MPL injection in both WT and CD4KO mice increased the DN T cells (2 folds compared to the PBS groups) at the site of injection (Fig. 4.7J).

Overall, MPL+Alum KO mice maintained approximately 4- to 6-fold higher levels of $MHCII^{high}$ macrophages and $CD11b^{high/low}$ DC populations compared to those in MPL+Alum WT mice. Also, 2- to 4-fold higher levels of $CD11b^{high/low}$ DC and DN T cell populations were observed in KO MPL mice than WT-MPL mice. These results suggest that differential cellularity of macrophages and DC populations together with DN T cells might be at least partially contributing to alternative B cell help in CD4KO mice.

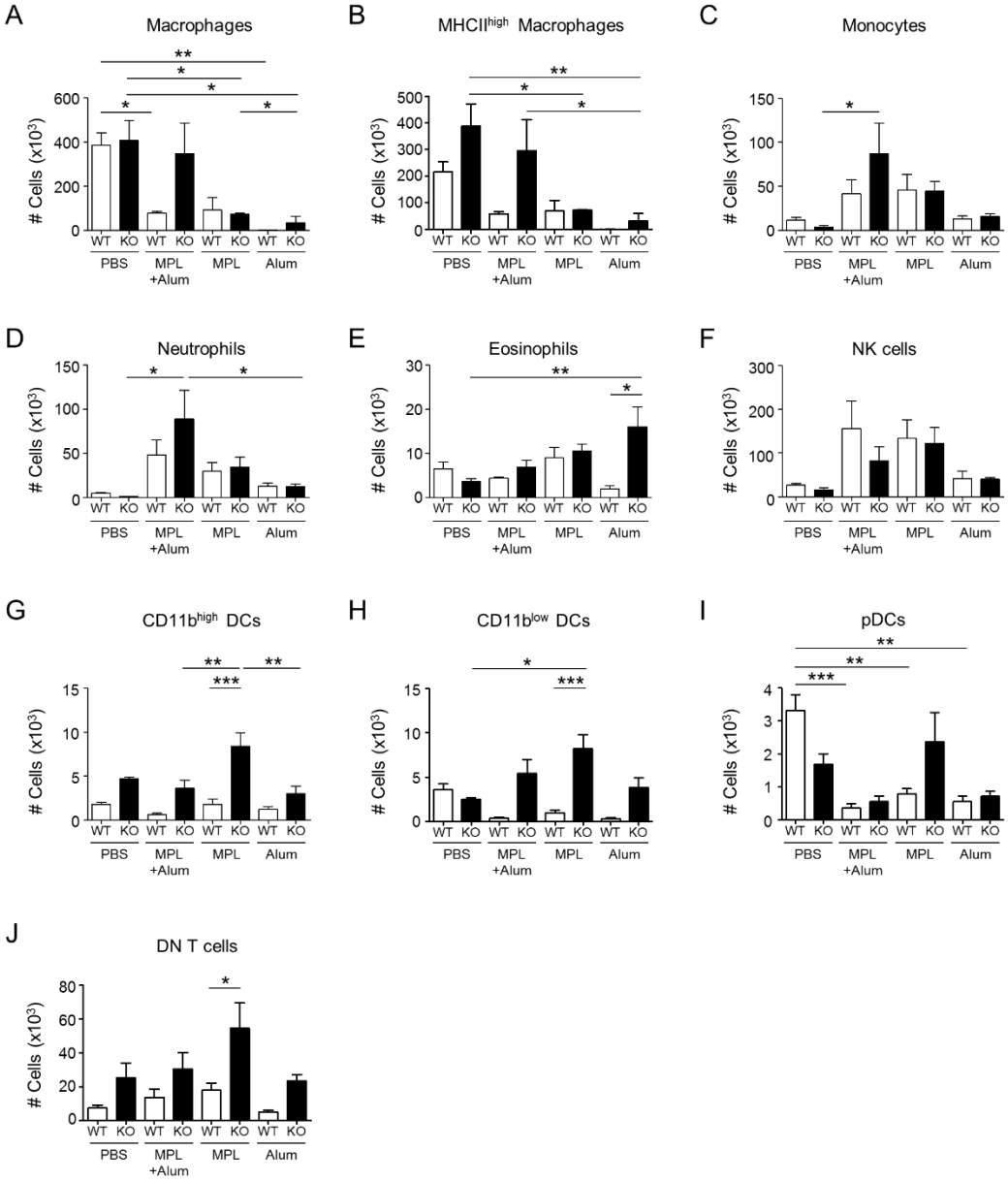

Figure 4.7 Recruitment of multiple immune cell phenotypes after adjuvant injection.
(**A**-**J**) Cellularity of different phenotypic cells in peritoneal exudates from WT and CD4KO mice (n=5). Cells in peritoneal exudates were collected at 24 h after adjuvant injection and their phenotypes and cellularity determined. (**A**) Macrophages; $CD11b^{+}F4/80^{+}$ (**B**) $MHCII^{high}$ macrophages; $CD11b^{+}F4/80^{+}MHCII^{high}$ (**C**) Monocytes: $CD11b^{+}Ly6c^{high}F4/80^{+}$ (**D**) Neutrophils; $CD11b^{+}Ly6c^{+}F4/80^{-}$ (**E**) Eosinophils; $CD11b^{+}SiglecF^{+}$ (**F**) $CD11b^{high}$ DCs; $CD11c^{+}CD11b^{high}MHCII^{high}$ (**G**) $CD11b^{low}$ DCs; $CD11c^{+}CD11b^{low}MHCII^{high}$ (**H**) pDCs; $CD11c^{+}B220^{+}MHCII^{high}$ (**I**) NK cells; $CD49b^{+}CD3^{-}$ (**J**) Double-negative (DN) T cells; $CD3^{+}CD4^{-}CD8^{-}$. All data were shown as mean ± SEM. Statistical significances were calculated by 1-way ANOVA and Tukey's multiple comparison test. *; $p<0.05$, **; $p<0.01$, and ***; $p<0.001$ as indicated among the groups.

4.2.8 MPL+Alum adjuvant combination attenuates the in vitro dendritic cell stimulatory effects by MPL

DCs are important cells to link between innate and adaptive immune responses. After 2 days cultures of DCs in the presence of adjuvants, cytokine levels in culture supernatants and activation marker expression on BMDCs were measured (Fig. 4.8A, B). MPL+Alum and MPL induced pro-inflammatory cytokine production by DCs, but Alum-treated DCs did not produce cytokines (Fig. 4.8A). MPL+Alum showed high levels of IL-6 and TNF-α but displayed a lower IL-12 cytokine level compared to MPL alone adjuvant. In terms of DC activation markers, MPL showed significantly higher levels of CD40, CD80 and CD86 expression than MPL+Alum on DCs (Fig. 4.8B). All adjuvants, MPL+Alum, MPL and Alum, increased $MHCII^{high}$ DC populations. These data indicate that Alum in MPL+Alum combination appears to attenuate stimulatory effects on DCs by MPL, a major player in *in vitro* activation of DCs.

To gain better understanding of *in vivo* adjuvant effects on reducing the cellularity of macrophages and DCs, we further tested *in vitro* cell death. Alum and MPL+Alum adjuvants were found to induce significant loss in cell viability after *in vitro* cultures of BM-derived primary cells (Fig. 4.8C).

To investigate further possible mechanism of MPL+Alum adjuvant combination, *in vitro* IgG production by B cells and proliferation of DN T cells cultured with or without adjuvant pre-treated BMDCs (Fig. 4.8D, E). MPL+Alum pre-treated BMDCs could support splenic B cells for IgG production *in vitro*, but adjuvant only could not (Fig. 4. 8D). In addition, DN T cell proliferation was stimulated by co-culture with MPL+Alum pre-treated BMDCs, and MHCII monoclonal antibody treatment could suppress its proliferation effects (Fig. 4.8E). In addition, to determine cognate or non-cognate help, we determined proliferation of DN T cells after incubation

with MHCII^{+} BMDCs stimulated with vaccine and non-vaccine antigens (Fig. 4.8F). Vaccine-treated BMDCs significantly increased the proliferation of DN T cells, but a different virus (A/Philippine H3N2) or ovalbumin-treated BMDCs did not (Fig. 4.8F). These results provide evidence that MHCII positive antigen presenting cells contribute to stimulating DN T cells and providing alternative B cell help in a genetically CD4 deficient condition.

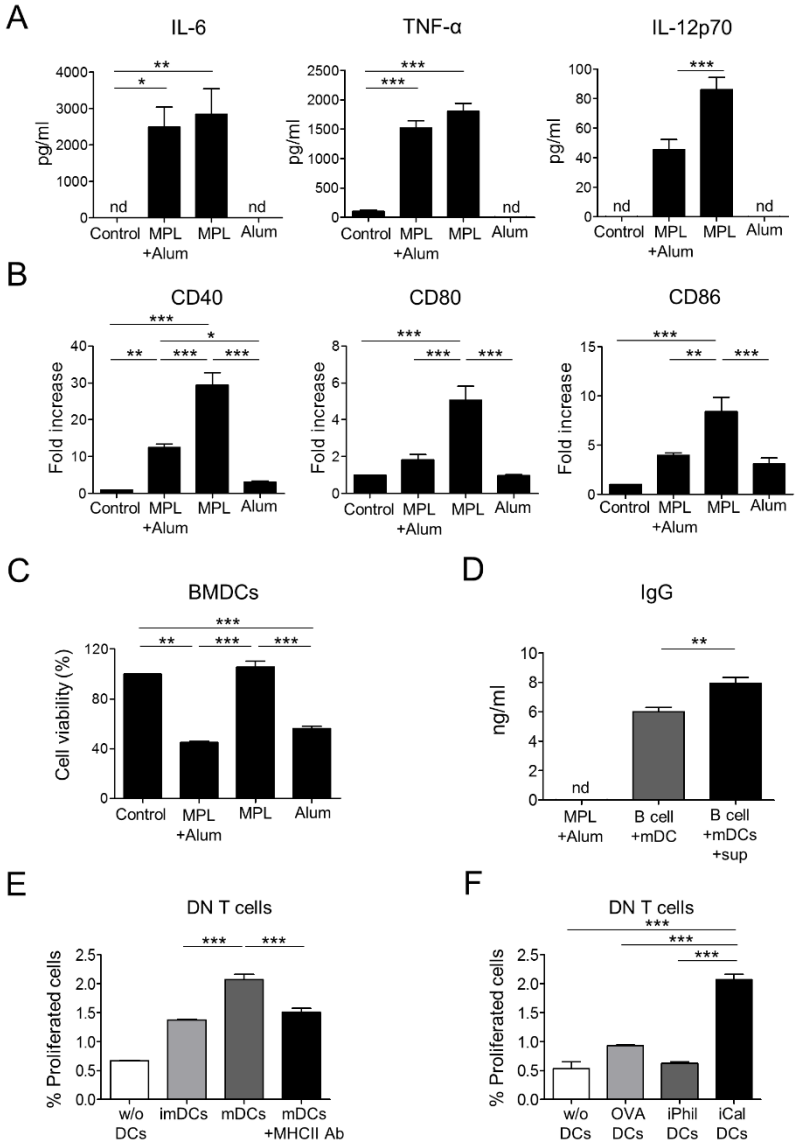

Figure 4.8 *In vitro* effects of adjuvants on DC activation or cell death.
(**A**) Pro-inflammatory cytokine production of BMDCs after adjuvant treatment. (**B**) Activation marker expression on adjuvant-treated BMDCs. Fold increase of marker expression were determined by mean fluorescence index of each groups compared to that of control group. BMDCs were generated from BM cells of WT mice. BMDCs were cultured with media (control), or adjuvants for 48 h. (**C**) Cell viability of BM derived DCs (BMDCs) treated with MPL+Alum, MPL or alum. Cell viability was determined by an MTT assay after 2 days culture with adjuvants. (**D**) *In vitro* antibody production by adjuvant-treated BMDCs. Spleen cells containing naïve B cells were harvested from naïve CD4KO mice and cultured with MPL+Alum, MPL+Alum pre-treated mature DCs (mDC), or mDC plus mDC culture supernatants (sup, a source of cytokines). The mDCs were prepared by pre-treating with adjuvants for 2 days. After 7 days' culture, total IgG levels in culture supernatants were determined by ELISA. (**E**) Percentages of proliferated double negative (DN, $CD4^-CD8^-$ in $CD3^+$ T cells) T cells after 5 days co-culture with or without BMDCs. w/o DCs; CD4KO mouse splenocytes containing DN T cells were cultured without BMDCs and proliferation of CFSE-labeled DN T cells was analyzed by flow cytometry. imDCs; DN T cells cultured with untreated control BMDCs. mDCs; DN T cells cultured with MPL+Alum pre-treated BMDCs. mDCs+MHCII Ab; DN T cells cultured with MPL+Alum and anti-mouse MHCII (clone M5/114.15.2) antibody (1 μg/ml) pre-treated BMDCs. (**F**) Percentages of proliferated double negative (DN, $CD4^-CD8^-$ in $CD3^+$ T cells) T cells after 5 days co-culture with different antigen-treated BMDCs. w/o DCs; CD4KO mouse splenocytes containing DN T cells were cultured without BMDCs. OVA DCs; DN T cells were cultured with ovalbumin pre-treated BMDCs. iPhil DCs; DN T cells were cultured with inactivated A/Philippine H3N2 virus pre-treated BMDCs. iCal DCs; DN T cells were cultured with inactivated A/California H1N1 virus vaccine strain pre-treated BMDCs. All data were shown as mean ± SEM. Statistical significance were calculated by 1-way ANOVA and Tukey's multiple comparison test. *; $p<0.05$, **; $p<0.01$ and ***; $p<0.001$ as indicated among the groups. nd; not detected.

4.3 Discussion

Subunit vaccines provide a safe alternative to live-attenuated virus vaccines but have poor immunogenicity, requiring effective adjuvants to enhance the vaccine efficacy. Immune-competent mouse models are often highly responsive to experimental vaccines and adjuvants; however, may not represent the efficacy expected in humans [93, 94]. It is also believed that adjuvant effects are mediated by specific types of activated $CD4^+$ T cells that would be educated via MHC II-expressing APCs through multiple innate immune cellular interactions and the production of inflammatory cytokines resulting from adjuvant stimulation [28, 95, 96, 97]. That is, vaccine adjuvants are important for modulating the types of $CD4^+$ T cells to induce the observed outcomes of adaptive immune responses in a conventional model. In contrast, the data in this study provide evidence that MPL+Alum adjuvant combination can mediate the induction of isotype-switched IgG antibodies conferring protective immunity in CD4KO mice comparable to those in WT mice even after 5 months of vaccination. Therefore, this study suggests an alternative pathway and/or cells in providing help to the B cells for IgG production in CD4KO mice in the context of MPL+Alum and MPL adjuvanted influenza vaccination.

Alum adjuvants were unable to induce IgG antibodies against split vaccine in CD4KO mice after prime. IgG1 antibodies after boost immunization of CD4KO mice with Alum were progressively waned to a further lower level after 3 months (Table 4.1). In contrast to Alum, MPL+Alum and MPL adjuvant effects were potent in WT and CD4KO mice even with prime only. The major difference between Alum and MPL+Alum is the induction of inflammatory cytokines, which was evident *in vitro* and *in vivo*. As expected, the results revealed that MPL or MPL+Alum activated BMDCs secrete IL-6 and TNF-α inflammatory cytokines, whereas Alum by itself did not. MPL+Alum did not directly stimulate $CD4^+$ T or B cells *in vitro* but was shown to directly

activate DCs *in vitro* primarily due to MPL, leading to the induction of antigen-specific T cells *in vivo* [98]. Therefore, micro-environment creating inflammatory cytokines by MPL+Alum and MPL is likely to play a major role in priming IgG isotype-switched B cell response in CD4KO mice. Previous studies demonstrated that mice lacking CD40 or $CD4^+$ T cells during sub-lethal primary infection induced only short-lived IgG antibodies waning within 60 days and no antibody-secreting plasma cells [71, 90]. Therefore, the results of long-lived IgG antibody responses mediated by MPL+Alum and MPL adjuvant in CD4KO mice are particularly notable.

The mechanisms of adjuvant effects on enhancing vaccine efficacy remain poorly understood, particularly in a CD4 deficient condition, although CD4-independent activation of $CD8^+$ T cells and B cells has been reported. Double negative αβ T cells were shown to play a role in generating CD4-independent isotype-switched IgG antibodies using CD4KO and T cell receptor β KO mouse models [41]. Another study demonstrated that both B7-1 (CD80) and B7-2 (CD86) costimulatory molecules on DCs were required for IgG1 and IgG2a responses [99]. TNF-α pathway was important for activating cytotoxic effector $CD8^+$ T cells in the absence of CD4 T cells [100]. This study provides evidence that a CD4 genetic defect led to developing other compensatory immune components even in a mock (PBS) treatment condition. PBS treatment of CD4 KO mice showed higher levels of MHCII ^{high} macrophages, $CD11b^{high}$ dendritic cells, DN T cells, and a lower level of pDCs compared to those in WT mice. Upon treatment with combination MPL+Alum adjuvant, CD4KO mice further increased cellularity of $MHCII^{high}$ macrophages, $CD11b^{high}$ and $CD11b^{low}$ dendritic cells (DCs) compared to those in WT mice in addition to comparable increases in monocytes, neutrophils, NK cells, and eosinophils. These cellular increases at the site of injection appeared to be correlated with high levels of cytokines (IL-6, TNF-α) and chemokines (MCP-1, RANTES) upon treatment of CD4KO mice with combination MPL+Alum adjuvant. Meanwhile,

MPL-treated CD4KO mice showed increased levels in DC populations ($CD11b^{high}$, $CD11b^{low}$ DCs, pDCs) and DN T cells compared to those in MPL-treated WT mice. We also observed further increased levels of DCs, but not macrophages compared to those in MPL+Alum treated CD4KO mice. Thus, it is possible that cellular components contributing to alternative B cell help in CD4KO mice are likely to be different between MPL (mostly various DC subsets, DN T cells) and combination MPL+Alum (mostly macrophages, minimally $CD11b^{low}$ DCs) adjuvants.

To gain further insight into possible roles of these compensatory immune components in providing alternative B cell help in CD4KO mice, we determined IgG responses in acutely CD4-depleted WT mice. We observed lower levels of IgG responses in CD4-depleted WT mice with MPL and MPL+Alum compared to those in CD4KO mice with the same adjuvanted vaccination. Lower protective efficacy was observed in CD4-depleted WT mice compared to that in CD4KO mice after MPL or MPL+Alum adjuvanted vaccination. Thus, it is possible that compensatory immune components including $MHCII^{high}$ macrophage and DC populations with DN T cells developed in CD4KO mice are partially contributing to overcoming defects in CD4 help to B cells for the generation of isotype-switched antibodies by MPL and combination MPL+Alum vaccination. In line with these results, MHCII KO mice with MPL+Alum adjuvant vaccination were found to induce lower levels of IgG responses by 32-fold than those in CD4 KO mice with same adjuvant vaccination (Table 4.1). In addition, MPL+Alum-activated BMDCs might have the capability to stimulate naïve splenic B cells to secrete IgG antibodies *in vitro*. Since efficient naïve $CD4^+$ T cell priming does not require B cells expressing MHCII [101], MHCII-expressing antigen presenting cells such as DCs and macrophages significantly contribute to the generation of isotype-switched IgG antibodies, probably via an alternative pathway different from conventional $CD4^+$ T cell help.

Adjuvant roles of Alum and MPL in MPL+Alum combination are yet to be fully understood. Differences in serum IgG antibody levels between MPL+Alum and MPL appeared to be greater at a later time point of 3 months boost in CD4KO mice (Table 4.1), which are further supported by antibody-secreting cell responses in spleens. Alum in AS04 (MPL+Alum) appeared to have a property of attenuating innate immune stimulating activities by MPL *in vitro* and *in vivo*. MPL was found to highly upregulate the expression of co-stimulatory molecules (CD40, CD80, and CD86) on BMDCs, which can provide an alternative B cell help to produce isotype switched antibodies [102]. Meanwhile, MPL+Alum appeared to moderately suppress the stimulatory effects of MPL on upregulating co-stimulatory molecules and IL-12 cytokine production during BMDC *in vitro* cultures. Attenuating acute induction of inflammatory cytokines would improve the safety for AS04 adjuvant formulated human vaccination.

Adjuvant-induced cell death has been known to be a mechanism of adjuvanticity for over a decade [103], although cell death is often considered an undesirable side effect. TNF family cytokines are classic inducers of programmed necrosis via receptor-interacting protein kinases, which promotes inflammation [104]. Alum was demonstrated to induce uric acid by causing sterile cell death [76]. Also, there is a well-known link between TLR-activation and cell death leading to pro-apoptotic activities [105]. We found that *in vitro* cultures of BMDCs with Alum or MPL+Alum resulted in cell death. In *in vivo* studies, WT mice with Alum, MPL+Alum, or MPL injection resulted in a significant loss of macrophages, $CD11b^{low}$ DCs, and pDCs in the peritoneal cavity. CD4KO mice with alum or MPL injection exhibited a significant loss in macrophages in the peritoneal cavity whereas MPL+Alum retained up to 80% of macrophages. Thus, MPL+Alum adjuvant combination might be contributing to protect macrophages from a severe cellular loss in

the *in vivo* injection site in WT mice compared to Alum, and more prominently in CD4KO mice compared to Alum and MPL.

5 CHAPTER 3. VIRUS-LIKE NANOPARTICLE AND DNA VACCINATION CONFERS PROTECTION AGAINST RESPIRATORY SYNCYTIAL VIRUS BY MODULATING INNATE AND ADAPTIVE IMMUNE CELLS

5.1 Summary

Respiratory syncytial virus (RSV) is an important human pathogen. Expression of virus structural proteins produces self-assembled virus-like nanoparticles (VLP). We investigated immune phenotypes after RSV challenge of immunized mice with VLP containing RSV F and G glycoproteins mixed with F-DNA (FdFG VLP). In contrast to formalin-inactivated RSV (FI-RSV) causing vaccination-associated eosinophilia, FdFG VLP immunization induced low bronchoalveolar cellularity, higher ratios of $CD11c^+$ versus $CD11b^+$ phenotypic cells and $CD8^+$ T versus $CD4^+$ T cells secreting interferon (IFN)-γ, T helper type-1 immune responses, and no sign of eosinophilia upon RSV challenge. Furthermore, RSV neutralizing activity, lung viral clearance, and histology results suggest that FdFG VLP can be comparable to live RSV in conferring protection against RSV and in preventing RSV disease. This study provides evidence that a combination of recombinant RSV VLP and plasmid DNA may have a potential anti-RSV prophylactic vaccine inducing balanced innate and adaptive immune responses.

5.2 Results

5.2.1 A combined VLP and DNA vaccine induces high IgG2a/IgG1 antibody ratios

Both F VLP and G VLP were shown to raise similar RSV neutralizing titers and control lung viral loads [63]. In addition, antibody responses specific for RSV G central domains were demonstrated to contribute to conferring protection and ameliorating RSV disease [106]. We found that FdFG VLP was more effective in inducing higher levels of IgG2a antibodies (Th1 type)

whereas F DNA alone was not highly immunogenic (Fig 5.1). Therefore, to further evaluate the protective immune responses and safety of FdFG VLP in comparison with FI-RSV and live RSV, mice were intramuscularly immunized with FdFGVLP, FI-RSV, or infected with live RSV (Fig. 5.2). At 3 weeks after prime and boost immunization, RSV specific serum antibodies were determined using FI-RSV as an ELISA coating antigen (Fig. 5.2A). Highest levels of IgG1 antibody were detected in the group of FI-RSV whereas FdFG VLP immunized mice showed lowest levels of IgG1 isotype antibody (Fig. 5.2A). The live RSV group showed a similar level of IgG1 and IgG2a antibodies specific for RSV after the 1^{st} infection, which was significantly increased after the 2^{nd} dose of infection (Fig. 5.2A, B). A higher level of IgG1 antibodies was induced in FI-RSV immunized mice compared to that in FdFG VLP immunized or live RSV infected mice (Fig. 5.2A, B). As a result, the FdFG VLP group showed the highest ratios of IgG2a/IgG1 in particular after prime immunization (Fig. 5.2B).

When ELISA was performed using the purified RSV F protein as a coating antigen, IgG1 antibodies were induced at higher levels by prime vaccination with FI-RSV than those by priming with FdFG VLP or infection with live RSV (Fig. 5.2C). In contrast, FdFG VLP immunization or live RSV infection induced higher levels of IgG2a antibodies specific for RSV F than those of IgG1. Consequently, higher ratios of IgG2a/IgG1 antibodies were induced in the FdFG VLP group, followed by live RSV infection (Fig. 5.2D).

FI-RSV immunization also induced significantly higher levels of RSV G protein specific IgG1 and IgG2a antibody responses than live RSV infection or FdFG VLP immunization after prime immunization (Fig. 5.2E). Because of low levels of IgG1 isotype antibodies, relatively higher ratios of IgG2a/IgG1 were observed in the FdFG group (Fig. 5.2F). The pattern and levels of antibody responses were maintained for over 6 months (data not shown). These results indicate

that FdFG VLP vaccine induces IgG2a antibodies predominantly recognizing the RSV F protein antigen. In line with high levels of IgG2a antibody responses, IFN-γ was secreted at higher levels by stimulation of whole splenocytes with live RSV, F or G VLP than the level of IFN-γ with FI-RSV (Fig. 5.3).

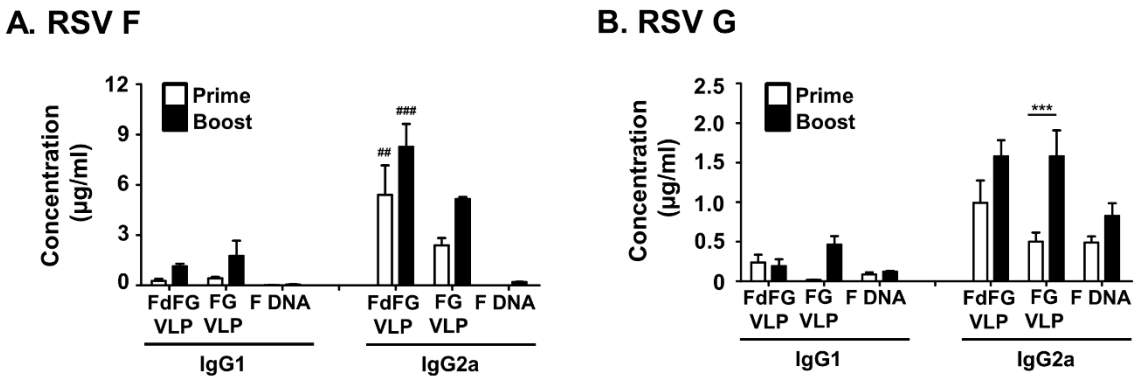

Figure 5.1 RSV-specific serum IgG isotype antibodies after individual vaccine components immunization. Serum samples were collected 3 weeks after prime and boost immunization from mice (n=15) that were immunized with F DNA+F VLP+G VLP RSV vaccine cocktail (50, 10, 10 µg for prime, 25, 5, 5 µg for boost, respectively), F VLP+G VLP (10, 10 µg for prime and boost, respectively) or F DNA (50 µg for prime and boost) at weeks 0 (prime) and 4 (boost). RSV-specific IgG1 and IgG2a levels were measured by ELISA. (A) RSV F protein specific IgG isotypes. (B) RSV G protein specific IgG isotypes. The results were representative of three independent experiments and presented by concentration (µg/ml) as mean± SEM (standard error of mean). Statistical analysis was by One-way ANOVA and Tukey's multiple comparison test. *** indicates $p<0.001$, between prime and boost immunized sera. $^{##}$ and $^{###}$ mean $p<0.01$ and 0.001, respectively, compared to the F DNA groups.

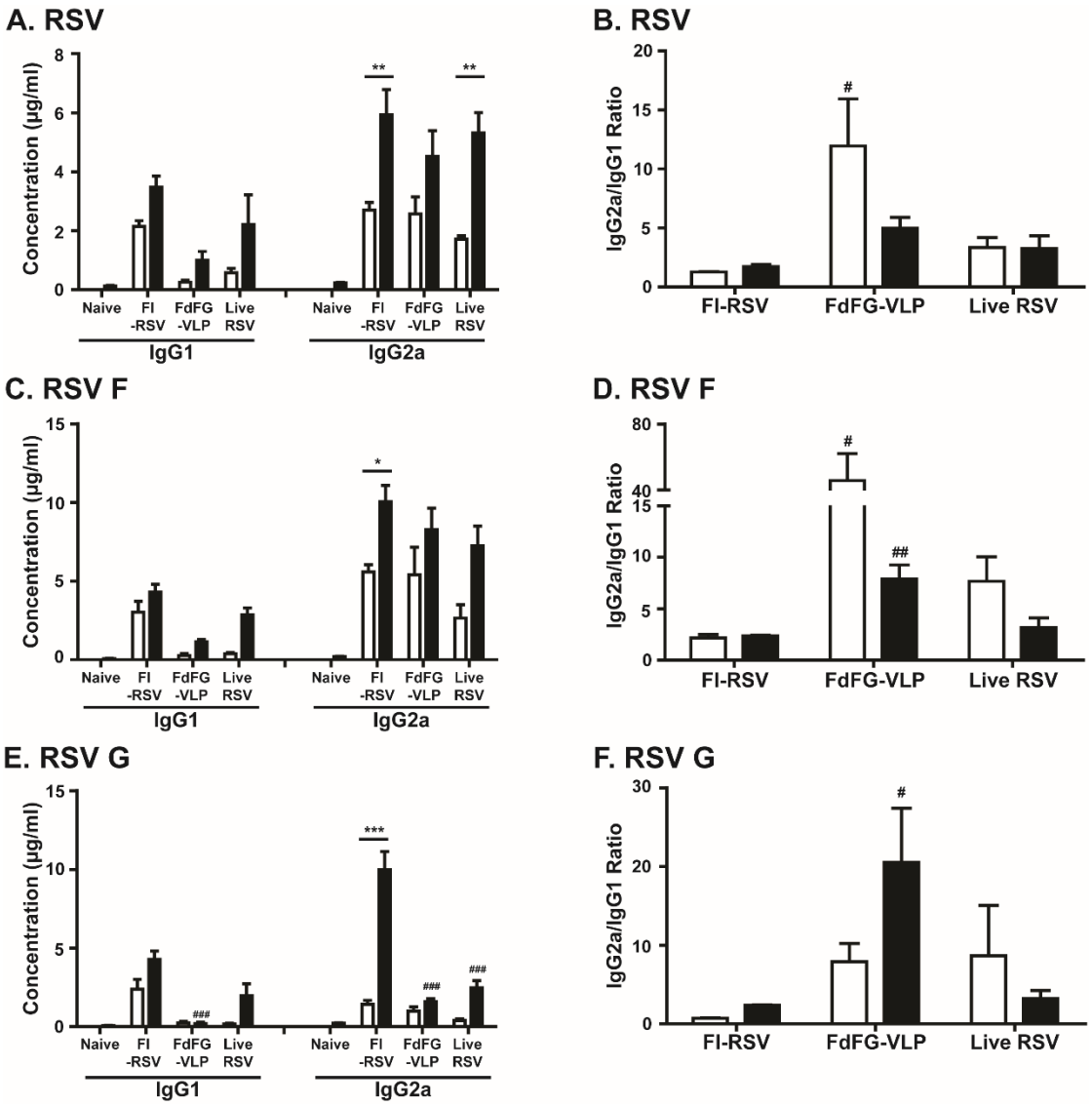

Figure 5.2 RSV-specific serum IgG isotype antibodies.
(A) RSV specific IgG1 and IgG2a antibodies. (B) Ratios of IgG2a/IgG1 antibodies specific to RSV. (C) IgG1 and IgG2a isotype antibodies specific for purified RSV F protein. (D) Ratios of IgG2a/IgG1 isotype antibodies specific for RSV F protein. (E) IgG1 and IgG2a isotype antibodies specific for purified RSV G protein. (F) Ratios of IgG2a/IgG1 isotype antibodies specific for RSV G protein. * and *** indicates $p<0.05$ and 0.001, respectively, between prime and boost immunized sera. $^{\#}$, $^{\#\#}$ and $^{\#\#\#}$ mean $p<0.05$, 0.01 and 0.001, respectively, between the FI-RSV and FdFG VLP groups. Naïve: unimmunized mice. FI-RSV: FI-RSV vaccine. FdFG-VLP: a combined vaccine of RSV F DNA, RSV F and G VLP. Live RSV: live RSV A2 strain.

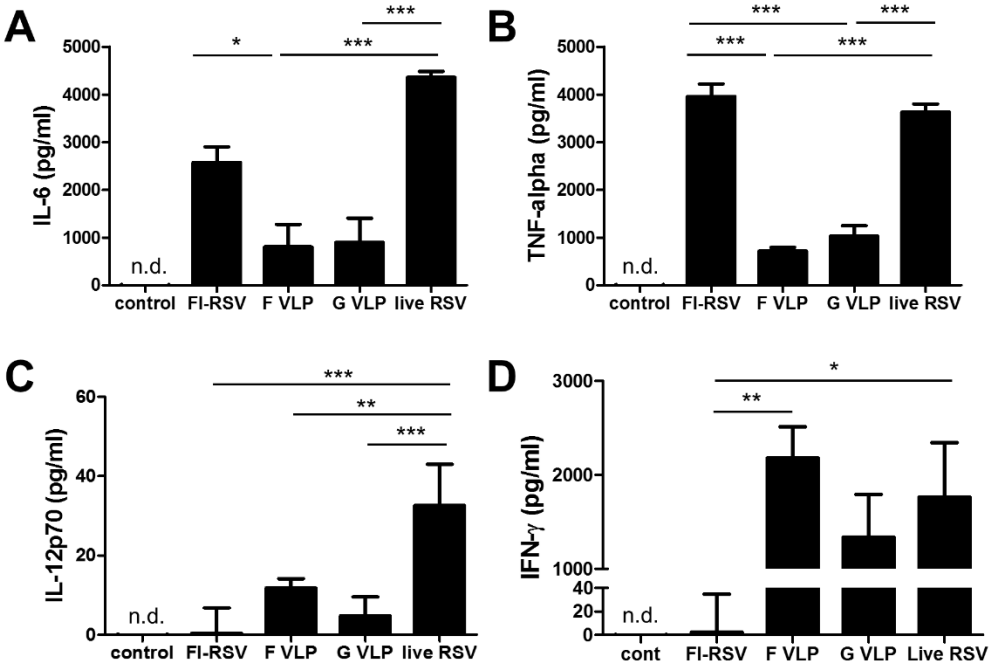

Figure 5.3 Cytokine production from bone marrow-derived dendritic cells and splenocytes after stimulation with RSV vaccines.
Bone marrow-derive dendritic cells (BMDCs) and splenocytes were treated with FI-RSV, F VLP, G VLP, or live RSV. After 2 days culture, cell culture supernatants were collected and used to determine IL-6 (A), TNF-alpha (B) and IL-12p70 (C) production in BMDC and IFN-γ production in splenocytes (D). The concentration of the cytokines were presented as mean ± SEM and the data were representative of three independent experiments. *, ** and *** bars with comparing groups indicates $p<0.05$, 0.01 and 0.001 by one-way ANOVA and Tukey's multiple comparison test.

5.2.2 Control of RSV replication by immunization with RSV vaccines

RSV neutralizing activity is considered an important protective immune correlate of RSV vaccines. To determine RSV neutralizing activity of immune sera, we performed neutralizing antibody titration by using the RSV A2 strain expressing red fluorescent monomeric Katushka 2 protein [68, 69]. Immune sera from the FI-RSV, FdFG-VLP and live RSV immunized mouse groups showed significantly decreased levels of fluorescent intensity compared to naïve mouse sera, indicating the inhibition of RSV infection (Fig. 5.4A). Up to 200 dilutions, approximately 50% decrease in RSV replication were observed in immune sera and there were no statistical significances among different vaccine immune sera (Fig. 5.4A). Thus, sera from FI-RSV, FdFG-

VLP and live RSV immunized mice exhibited high levels of RSV neutralizing activities compared to naïve sera.

To determine whether immunization with FI-RSV or FdFG VLP could protect mice against RSV replication, immunized or previously infected mice were intranasally challenged with RSV (1×10^6 PFU/mouse) at 26 weeks of post boost immunization. RSV titers were analyzed in the lung samples collected at day 5 post RSV challenge (Fig. 5.4B). Unimmunized naïve mice that were infected with RSV showed the highest levels of lung viral loads. RSV was detected at significantly lower levels in the lungs from mice that were previously immunized with FI-RSV or FdFG VLP, or previously infected with RSV compared to those of naïve mice (Fig. 5.4B). Thus, mice that were immunized with FI-RSV or FdFG VLP controlled RSV replication in lungs after RSV challenge infection.

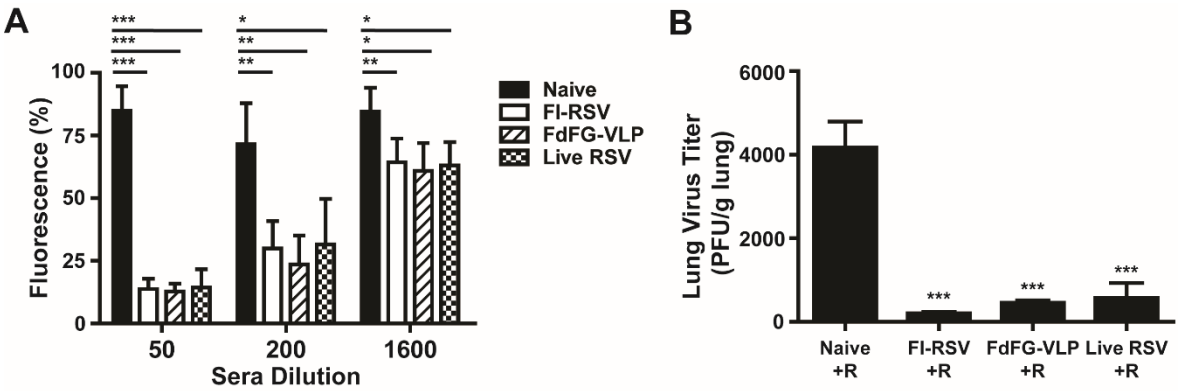

Figure 5.4 FdFG VLP immunization induces RSV neutralizing activity and controls lung viral loads.
(A) RSV neutralizing activity in immunized sera. Data were presented as mean fluorescence percentages ± SEM. *, ** and *** indicates $p<0.05$, 0.01 and 0.001, respectively, by student t test. (B) Lung RSV titers from naïve and immunized mice after RSV challenge. The results were representative out of 3 independent experiments. *** indicates $p<0.001$ compared to the Naïve+R group.

5.2.3 FdFG VLP immunization prevents severe cellular infiltration into airway upon RSV infection

Phenotypes of immune cells contributing to RSV disease or protection are not completely defined. We determined whether FdFG VLP immunization would reduce infiltrating cells into airway upon RSV infection compared to FI-RSV immunization (Fig. 5.5). Naïve mice without infection exhibited low percentages (data not shown) and cellularity of lymphocytes (Fig. 5.5B). At day 5 post RSV infection, naïve mice showed a moderate increase in lymphocytes and cellularity (Fig. 5.5A, B). As expected, FI-RSV immunized mice showed the highest cellular infiltrates with large size cell populations (Region 1 gate, Fig. 5.5) which include granulocytes, dendritic cells, and monocytes and macrophages in bronchoalveolar cells (Table 5.1, Fig. 5.5B). FdFG VLP immunized mice showed a lower level of cellularity in bronchoalveolar cells compared to those in FI-RSV immunized mice (Fig. 5.5B). Live RSV group that was previously infected two times with RSV also caused substantial levels of lymphocytes and granular/myeloid cells, which is higher than those by FdFG VLP immunization (Fig. 5.5B). The region 1 gated BAL cells of FI-RSV immunized mice were found to be smaller in size than those in naïve, FdFG VLP, or live RSV mice (Fig. 5.5A) and most cells in the region 1 gate from the FI-RSV group are likely to be eosinophils (Fig. 5.7). Mice with FdFG VLP immunization showed a similar pattern of region 1 large cell populations as RSV-reinfected mice in response to RSV challenge (Fig. 5.5B).

Table 5.1 Cellularity of BAL cells in the immunized mice after RSV infection.
The region 1 and 2 gates are indicted in the Fig. 5.5. Each indicated phenotypic BAL cell populations were calculated with the percentages of each cell population according to flow cytometry analysis and total cell counts by trypan-blue dye staining. The data are expressed as mean ± SEM out of three independent experiments. BAL cells were analyzed at day 5 post RSV challenge (1x 106 PFU/mouse) of immunized mice (n=5). Naïve; unimmunized mice. Naïve+R; naïve mice infected with RSV. FI-RSV+R; FI- RSV group challenged with RSV. FdFG-VLP+R; FdFG VLP group challenged with RSV. Live RSV+R; Live RSV group infected with RSV. *, ** and ***; $p<0.05$, $p<0.01$ and $p<0.001$, respectively, compared to the naïve group. # and ##; $p<0.05$ and $p<0.01$ compared to the FI-RSV+R group by One-way ANOVA and Tukey's multiple comparison test.

($\times 10^3$ cells/mouse)

	Naïve	Naïve+R	FI-RSV+R	FdFG-VLP+R	Live RSV+R
Leukocytes ($CD45^+$)	117.6±49.1	652.4±225.7	1938.6±296.1***	656.3±94.1$^{\#\#}$	1609.9±256.8**
Region 1 gated cells	95.0±37.3	298.2±73.0	1126.0±283.3**	323.0±76.0$^{\#}$	582.7±39.8
$CD11b^+CD11c^+$	0.3±0.1	12.5±10.2	60.0±35.4	32.6±9.3	53.1±24.9
$CD11b^-CD11c^+$	87.7±36.7	180.8±120.6	123.5±15.3	164.2±61.1	212.4±98.9
$CD11b^+CD11c^-$	2.1±1.3	29.8±14.4	633.4±219.3**	82.0±11.8$^{\#}$	155.8±52.6$^{\#}$
Eosinophils ($CD11b^+CD11c^-$ $SiglecF^+$)	1.0±0.4	9.1±7.0	590.4±309.0	7.2±3.6	17.1±1.4
Region 2 gated cells	4.8±4.1	259.4±205.8	562.7±112.8	212.5±42.8	698.9±261.4
$CD4^+$	3.5±2.8	183.1±150.2	447.4±82.4	148.4±45.5	493.1±194.5
$CD8^+$	1.2±1.2	76.0±55.8	115.0±30.7	63.7±8.2	204.8±68.2*

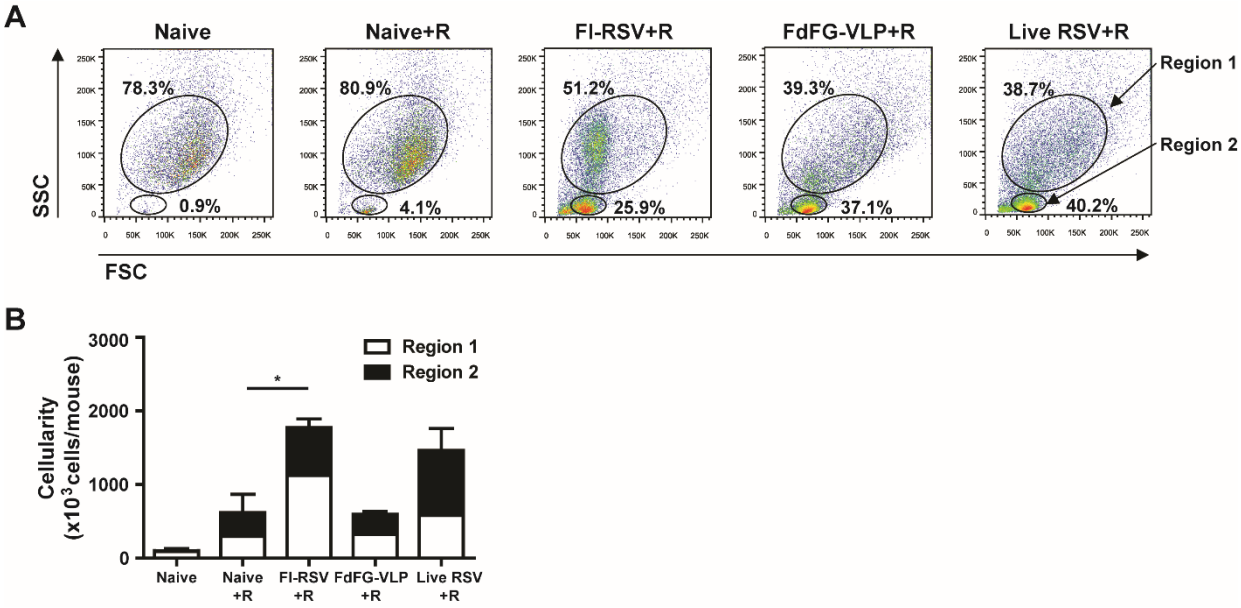

Figure 5.5 FdFG VLP immunization lowers bronchoalveolar cellularity compared to FI-RSV or live RSV. (A) Flow cytometry profiles of BAL cells based on forward (size) and side (granularity) scattering. (B) Cellularity of Region 1 and 2 in BAL fluids. Cellularity was presented from the results of total BAL cell numbers per mouse multiplied by percentages of each population. The data are presented as mean ± SEM. * indicates $p<0.05$.

5.2.4 FdFG VLP immunization modulates innate CD11b$^+$ and CD11c$^+$ cells in BALF

A better understanding of cellular phenotypes in BALF following RSV vaccination would be informative for determining immune responses associated with protection or lung inflammatory disease. The FI-RSV group showed a higher level of myeloid marker CD11b$^+$ cells compared to FdFG VLP or live RSV at day 5 post RSV challenge (Fig. 5.6A). FdFG VLP immunization of mice induced a moderate range in levels of CD11b$^+$ cells similar to that in the live RSV group after RSV challenge. In contrast, CD11c$^+$ cells were found at higher levels in the FdFG VLP group compared to the FI-RSV group. That is, the FdFG VLP group exhibited a trend of increasing CD11c$^+$ cells and lowering CD11b$^+$ cells, which is similar to a pattern observed with the group of live RSV infection. As a result, the ratios of CD11c$^+$ versus CD11b$^+$ cells were highest in the FdFG VLP group whereas FI-RSV showed the lowest level of CD11c$^+$ cells among the groups after RSV challenge (Fig. 5.6B, C). CD45$^+$CD11c$^+$ cells appeared to be alveolar macrophages with a F4/80$^+$

phenotype (data not shown) and the majority of $CD45^+CD11b^+CD11c^-$ cells seemed to be eosonophils (Fig. 5.7). These results suggest that an imbalance in $CD11c^+$ versus $CD11b^+$ cells and cell types in airway might be an important parameter contributing to FI-RSV vaccination-induced lung inflammatory disease with severe infiltrates around the airways and interstitial spaces (Fig 5.8).

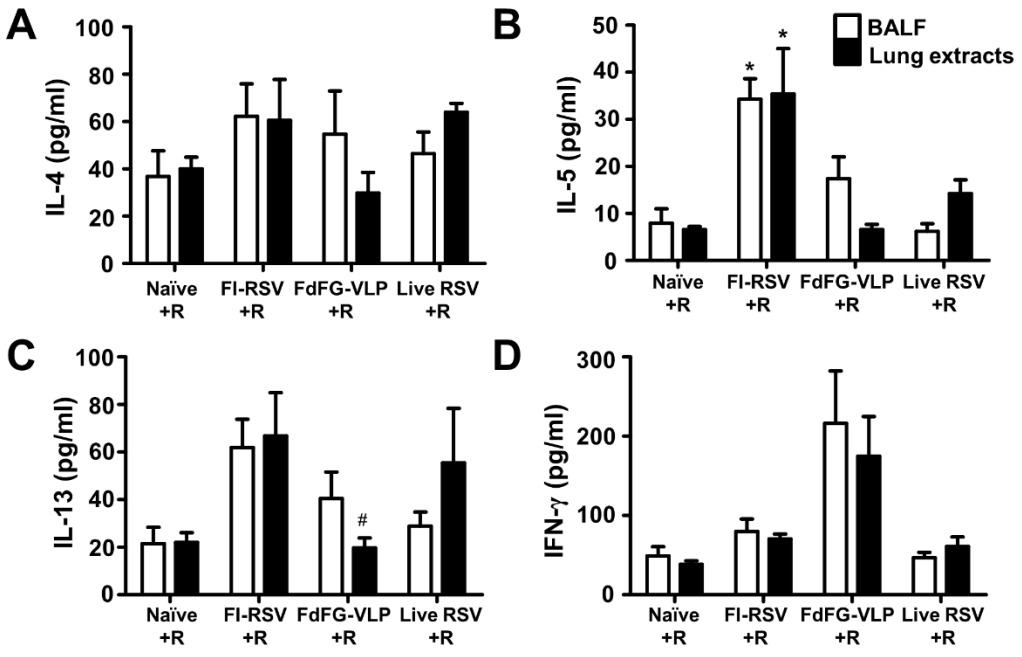

Figure 5.6 Distribution of CD11b and CD11c positive cells in bronchoalveolar lavage fluids.
(A) Flow cytometry profiles gated on CD11b and CD11c. $CD45^+$ granulocyte/myeloid cells in BAL were gated by CD11b and CD11c expression. (B) $CD11b^-CD11c^+$ (upper-left in A)/$CD11b^+CD11c^-$ (lower-right in A) ratios. (C) $CD11b^+CD11c^+$ (upper-right in A)/$CD11b^+CD11c^-$ (lower-right in A) ratios. The ratios are presented as mean ± SEM. * indicates $p<0.05$ by student t test.

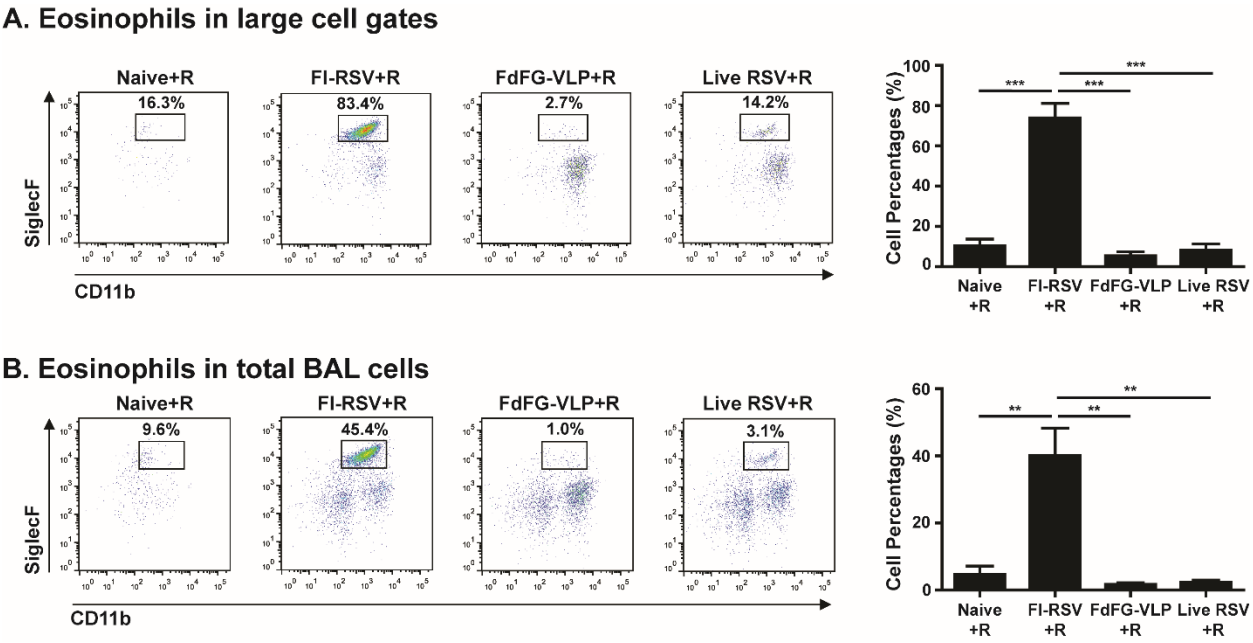

Figure 5.7 FdFG VLP immunization does not induce eosinophilia upon RSV challenge.
(A) Eosinophils ($CD11b^{+}SiglecF^{+}$) in $CD45^{+}CD11c^{-}$ large cell gates of BAL cells. (B) Eosinophils ($CD11b^{+}SiglecF^{+}$) in $CD45^{+}CD11c^{-}$ total BAL cells. The mean percentage data are presented in right panels as mean ± SEM. *, **, and *** indicate $p<0.05$, 0.01, and 0.001, respectively.

Figure 5.8 Comparison of pulmonary histopathology after RSV challenge.
(A) Representative pulmonary histopathology of lung tissue sections is shown in each group of mice at day 5 post RSV challenge. Representative images of peribronchiolar regions after hematoxylin and eosin (H&E) staining were

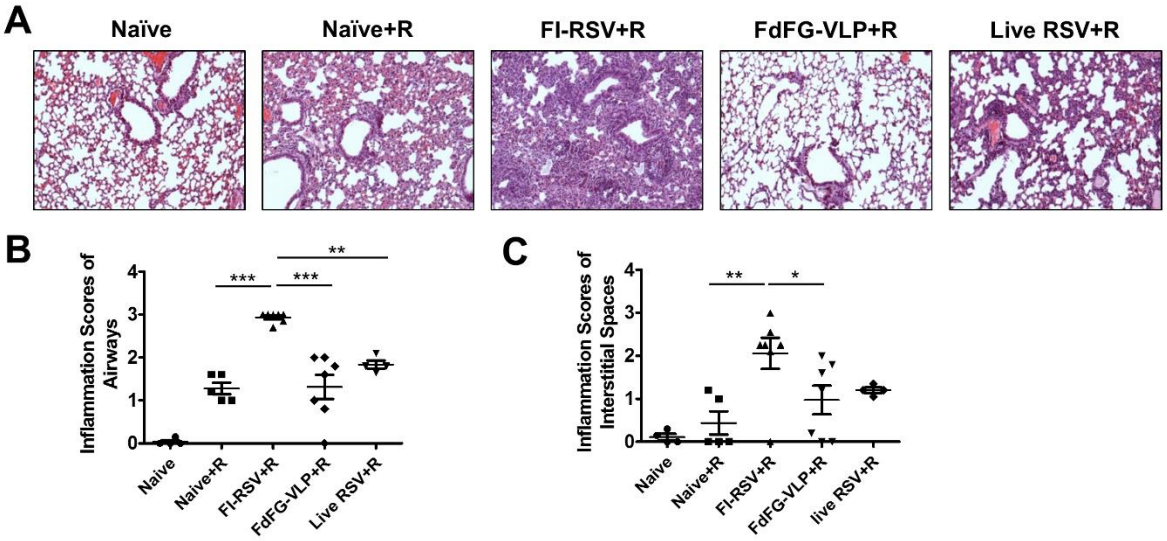

acquired at a magnification of ×100. (B) Inflammation scores of airways. (C) Inflammation scores of interstitial spaces. *, ** and *** indicates $p<0.05$, 0.01 and 0.001 by one-way ANOVA and Tukey's multiple comparison test. Naïve+R; naïve mice challenged with RSV. FI-RSV+R; FI-RSV group challenged with RSV. FdFG-VLP+R; FdFG VLP group challenged with RSV. Live RSV+R; Live RSV group challenged with RSV.

5.2.5 FdFG VLP immunization does not induce eosinophilia upon RSV infection

Eosinophils were demonstrated to have the phenotypes of $CD45^+CD11c^-CD11b^+SiglecF^+$ and enriched in inflamed lung tissues [107, 108]. At day 5 post RSV challenge, the FI-RSV immunized group induced prominently a population with $CD11b^+SiglecF^+$ cells, which was approximately 83% out of the $CD45^+CD11c^-$ large cell gated populations (Fig. 5.7A) and 45% out of total BALF cells (Fig. 5.7B). High levels of eosinophils showed a correlation with severe infiltrates around the bronchial airways and interstitial spaces from the lung histology of FI-RSV immune mice (Fig 5.8). A low but distinct population with $CD45^+CD11c^-CD11b^+SiglecF^+$ cells at a level of approximately 14% (Fig. 5.7A) was also observed in the live RSV group after RSV challenge. Importantly, the group of mice immunized with FdFG VLP vaccine did not show such a distinct population of $CD11b^+SiglecF^+$ cells. Unimmunized naïve mice also showed $CD11b^+SiglecF^+$ phenotypic cells even at a low level after RSV infection (Fig. 5.7). Therefore, results in this study provide evidence that FdFG VLP immunization would not induce pulmonary eosinophilia whereas FI-RSV immunization induces severe eosinophilia and live RSV re-infections may induce a low level of eosinophils.

5.2.6 FdFG VLP immunization increases the ratios of adaptive $CD8^+/CD4^+$ cells secreting IFN-γ in BAL lymphocytes

Previous studies demonstrated that FI-RSV immunized mice had an increased number of $CD4^+$ T cells infiltrating BALF after RSV challenge, which was shown to be involved in vaccine-enhanced lung disease [109]. Thus, it was assumed that a reverse trend would be beneficial in preventing lung disease. $CD4^+$ T cells and $CD8^+$ T cells in BALF were analyzed day 5 post RSV challenge (Fig. 5.9). FI-RSV immunization induced high $CD4^+$ T cells in BALF after RSV challenge. In contrast,

FdFG VLP immunization resulted in approximately 3-fold lower $CD4^+$ cellularity in BALF compared to that induced by FI-RSV immunization or by live RSV infection (Table 5.1). Overall, the ratios of $CD8^+/CD4^+$ T cells were relatively higher in the FdFG VLP and live RSV group than those in the FI-RSV group (Fig. 5.9B).

It was demonstrated that IFN-γ can have both beneficial protective and detrimental systemic disease effects [53], indicating that IFN-γ response should be balanced to avoid disease after RSV challenge. Intracellular IFN-γ cytokine staining of cells in BALF was presented (Fig. 5.9). FI-RSV immunization induced highest levels of IFN-γ producing $CD4^+$ T cells (32.8% of total $CD3^+$ T cells, Fig. 5.9A) whereas the FdFG VLP group showed a relatively low level of IFN-γ^+ $CD4^+$ T cells (16.4%, Fig. 5.9A). Since the $CD4^+$ T cellularity in the FI-RSV group showed 3 fold higher than that in the FdFG VLP group (Table 5.1), the total IFN-γ producing $CD4^+$ T cells induced by FI-RSV immunization were approximately 5- to 6-fold higher than those by FdFG VLP immunization. Interestingly, live RSV showed an intermediate level of IFN-γ secreting $CD4^+$ T cells (22.7%, Fig. 5.9A). In line with high levels of IFN-γ producing $CD4^+$ T cells and eosinophils, we found that FI-RSV and live RSV more strongly stimulated *in vitro* bone marrow derived dendritic cells (BMDCs) to secrete proinflammatory cytokines IL-6 and TNF-α than RSV F or G VLP (Fig. 5.3).

$CD8^+$ T cells were reported more likely to contribute to protection against RSV [110]. Contrary to IFN-γ^+ $CD4^+$ T cells, a reverse pattern of IFN-γ producing $CD8^+$ T cells between FI-RSV and FdFG VLP groups was observed in T cells from BALF after RSV challenge. The FdFG VLP group showed the highest level of IFN-γ^+ $CD8^+$ T cells (26.8% of total $CD3^+$ T cells, Fig. 5.9A, C). FI-RSV immunization induced a lowest level of IFN-γ^+ $CD8^+$ T cells (11.7%, Fig. 5.9A, C). Interestingly, FI-RSV was not effective in IL-12 Th1 type cytokine production from *in vitro*

BMDC cultures (Fig. 5.3). An intermediate level of IFN-γ^+ $CD8^+$ T cells was observed in the live RSV group (19.9%, Fig. 5.9A, C). Accordingly, the ratios of $CD8^+$ and $CD4^+$ T cells producing IFN-γ were highest in the FdFG VLP group (Fig. 5.9C), indicating that FdFG VLP immunization can modulate IFN-γ secreting $CD4^+$ and $CD8^+$ T cells infiltrating into airway upon RSV challenge. To further determine whether FdFG VLP could modulate the expression of cytokines in lung microenvironment, we determined IL-4, IL-5, IL-13 Th2 type and IFN-γ Th1 type cytokines in BALF as well as in lung extract (Fig. 5.10) after RSV challenge of immunized mice. Lung extracts from FI-RSV immunized mice showed a trend of increasing Th2 cytokines (IL-4, IL-5, IL-13) whereas FdFG VLP immunization resulted in an increase of IFN- γ production in lung milieu. A similar pattern of cytokines was observed in BALF samples (Fig. 5.10). Therefore, a pattern of increasing Th2 cytokines in lungs of FI-RSV immune mice might have contributed to inflammatory RSV disease.

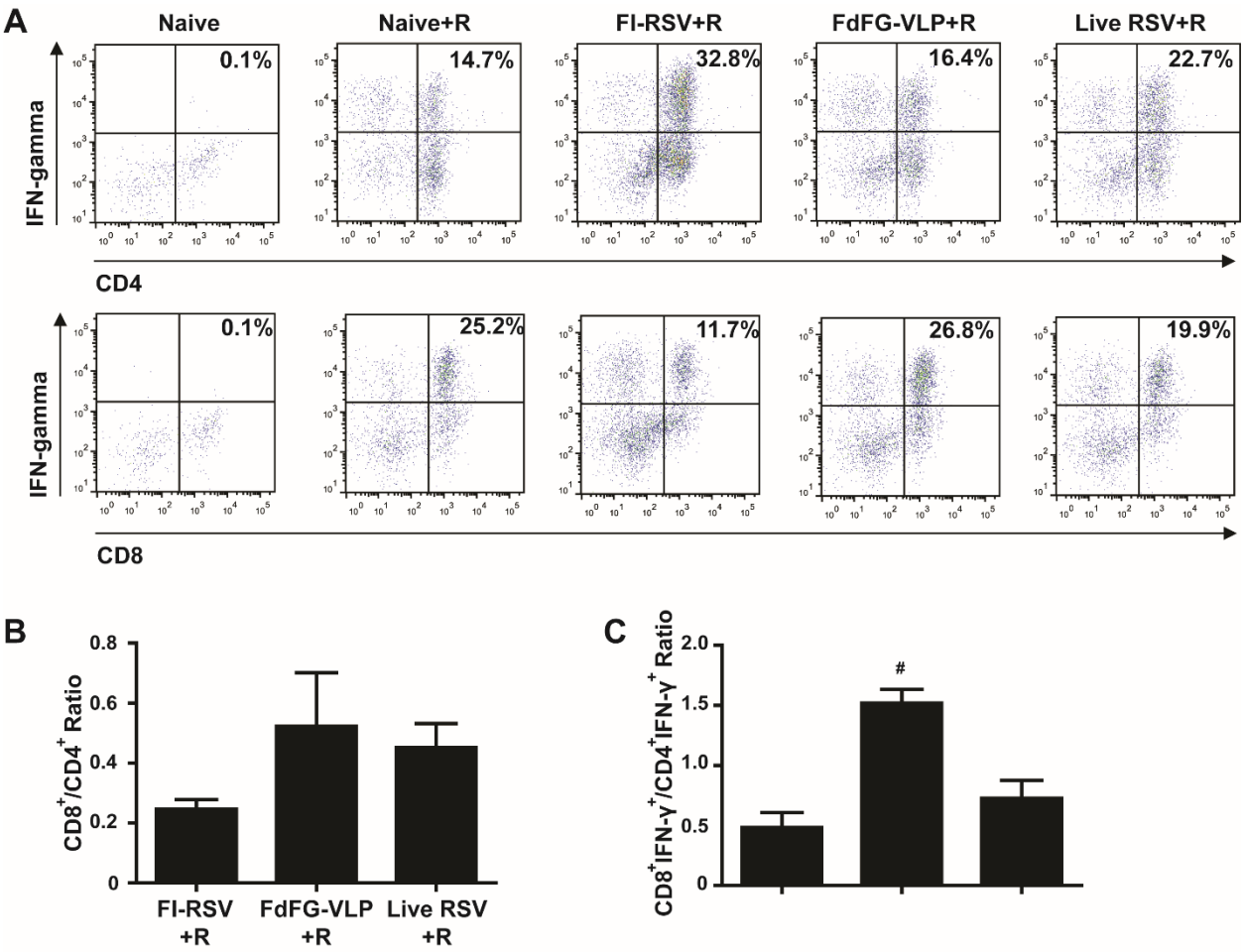

Figure 5.9 IFN-γ producing lymphocytes in bronchoalveolar lavage fluids.
(A) IFN-γ^+ cell percentages in $CD4^+$ and $CD8^+$ lymphocyte ($CD3^+$) populations. The dot plots are representative of three independent intracellular cytokine staining experiments. (B) Ratios of $CD8^+$ to $CD4^+$ T cells in total lymphocyte population. (C) Ratios of IFN-γ producing $CD8^+$ to $CD4^+$ T cells in BAL lymphocytes. Ratios are presented as mean ± SEM. $^{\#}$ indicates $p<0.05$ compared to the FI-RSV+R group.

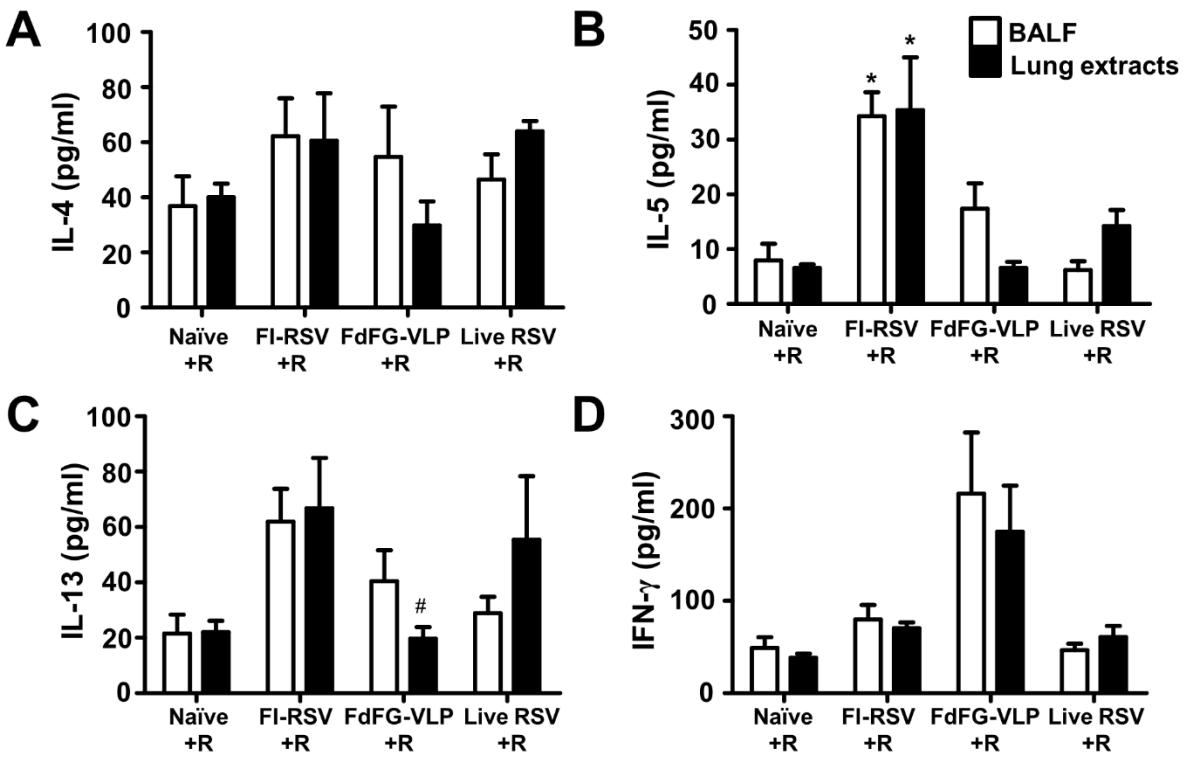

Figure 5.10 Cytokine profiles in bronchoalveolar lavage fluid of RSV challenged mice.
Bronchoalveolar lavage fluid (BALF) was collected from the immunized mice day 5 post RSV challenge and used to determine IL-4 (A), IL-5 (B), IL-13 (C), and IFN-γ (D). The concentration of the cytokines were presented as mean ± SEM and the data were representative of three independent experiments. * indicates $p<0.05$ compared to all other groups and # indicates $p<0.05$ compared to FI-RSV+R group by one-way ANOVA and Tukey's multiple comparison test.

5.3 Discussion

Protective immune correlates are not well understood because there is no licensed RSV vaccine. In particular, cellular phenotypes contributing to protection and disease remain largely unknown after RSV vaccination. Results in this study provide evidence that FdFG VLP could confer protection against RSV by preventing pulmonary eosinophilia and modulating cellular phenotypes as well as cellularity of infiltrates and IFN-γ secreting cells in addition to inducing Th1 type antibodies and cytokines.

FdFG VLP vaccination induced antibodies recognizing RSV, predominantly binding to the RSV F protein antigen and little to the RSV G antigen. After prime immunization with FdFG VLP, higher levels of IgG2a antibodies for RSV F were observed than those for RSV G (Fig. 5.2C and E), indicating that RSV F is more immunogenic than RSV G and this result is consistent with those in mice that were immunized with NDV VLPs containing both RSV F and G proteins [111]. After boost immunization, IgG2a antibodies for RSV G were increased. Meanwhile, IgG1 antibodies specific for RSV F were relatively increased after boost immunization. Accordingly, IgG2a/IgG1 ratios showed an opposite direction between RSV F and RSV G specific antibodies after boost immunization (Fig. 5.2D, F). Therefore, antibody isotype profiles and distribution between RSV F and G specific antibodies may reflect an intrinsic difference in immunogenicity and protection.

RSV F is known to be an agonist for Toll-like receptor 4 (TLR4) [112]. There seems to be a certain correlation between TLR4 polymorphism and RSV disease severity [113]. TLR is known to regulate host immune responses against RSV [114]. High levels of IgG2a antibodies to RSV F than those to RSV G might be due to an effective stimulation of dendritic cells via TLR4 by F VLP. RSV neutralizing monoclonal antibodies targeting the RSV F protein have been licensed, making the F protein an attractive vaccine target [115]. Thus, it might be desirable that FdFG VLP

immunization induced antibody immune responses that are predominantly specific for RSV F. Immune responses to RSV G were shown to be effective in controlling lung viral loads [63,116], and also to cause eosinophilia and secrete Th2 cytokines[117, 118]. Also, purified RSV F protein vaccine was shown to induce a Th2-like response[119]. Higher levels of IgG2a antibodies were induced by immunization with FdFG VLP. Therefore, it should be informative to determine the contributions of each RSV FdFG VLP vaccine component to RSV protection and disease. Inclusion of F DNA in the FG VLP was found to contribute to further increasing IgG2a antibody responses (Fig. 5.1). An enhanced Th1-like response induced by FdFG VLP might be due to the endogenous expression of genetic RSV F DNA vaccine plus intrinsic property of a nano-particulate nature of VLP. In support of this property of VLPs, influenza hemagglutinin proteins presented on VLP induced strong IgG2a isotype and IFN-γ producing T cell responses compared to soluble hemagglutinin proteins[89] .

There are some controversies regarding the efficacy of lung viral clearance in FI-RSV immunized animals. Low RSV neutralizing antibodies were reported to be induced by FI-RSV immunization[116, 120, 121]. Accordingly, low efficacy of lung viral clearance was shown in FI-RSV immunized mice[116, 121]. In contrast, other previous studies demonstrated that FI-RSV immunized mice or cotton rats controlled RSV lung viral loads after infection[122, 123, 124, 125, 126]. It is not clear yet why lung viral clearance efficacies and RSV neutralizing titers are various among different studies on FI-RSV immunizations in animal models. FI-RSV preparation, doses of FI-RSV vaccines, animal models, and assay methods may influence the outcomes of FI-RSV vaccination efficacy despite its observed histopathology.

In this study, the total cell numbers of granulocyte/myeloid large cell populations and lymphocytes infiltrating BALF were found to be highest in the FI-RSV group. In contrast, FdFG

VLP immunization did not result in significant infiltrates of leukocytes into BALF, and their bronchoalveolar cellularity was significantly lower than that by FI-RSV immunization following subsequent RSV infection. The group of mice intramuscularly immunized with FdFG VLP showed lower levels of granulocyte/myeloid cells and lymphocytes infiltrated into BALF upon RSV challenge even compared to those observed in the group of live RSV. Therefore, based on the results in this study, FdFG VLP is less likely to induce inflammatory cellular infiltrates into lungs upon RSV challenge compared to live RSV infection even at 26 weeks after immunization.

FI-RSV immunization resulted in granulocyte/myeloid cells (region 1 gated cells in Fig. 5.5) that were smaller in size as shown by forward light scattering, and the majority (~80%) of this region 1 gated granulocyte/myeoloid cell population was found to have eosinophil phenotypic markers ($CD45^+CD11c^-CD11b^+SiglecF^+$). The marked increase in pulmonary eosinophilia is a hallmark of FI-RSV vaccine-enhanced disease[49, 65]. Also, the ratios of $CD11c^+$ cell phenotypes and $CD11b^+$ myeloid cell phenotypes ($CD11c^+/CD11b^+$) were very low in the FI-RSV group. Whereas, the FdFG VLP and live RSV groups of mice showed larger in size but low numbers of BALF granulocyte/myeloid cells that were composed of high levels of $CD11c^+$ phenotypic cells, and low levels of eosinophils. The FdFG VLP group showed even a lower level of eosinophils when compared to that in the live RSV group. The majority of $CD11c^+$ phenotypic cells in mice with FdFG VLP vaccine appeared to be alveolar macrophages with a $F4/80^+$ phenotype (data not shown) but further detailed studies should be carried out to define these cell types. The $CD11c^+$ phenotypic cells were shown to play a crucial role in inducing Th1-polarized adaptive immune responses [97, 127]. $CD11b^+$ phenotypic cells were reported to promote the recruitment of leukocytes by pro-inflammatory cytokines following infection [128, 129]. The high levels of $CD11b^+$ cells in BALF may be correlated with a property of FI-RSV in stimulating BMDCs to secrete IL-6 and

TNF-α cytokines but not IL-12 or IFN-γ cytokines (Fig. 5.1). In contrast, F VLP was less effective in stimulating BMDCs to secrete IL-6 and TNF-α cytokines. We observed a similar pattern of cellular phenotypes in lungs but less prominent compared to those in BALF (data not shown). Further characterization of these infiltrating cells in BALF and lungs after vaccination and RSV challenge will provide an informative insight into designing a safer vaccine against RSV. The results in this study suggest that modulation of innate immune cells in BALF by FdFG VLP vaccination plays an important role in conferring protection against RSV eosinophilic inflammatory disease.

T cells are known to contribute to RSV disease as well as protection, indicating that a balance between $CD4^+$ T cells and $CD8^+$ T cells is important[109, 130]. It is highly significant to note that, among groups, FdFG VLP immunized mice showed highest levels of BALF $CD8^+$ T cells producing IFN-γ, which resulted in the highest ratio of $CD8^+/CD4^+$ T cells making IFN-γ. In contrast, FI-RSV mice exhibited highest levels of BALF $CD4^+$ T cells producing IFN-γ, giving the lowest ratio of $CD8^+/CD4^+$ T cells making IFN-γ. Live RSV mice showed over 2 fold less ratio of $CD8^+/CD4^+$ T cells making IFN-γ compared to those in FdFG VLP immunized mice. We also found that the cellularity of BALF $CD4^+$ T cells was highest in FI-RSV mice and then followed by live RSV mice whereas FdFG VLP mice showed relatively a low level of $CD4^+$ T cellularity in BALF. In addition to total BALF cellularity, high levels of IL-4 secreting lung and spleen cells were detected in FI-RSV immunized mice but not in FdFG VLP immunized mice (data not shown). In support of results in this study, IFN-γ producing $CD8^+$ T cells were shown to inhibit Th2 responses and pulmonary RSV disease[131]. Histopathology results of lung tissue sections suggest that FI-RSV immunization induced severe pulmonary inflammation, and moderate lung inflammation was observed with live RSV re-infections and unimmunized mice upon RSV

infection (Fig. 5.8). In contrast, FdFG VLP immunization did not induce such pulmonary inflammatory disease (Fig. 5.8). Therefore, in addition to high cellularity in BALF, high levels of eosinophils, IL-4 and IFN-γ producing $CD4^+$ T cells, and Th2 cytokines may be all together contributing to RSV lung disease upon infection, resulting in severe pulmonary histopathology.

6 CONCLUSIONS

6.1 Diseases prevented by vaccine with adjuvants

Humans are immunized with many different kinds of vaccines throughout life to prevent infectious diseases. With adjuvants, the antigen-specific immune responses can be increased and many infectious diseases can be prevented by effective vaccination with adjuvants[14]. Young children, the elderly and the human immunodeficiency virus infected patients have high risk to be infected by pathogens such as influenza virus so that they are required to get vaccinations. However, most of commercial vaccines are for healthy population, and vaccine efficacy is low in the immune-compromised individuals. More effective new adjuvants need to be developed for improving the vaccine efficacy for this population[14, 20, 132, 133]. Young infants and immune-compromised populations may have defects in $CD4^+$ T helper cells due to the immature immune system, aging or virus infection in $CD4^+$ T cells, respectively[14]. It is significant to investigate the adjuvant effects in the absence of $CD4^+$ T cells. Few vaccine adjuvants have been licensed and used for human vaccines. In addition, the detailed action mechanisms of adjuvants have not been fully understood. It is highly significant to better understand vaccine adjuvants mechanisms to improve the efficacy of adjuvants and develop new adjuvants as well.

It is the first study to test vaccine and adjuvant effects in CD4-deficient immune-compromised CD4KO mice. Previous studies demonstrated the $CD4^+$ T cell dependent mechanisms using wild-type mouse models. That is, the previous studies of vaccines and adjuvants have focused on the antigen-specific immune responses of $CD4^+$ T cells. There has been no study to investigate the effects of vaccine adjuvants in the absence of $CD4^+$ T cells. Therefore, the adjuvant studies using CD4-knock-out mice and $CD4^+$ T cell-dependent antigen can provide further understanding of the action mechanisms of the adjuvants and vaccines. This study will

provide a new mechanism of vaccine and adjuvants that can improve the protective immune responses against the pathogens.

6.2 Mechanisms of vaccine adjuvants in immune competent condition

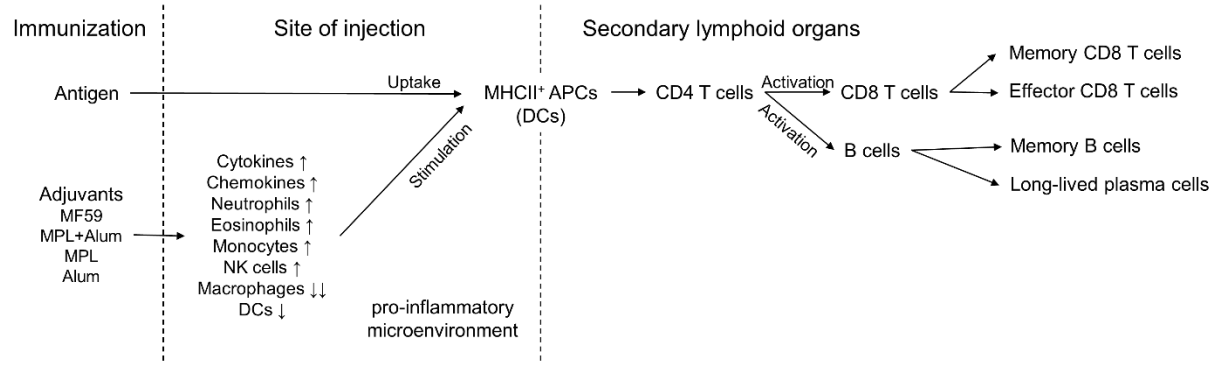

Figure 6.1 Conventional vaccine adjuvant mechanism

Adjuvants are basically innate immune stimulators and form pro-inflammatory microenvironments at the site of injection (Fig. 6.1). Conventionally, adjuvants increases chemokine and inflammatory cytokine production and recruits various innate immune cells such as neutrophils and monocytes at the injection site [79]. The activation of T cells depends on antigen presenting cells (APCs), such as dendritic cells (DCs) of the innate immune system. It has been well established that $CD4^+$ T cells provide critical help for inducing long-lived protective antibody production by B cells [134] and for generating effective $CD8^+$ memory T cells [135]. Thus, it is believed that adjuvant effects on enhancing antibody responses to T cell-dependent vaccine antigens are mediated by $CD4^+$ T helper cells through adjuvant-activated innate immune components as demonstrated in many studies [136, 137, 138, 139, 140, 141, 142]. A conventional concept is that adjuvants activate innate immune components, which subsequently determines a specific type of T helper cells in orchestrating the quantity and quality of protective antibodies [24, 28, 139].

6.3 Immune mechanisms of vaccine adjuvants in CD4-deficient condition

The roles of $CD4^+$ T cells in the adjuvant effects and underlying mechanisms by which adjuvants work largely remain unknown. This study demonstrated protective immunity to T-dependent vaccine antigen in CD4KO mice, which is mediated by MF59 and MPL+Alum adjuvants (Fig. 6.2). Immune parameters investigated include isotype-switched antibodies, long-lived IgG antibody-producing cells, protective HAI antibodies and cellular mechanisms of the adjuvants in a CD4-deficient condition (Fig. 6.2).

MF59 was more potent in acutely inducing inflammatory cytokines and in recruiting innate immune cells compared to alum. Cell death and uric acid appear to be a mechanism for adjuvant effects by MF59. Partial retention of macrophages from significant cell depletion and recruitment of DC populations in addition to monocytes and neutrophils at the site of injection might be contributing to MF59 adjuvant effects particularly in CD4KO mice.

MPL+Alum showed effective adjuvant effects on inducing IgG isotype-switched antibodies and conferring protective immunity in CD4KO mice, which was more effective compared to those in WT mice with influenza vaccine only or Alum-adjuvanted vaccination. MPL+Alum showed moderate levels of cytokines and chemokines in the peritoneal cavity after injection of CD4KO mice. MPL+Alum appears to have differential effects on generating local inflammatory micro-environment, maintaining macrophages, and attenuating acute inflammation compared to those of MPL and Alum. MHCII-expressing cellular components, DN T cells, and soluble cytokines and chemokines at the site of injection are likely to be the major contributing factors in providing alternative help to B cells for inducing IgG antibody responses in the context of MPL+Alum adjuvanted influenza vaccination of CD4KO mice.

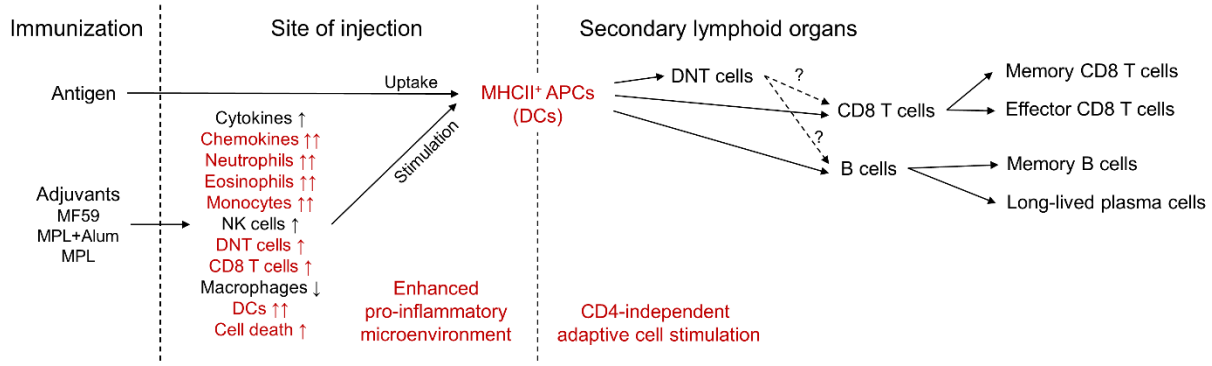

Figure 6.2 Alternative vaccine adjuvant mechanisms in CD4KO mice

6.4 Comparisons of vaccine adjuvants in terms of CD4-dependency

The adjuvants in this study showed different adjuvant efficacy in CD4KO mice and CD4-depleted wild-type mice with the same T-cell dependent vaccine antigen. MF59 showed the strongest CD4-independent adjuvant effects. MPL and MPL+Alum combination showed a moderate level of CD4-dependency, but they induced sufficient protection in CD4-deficient mice. Alum was the representative CD4-dependent vaccine adjuvants and it was used as a control of vaccine adjuvant in this study.

Most of vaccine adjuvants were known to play a role as an innate immune stimulator. They stimulate the innate immune system at the site of injection and then induce innate and adaptive immune cell recruitment and activation. In this study, all adjuvants, MF59, MPL+Alum, MPL, and Alum, induced eosinophils, neutrophils, monocytes, and NK cells recruitment at the peritoneal cavity. It supported the previous findings that adjuvants caused pro-inflammatory micro-environments at the site of injection.

However, macrophages and dendritic cells, which are representative $MHCII^+$ antigen-presenting cells (APCs), showed different tendency of cell recruitment by adjuvants and CD4-deficient condition. In wild-type mice, macrophages and DCs in the peritoneal cavity were

decreased by adjuvant treatment. This is because of adjuvant-induced cell death and increase of other inflammatory cells. In contrast, in CD4KO mice, the numbers of DCs were increased by adjuvant treatment and the levels of DC recruitment were consistent with the CD4-independency of the vaccine adjuvants (MF59>MPL>MPL+Alum). In case of macrophages, even the actual numbers were reduced by adjuvant treatments, but the levels of decrease (15~92%) were lower than wild-type (74~99%). Thus, the more dendritic cells and macrophages were retained in the CD4-independent vaccine adjuvant-treated CD4KO mice. In addition to APCs, $CD8^+$ T cells and DN T cells were increased in MF59, MPL+Alum, MPL-treated CD4KO mice (Fig. 6.3).

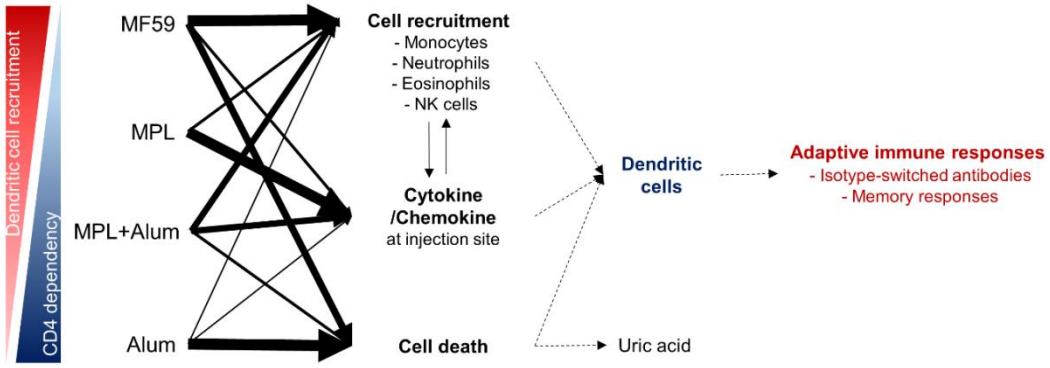

Figure 6.3 Comparisons of CD4-dependency and mechanisms of vaccine adjuvants.
The widths of the arrows from each adjuvants mean the strength/effects of the each adjuvants to induce following immune responses. MF59 induced more cell recruitment, moderate cell death and weak cytokine production. MPL induced high levels of cytokine production at the injection site, but weak cell recruitment and no cell death. Moderate levels of cell recruitment, cytokine production and cell death were elicited by MPL+Alum and the effects of alum was mostly by cell death.

In addition to characteristic of each adjuvant, in this study, different CD4-deficient mouse models were used to investigate CD4-dependent/independent adjuvant effects. CD4KO mice, which is genetically modified to delete CD4 gene expression, can be a model to test CD4-dependency of adjuvants. However, these CD4KO mice with a genetic defect in the CD4 gene expression are known to have developed compensatory cell populations, such as double-negative (DN) T cells[143] and MHCII-restrictive $CD8^+$ T cells[77, 144]. These compensatory cells might have

played roles in inducing antibody production and protection instead of $CD4^+$ T cells. To better understand the roles of CD4 T cells in inducing immunity using a model of CD4-depleted B6 WT mice, $CD4^+$ T cells are acutely depleted after development, therefore the roles of $CD4^+$ T cells can be investigated in a more stringent condition compared to those in CD4KO mice. MF59 adjuvant plus flu vaccination overcomes the acute CD4-depletion and induce comparable levels of antibodies, whereas MPL and MPL+Alum showed partial CD4 dependence in CD4-depleted situation compared to untreated WT mice.

$CD4^+$ T cells are undergone positive/negative selection when they are differentiated in thymus by $MHCII^+$ thymus epithelial cells[145]. The helper function of CD4 T cells in the immune system is mediated via the recognition of peptide antigens presented on $MHCII^+$ APCs. Thus, both CD4 cells and MHCII expressing cells are deficient in MHCIIKO mice. Using an MHCIIKO mouse model, this study was extended to determine whether $MHCII^+$ cells are important to induce antibody production and protection against pathogens in comparison with those in CD4KO mice. In MHCIIKO mice, antigen-specific antibodies were barely produced by vaccination with adjuvants, indicating that $MHCII^+$ cells might have played a critical role in exhibiting CD4-independent adjuvant effects in CD4KO mice. All these experimental results of roles of DN T cells and $MHCII^+$ APCs are contributing to better understanding of immune mechanisms of CD4-independent vaccine adjuvants to overcome the CD4-deficiency and elicit protective immune responses against pathogens. These findings suggest a new paradigm in the adjuvant action mechanisms.

Table 6.1 Comparison of different CD4-deficient mice models

	CD4KO	CD4-depleted WT	MHCIIKO
Cause of CD4-deficiency	Genetically deleted	Anti-CD4 mAb	Genetically deleted
Method of CD4-deficiency	Developmental defect	Acute depletion	Developmental defect
Additional defect	Unknown	Unknown	No $MHCII^+$ cells
Compensation of CD4 T cells	MHCII-restricted DN T cells/CD8 T cells	$MHCII^+$ cells	-
IgG Antibody production by MF59/MPL+Alum	High	High (MF59) Moderate (MPL+Alum)	No significant vaccine-specific IgG antibodies
Application	Easily check CD4-dependency of adjuvants/vaccines	More stringent mice model to test CD4-dependency	To test roles of both MHCII and CD4 positive cells
Limitation	The cells compensating CD4 T cells	Unknown adverse effects by mAbs Still remaining CD4 T cells in lymphoid organs	Hard to induce immune responses

6.5 Cellular mechanisms of RSV vaccines

Respiratory syncytial virus (RSV) is a major cause of pneumonia and bronchiolitis in infants and in the elderly, but there is no licensed RSV vaccine. A particular obstacle is the safety concern of vaccine-enhanced RSV disease. It is of high priority to develop an effective and safe RSV vaccine. Therefore, it is significant to investigate the cellular mechanisms of RSV vaccines.

FdFG VLP nanoparticulate vaccine could provide protection against RSV without causing eosinophilia. Phenotypic analysis of BALF cells suggested that FdFG VLP vaccination induced apparently balanced immune responses of $CD11c^+$ phenotypic cells and IFN-γ producing $CD8^+$ T cells locally. Also, high levels of $CD11b^+$ eosinophils and IFN-γ producing CD4 appeared to contribute to FI-RSV vaccination-induced pulmonary RSV disease. These results provide first evidence that RSV vaccines based on VLP in combination with F DNA genetic vaccine can be

developed as an effective and safe RSV vaccine inducing protective immunity comparable or better than live RSV.

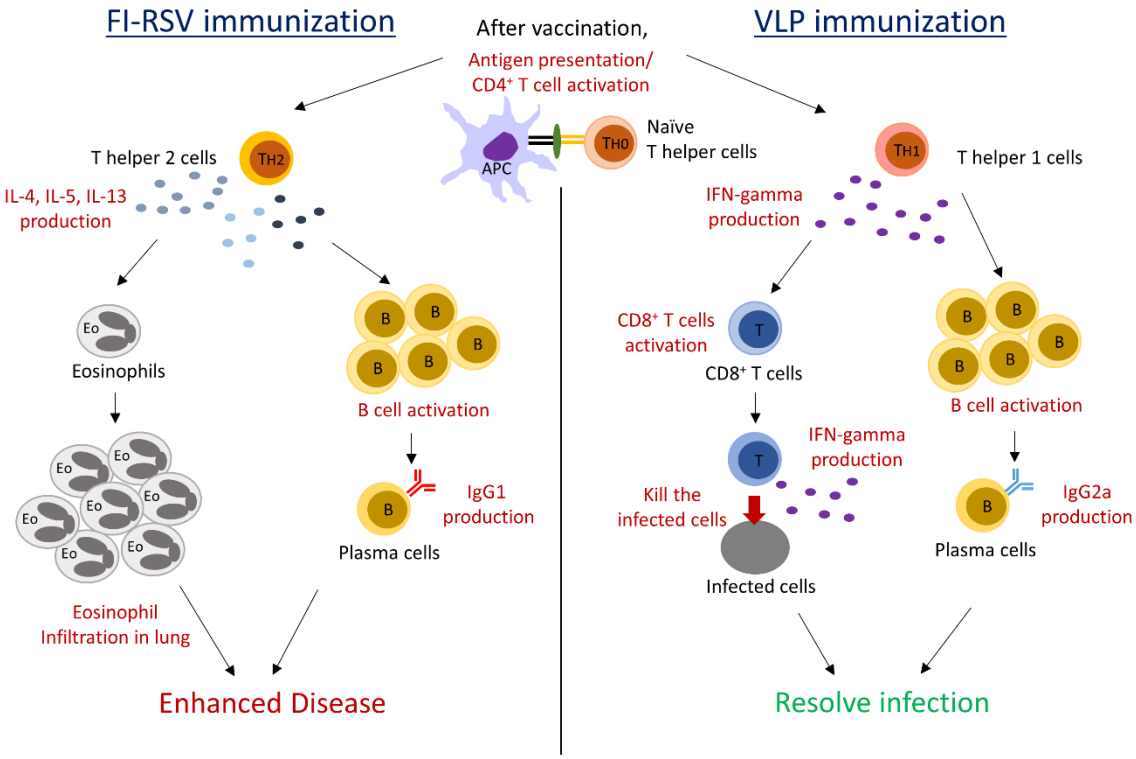

Figure 6.4 Mechanisms of RSV vaccines

REFERENCES

1. Centers for Disease C, Prevention. Estimates of deaths associated with seasonal influenza --- United States, 1976-2007. *MMWR Morbidity and mortality weekly report* 2010, **59**(33)**:** 1057-1062.

2. Thompson WW, Shay DK, Weintraub E, Brammer L, Cox N, Anderson LJ, *et al.* Mortality associated with influenza and respiratory syncytial virus in the United States. *Jama* 2003, **289**(2)**:** 179-186.

3. Taubenberger JK, Kash JC. Influenza virus evolution, host adaptation, and pandemic formation. *Cell host & microbe* 2010, **7**(6)**:** 440-451.

4. Webster RG, Bean WJ, Gorman OT, Chambers TM, Kawaoka Y. Evolution and ecology of influenza A viruses. *Microbiological reviews* 1992, **56**(1)**:** 152-179.

5. Jalilian B, Christiansen SH, Einarsson HB, Pirozyan MR, Petersen E, Vorup-Jensen T. Properties and prospects of adjuvants in influenza vaccination - messy precipitates or blessed opportunities? *Molecular and cellular therapies* 2013, **1:** 2.

6. Tong S, Zhu X, Li Y, Shi M, Zhang J, Bourgeois M, *et al.* New world bats harbor diverse influenza A viruses. *PLoS pathogens* 2013, **9**(10)**:** e1003657.

7. Russell RJ, Haire LF, Stevens DJ, Collins PJ, Lin YP, Blackburn GM, *et al.* The structure of H5N1 avian influenza neuraminidase suggests new opportunities for drug design. *Nature* 2006, **443**(7107)**:** 45-49.

8. Iwasaki A, Pillai PS. Innate immunity to influenza virus infection. *Nature reviews Immunology* 2014, **14**(5)**:** 315-328.

9. Bridges CB, Kuehnert MJ, Hall CB. Transmission of influenza: implications for control in health care settings. *Clinical infectious diseases : an official publication of the Infectious Diseases Society of America* 2003, **37**(8)**:** 1094-1101.

10. Finelli L, Fiore A, Dhara R, Brammer L, Shay DK, Kamimoto L, *et al.* Influenza-associated pediatric mortality in the United States: increase of Staphylococcus aureus coinfection. *Pediatrics* 2008, **122**(4)**:** 805-811.

11. Lin JC, Nichol KL. Excess mortality due to pneumonia or influenza during influenza seasons among persons with acquired immunodeficiency syndrome. *Archives of internal medicine* 2001, **161**(3)**:** 441-446.

12. Taubenberger JK, Morens DM. The pathology of influenza virus infections. *Annual review of pathology* 2008, **3:** 499-522.

13. Treanor J. Influenza vaccine--outmaneuvering antigenic shift and drift. *The New England journal of medicine* 2004, **350**(3)**:** 218-220.

14. Rappuoli R, Mandl CW, Black S, De Gregorio E. Vaccines for the twenty-first century society. *Nature reviews Immunology* 2011, **11**(12)**:** 865-872.

15. Plotkin SA. Correlates of protection induced by vaccination. *Clinical and vaccine immunology : CVI* 2010, **17**(7)**:** 1055-1065.

16. Pulendran B, Oh JZ, Nakaya HI, Ravindran R, Kazmin DA. Immunity to viruses: learning from successful human vaccines. *Immunological reviews* 2013, **255**(1)**:** 243-255.

17. Taylor JJ, Pape KA, Jenkins MK. A germinal center-independent pathway generates unswitched memory B cells early in the primary response. *The Journal of experimental medicine* 2012, **209**(3)**:** 597-606.

18. Vajo Z, Kosa L, Visontay I, Jankovics M, Jankovics I. Inactivated whole virus influenza A (H5N1) vaccine. *Emerging infectious diseases* 2007, **13**(5)**:** 807-808.

19. Izurieta HS, Haber P, Wise RP, Iskander J, Pratt D, Mink C, *et al.* Adverse events reported following live, cold-adapted, intranasal influenza vaccine. *Jama* 2005, **294**(21)**:** 2720-2725.

20. Mbow ML, De Gregorio E, Valiante NM, Rappuoli R. New adjuvants for human vaccines. *Current opinion in immunology* 2010, **22**(3)**:** 411-416.

21. Tripp RA, Tompkins SM. Virus-vectored influenza virus vaccines. *Viruses* 2014, **6**(8)**:** 3055-3079.

22. Hovden AO, Cox RJ, Haaheim LR. Whole influenza virus vaccine is more immunogenic than split influenza virus vaccine and induces primarily an IgG2a response in BALB/c mice. *Scandinavian journal of immunology* 2005, **62**(1)**:** 36-44.

23. McKee AS, MacLeod MK, Kappler JW, Marrack P. Immune mechanisms of protection: can adjuvants rise to the challenge? *BMC biology* 2010, **8:** 37.

24. Coffman RL, Sher A, Seder RA. Vaccine adjuvants: putting innate immunity to work. *Immunity* 2010, **33**(4)**:** 492-503.

25. Eisenbarth SC, Colegio OR, O'Connor W, Sutterwala FS, Flavell RA. Crucial role for the Nalp3 inflammasome in the immunostimulatory properties of aluminium adjuvants. *Nature* 2008, **453**(7198)**:** 1122-1126.

26. Kool M, Petrilli V, De Smedt T, Rolaz A, Hammad H, van Nimwegen M, *et al.* Cutting edge: alum adjuvant stimulates inflammatory dendritic cells through activation of the NALP3 inflammasome. *Journal of immunology* 2008, **181**(6)**:** 3755-3759.

27. Sharp FA, Ruane D, Claass B, Creagh E, Harris J, Malyala P, *et al.* Uptake of particulate vaccine adjuvants by dendritic cells activates the NALP3 inflammasome. *Proceedings of the National Academy of Sciences of the United States of America* 2009, **106**(3)**:** 870-875.

28. O'Hagan DT, Ott GS, De Gregorio E, Seubert A. The mechanism of action of MF59 - an innately attractive adjuvant formulation. *Vaccine* 2012, **30**(29)**:** 4341-4348.

29. Seubert A, Monaci E, Pizza M, O'Hagan DT, Wack A. The adjuvants aluminum hydroxide and MF59 induce monocyte and granulocyte chemoattractants and enhance monocyte differentiation toward dendritic cells. *Journal of immunology* 2008, **180**(8)**:** 5402-5412.

30. Akira S, Takeda K. Toll-like receptor signalling. *Nature reviews Immunology* 2004, **4**(7)**:** 499-511.

31. Didierlaurent AM, Morel S, Lockman L, Giannini SL, Bisteau M, Carlsen H, *et al.* AS04, an aluminum salt- and TLR4 agonist-based adjuvant system, induces a transient localized innate immune response leading to enhanced adaptive immunity. *Journal of immunology* 2009, **183**(10)**:** 6186-6197.

32. Casella CR, Mitchell TC. Putting endotoxin to work for us: monophosphoryl lipid A as a safe and effective vaccine adjuvant. *Cellular and molecular life sciences : CMLS* 2008, **65**(20)**:** 3231-3240.

33. Huleatt JW, Nakaar V, Desai P, Huang Y, Hewitt D, Jacobs A, *et al.* Potent immunogenicity and efficacy of a universal influenza vaccine candidate comprising a recombinant fusion protein linking influenza M2e to the TLR5 ligand flagellin. *Vaccine* 2008, **26**(2)**:** 201-214.

34. Huleatt JW, Jacobs AR, Tang J, Desai P, Kopp EB, Huang Y, *et al.* Vaccination with recombinant fusion proteins incorporating Toll-like receptor ligands induces rapid cellular and humoral immunity. *Vaccine* 2007, **25**(4)**:** 763-775.

35. Pashine A, Valiante NM, Ulmer JB. Targeting the innate immune response with improved vaccine adjuvants. *Nature medicine* 2005, **11**(4 Suppl)**:** S63-68.

36. Sha Z, Kang SM, Compans RW. Mucosal immunization of CD4+ T cell-deficient mice with an inactivated virus induces IgG and IgA responses in serum and mucosal secretions. *Virology* 2005, **331**(2)**:** 387-395.

37. Geeraedts F, Bungener L, Pool J, ter Veer W, Wilschut J, Huckriede A. Whole inactivated virus influenza vaccine is superior to subunit vaccine in inducing immune responses and secretion of proinflammatory cytokines by DCs. *Influenza and other respiratory viruses* 2008, **2**(2)**:** 41-51.

38. Sailaja G, Skountzou I, Quan FS, Compans RW, Kang SM. Human immunodeficiency virus-like particles activate multiple types of immune cells. *Virology* 2007, **362**(2)**:** 331-341.

39. Quan FS, Ko EJ, Kwon YM, Joo KH, Compans RW, Kang SM. Mucosal adjuvants for influenza virus-like particle vaccine. *Viral immunology* 2013, **26**(6)**:** 385-395.

40. Wykes M, MacPherson G. Dendritic cell-B-cell interaction: dendritic cells provide B cells with CD40-independent proliferation signals and CD40-dependent survival signals. *Immunology* 2000, **100**(1)**:** 1-3.

41. Sha Z, Compans RW. Induction of CD4(+) T-cell-independent immunoglobulin responses by inactivated influenza virus. *Journal of virology* 2000, **74**(11)**:** 4999-5005.

42. Dorfmeier CL, Lytle AG, Dunkel AL, Gatt A, McGettigan JP. Protective vaccine-induced CD4(+) T cell-independent B cell responses against rabies infection. *Journal of virology* 2012, **86**(21)**:** 11533-11540.

43. Yao Q, Zhang R, Guo L, Li M, Chen C. Th cell-independent immune responses to chimeric hemagglutinin/simian human immunodeficiency virus-like particles vaccine. *Journal of immunology* 2004, **173**(3)**:** 1951-1958.

44. Collins PL, Chanock RM, Murphy B. Respiratory Syncytial Virus, p. 1443-1485 In: Fields Virology, Knipe DM, Howley PM, eds. Vol 1. 4th ed. Philadelphia: Lippncott Williams & Wilkins press. 2001**:** 1533-1579.

45. Karron RA. Respiratory syncytial virus and parainfluenza virus vaccines, p. 1283–1293. In S. A. Plotkin, W. A. Orenstein, and P. A. Offit (ed.), Vaccines, 5th ed. Saunders-Elsevier, Philadelphia, PA. 2008.

46. Falsey AR, Hennessey PA, Formica MA, Cox C, Walsh EE. Respiratory syncytial virus infection in elderly and high-risk adults. *N Engl J Med* 2005, **352**(17)**:** 1749-1759.

47. Collins PL, Graham BS. Viral and host factors in human respiratory syncytial virus pathogenesis. *Journal of virology* 2008, **82**(5)**:** 2040-2055.

48. Kapikian AZ, Mitchell RH, Chanock RM, Shvedoff RA, Stewart CE. An epidemiologic study of altered clinical reactivity to respiratory syncytial (RS) virus infection in children previously vaccinated with an inactivated RS virus vaccine. *Am J Epidemiol* 1969, **89**(4)**:** 405-421.

49. Kim HW, Canchola JG, Brandt CD, Pyles G, Chanock RM, Jensen K, *et al.* Respiratory syncytial virus disease in infants despite prior administration of antigenic inactivated vaccine. *Am J Epidemiol* 1969, **89**(4)**:** 422-434.

50. Delgado MF, Coviello S, Monsalvo AC, Melendi GA, Hernandez JZ, Batalle JP, *et al.* Lack of antibody affinity maturation due to poor Toll-like receptor stimulation leads to enhanced respiratory syncytial virus disease. *Nat Med* 2009, **15**(1)**:** 34-41.

51. Hancock GE, Heers KM, Smith JD, Scheuer CA, Ibraghimov AR, Pryharski KS. CpG containing oligodeoxynucleotides are potent adjuvants for parenteral vaccination with the fusion (F) protein of respiratory syncytial virus (RSV). *Vaccine* 2001, **19**(32)**:** 4874-4882.

52. Murphy BR, Sotnikov AV, Lawrence LA, Banks SM, Prince GA. Enhanced pulmonary histopathology is observed in cotton rats immunized with formalin-inactivated respiratory syncytial virus (RSV) or purified F glycoprotein and challenged with RSV 3-6 months after immunization. *Vaccine* 1990, **8**(5)**:** 497-502.

53. Castilow EM, Olson MR, Meyerholz DK, Varga SM. Differential role of gamma interferon in inhibiting pulmonary eosinophilia and exacerbating systemic disease in fusion protein-immunized mice undergoing challenge infection with respiratory syncytial virus. *Journal of virology* 2008, **82**(5)**:** 2196-2207.

54. Valosky J, Hishiki H, Zaoutis TE, Coffin SE. Induction of mucosal B-cell memory by intranasal immunization of mice with respiratory syncytial virus. *Clinical and diagnostic laboratory immunology* 2005, **12**(1)**:** 171-179.

55. Schmidt MR, McGinnes LW, Kenward SA, Willems KN, Woodland RT, Morrison TG. Long-term and memory immune responses in mice against Newcastle disease virus-like particles containing respiratory syncytial virus glycoprotein ectodomains. *Journal of virology* 2012, **86**(21)**:** 11654-11662.

56. Hall CB, Walsh EE, Long CE, Schnabel KC. Immunity to and frequency of reinfection with respiratory syncytial virus. *The Journal of infectious diseases* 1991, **163**(4)**:** 693-698.

57. Piedra PA. Clinical experience with respiratory syncytial virus vaccines. *The Pediatric infectious disease journal* 2003, **22**(2 Suppl)**:** S94-99.

58. Bont L, Versteegh J, Swelsen WT, Heijnen CJ, Kavelaars A, Brus F, *et al.* Natural reinfection with respiratory syncytial virus does not boost virus-specific T-cell immunity. *Pediatric research* 2002, **52**(3)**:** 363-367.

59. Hall CB, Walsh EE, Long CE, Schnabel KC. Immunity to and frequency of reinfection with respiratory syncytial virus. *The Journal of infectious diseases* 1991, **163**(4)**:** 693-698.

60. Bont L, Versteegh J, Swelsen WT, Heijnen CJ, Kavelaars A, Brus F, *et al.* Natural reinfection with respiratory syncytial virus does not boost virus-specific T-cell immunity. *Pediatric research* 2002, **52**(3)**:** 363-367.

61. Kang SM, Song JM, Quan FS, Compans RW. Influenza vaccines based on virus-like particles. *Virus research* 2009, **143**(2)**:** 140-146.

62. Zeltins A. Construction and characterization of virus-like particles: a review. *Molecular biotechnology* 2013, **53**(1)**:** 92-107.

63. Quan FS, Kim Y, Lee S, Yi H, Kang SM, Bozja J, *et al.* Viruslike particle vaccine induces protection against respiratory syncytial virus infection in mice. *The Journal of infectious diseases* 2011, **204**(7)**:** 987-995.

64. Kim HW, Canchola JG, Brandt CD, Pyles G, Chanock RM, Jensen K, *et al.* Respiratory syncytial virus disease in infants despite prior administration of antigenic inactivated vaccine. *American journal of epidemiology* 1969, **89**(4)**:** 422-434.

65. Openshaw PJ, Culley FJ, Olszewska W. Immunopathogenesis of vaccine-enhanced RSV disease. *Vaccine* 2001, **20 Suppl 1:** S27-31.

66. Stokes KL, Currier MG, Sakamoto K, Lee S, Collins PL, Plemper RK, *et al.* The respiratory syncytial virus fusion protein and neutrophils mediate the airway mucin response to pathogenic respiratory syncytial virus infection. *Journal of virology* 2013, **87**(18)**:** 10070-10082.

67. Prince GA, Curtis SJ, Yim KC, Porter DD. Vaccine-enhanced respiratory syncytial virus disease in cotton rats following immunization with Lot 100 or a newly prepared reference vaccine. *J Gen Virol* 2001, **82**(Pt 12)**:** 2881-2888.

68. Shcherbo D, Shemiakina, II, Ryabova AV, Luker KE, Schmidt BT, Souslova EA, *et al.* Near-infrared fluorescent proteins. *Nat Methods* 2010, **7**(10)**:** 827-829.

69. Hotard AL, Shaikh FY, Lee S, Yan D, Teng MN, Plemper RK, *et al.* A stabilized respiratory syncytial virus reverse genetics system amenable to recombination-mediated mutagenesis. *Virology* 2012, **434**(1)**:** 129-136.

70. Reed LJ, Muench H. A simple method of estimating fifty percent endpoints. *Am J Hygiene* 1938, **27:** 493-497.

71. Lee BO, Rangel-Moreno J, Moyron-Quiroz JE, Hartson L, Makris M, Sprague F, *et al.* CD4 T cell-independent antibody response promotes resolution of primary influenza infection and helps to prevent reinfection. *Journal of immunology* 2005, **175**(9)**:** 5827-5838.

72. Tonti E, Fedeli M, Napolitano A, Iannacone M, von Andrian UH, Guidotti LG, *et al.* Follicular helper NKT cells induce limited B cell responses and germinal center formation in the absence of CD4(+) T cell help. *Journal of immunology* 2012, **188**(7)**:** 3217-3222.

73. Aimanianda V, Haensler J, Lacroix-Desmazes S, Kaveri SV, Bayry J. Novel cellular and molecular mechanisms of induction of immune responses by aluminum adjuvants. *Trends in pharmacological sciences* 2009, **30**(6)**:** 287-295.

74. Hogenesch H. Mechanism of immunopotentiation and safety of aluminum adjuvants. *Frontiers in immunology* 2012, **3:** 406.

75. Kool M, Soullie T, van Nimwegen M, Willart MA, Muskens F, Jung S, *et al.* Alum adjuvant boosts adaptive immunity by inducing uric acid and activating inflammatory dendritic cells. *The Journal of experimental medicine* 2008, **205**(4)**:** 869-882.

76. Kono H, Chen CJ, Ontiveros F, Rock KL. Uric acid promotes an acute inflammatory response to sterile cell death in mice. *J Clin Invest* 2010, **120**(6)**:** 1939-1949.

77. Tyznik AJ, Sun JC, Bevan MJ. The CD8 population in CD4-deficient mice is heavily contaminated with MHC class II-restricted T cells. *The Journal of experimental medicine* 2004, **199**(4)**:** 559-565.

78. Seubert A, Calabro S, Santini L, Galli B, Genovese A, Valentini S, *et al.* Adjuvanticity of the oil-in-water emulsion MF59 is independent of Nlrp3 inflammasome but requires the adaptor protein MyD88. *Proceedings of the National Academy of Sciences of the United States of America* 2011, **108**(27)**:** 11169-11174.

79. Calabro S, Tortoli M, Baudner BC, Pacitto A, Cortese M, O'Hagan DT, *et al.* Vaccine adjuvants alum and MF59 induce rapid recruitment of neutrophils and monocytes that participate in antigen transport to draining lymph nodes. *Vaccine* 2011, **29**(9)**:** 1812-1823.

80. El Sahly H. MF59™ as a vaccine adjuvant: a review of safety and immunogenicity. *Expert review of vaccines* 2010, **9**(10)**:** 1135-1141.

81. Monaci E, Mancini F, Lofano G, Bacconi M, Tavarini S, Sammicheli C, *et al.* MF59- and Al(OH)3-Adjuvanted Staphylococcus aureus (4C-Staph) Vaccines Induce Sustained Protective Humoral and Cellular Immune Responses, with a Critical Role for Effector CD4 T Cells at Low Antibody Titers. *Frontiers in immunology* 2015, **6:** 439.

82. Mosca F, Tritto E, Muzzi A, Monaci E, Bagnoli F, Iavarone C, *et al.* Molecular and cellular signatures of human vaccine adjuvants. *Proceedings of the National Academy of Sciences of the United States of America* 2008, **105**(30)**:** 10501-10506.

83. Neumann K, Castineiras-Vilarino M, Hockendorf U, Hannesschlager N, Lemeer S, Kupka D, *et al.* Clec12a is an inhibitory receptor for uric acid crystals that regulates inflammation in response to cell death. *Immunity* 2014, **40**(3)**:** 389-399.

84. Shi Y, Evans JE, Rock KL. Molecular identification of a danger signal that alerts the immune system to dying cells. *Nature* 2003, **425**(6957)**:** 516-521.

85. Jacobson LS, Lima H, Jr., Goldberg MF, Gocheva V, Tsiperson V, Sutterwala FS, *et al.* Cathepsin-mediated necrosis controls the adaptive immune response by Th2 (T helper type 2)-associated adjuvants. *The Journal of biological chemistry* 2013, **288**(11)**:** 7481-7491.

86. Vesikari T, Forsten A, Herbinger KH, Cioppa GD, Beygo J, Borkowski A, *et al.* Safety and immunogenicity of an MF59((R))-adjuvanted A/H5N1 pre-pandemic influenza vaccine in adults and the elderly. *Vaccine* 2012, **30**(7)**:** 1388-1396.

87. Young BE, Sadarangani SP, Leo YS. The avian influenza vaccine Emerflu. Why did it fail? *Expert review of vaccines* 2015, **14**(8)**:** 1125-1134.

88. Mestas J, Hughes CC. Of mice and not men: differences between mouse and human immunology. *Journal of immunology* 2004, **172**(5)**:** 2731-2738.

89. Song JM, Hossain J, Yoo DG, Lipatov AS, Davis CT, Quan FS, *et al.* Protective immunity against H5N1 influenza virus by a single dose vaccination with virus-like particles. *Virology* 2010, **405**(1)**:** 165-175.

90. Tonti E, Fedeli M, Napolitano A, Iannacone M, von Andrian UH, Guidotti LG, *et al.* Follicular helper NKT cells induce limited B cell responses and germinal center formation in the absence of CD4(+) T cell help. *J Immunol* 2012, **188**(7)**:** 3217-3222.

91. Grusby MJ, Johnson RS, Papaioannou VE, Glimcher LH. Depletion of CD4+ T cells in major histocompatibility complex class II-deficient mice. *Science* 1991, **253**(5026)**:** 1417-1420.

92. O E, Lee YT, Ko EJ, Kim KH, Lee YN, Song JM, *et al.* Roles of major histocompatibility complex class II in inducing protective immune responses to influenza vaccination. *Journal of virology* 2014, **88**(14)**:** 7764-7775.

93. Mestas J, Hughes CC. Of mice and not men: differences between mouse and human immunology. *J Immunol* 2004, **172**(5)**:** 2731-2738.

94. Dormitzer PR, Galli G, Castellino F, Golding H, Khurana S, Del Giudice G, *et al.* Influenza vaccine immunology. *Immunological reviews* 2011, **239**(1)**:** 167-177.

95. McAleer JP, Vella AT. Educating CD4 T cells with vaccine adjuvants: lessons from lipopolysaccharide. *Trends Immunol* 2010, **31**(11)**:** 429-435.

96. McKee AS, MacLeod MK, Kappler JW, Marrack P. Immune mechanisms of protection: can adjuvants rise to the challenge? *BMC Biol* 2010, **8:** 37.

97. McAleer JP, Zammit DJ, Lefrancois L, Rossi RJ, Vella AT. The lipopolysaccharide adjuvant effect on T cells relies on nonoverlapping contributions from the MyD88 pathway and CD11c+ cells. *Journal of immunology* 2007, **179**(10)**:** 6524-6535.

98. Didierlaurent AM, Morel S, Lockman L, Giannini SL, Bisteau M, Carlsen H, *et al.* AS04, an aluminum salt- and TLR4 agonist-based adjuvant system, induces a transient localized

innate immune response leading to enhanced adaptive immunity. *J Immunol* 2009, **183**(10)**:** 6186-6197.

99. Rauschmayr-Kopp T, Williams IR, Borriello F, Sharpe AH, Kupper TS. Distinct roles for B7 costimulation in contact hypersensitivity and humoral immune responses to epicutaneous antigen. *Eur J Immunol* 1998, **28**(12)**:** 4221-4227.

100. Zimmerer JM, Horne PH, Fiessinger LA, Fisher MG, Pham TA, Saklayen SL, *et al.* Cytotoxic effector function of CD4-independent, CD8(+) T cells is mediated by TNF-alpha/TNFR. *Transplantation* 2012, **94**(11)**:** 1103-1110.

101. Williams GS, Oxenius A, Hengartner H, Benoist C, Mathis D. CD4+ T cell responses in mice lacking MHC class II molecules specifically on B cells. *Eur J Immunol* 1998, **28**(11)**:** 3763-3772.

102. Rau FC, Dieter J, Luo Z, Priest SO, Baumgarth N. B7-1/2 (CD80/CD86) direct signaling to B cells enhances IgG secretion. *Journal of immunology* 2009, **183**(12)**:** 7661-7671.

103. Ferguson TA, Choi J, Green DR. Armed response: how dying cells influence T-cell functions. *Immunological reviews* 2011, **241**(1)**:** 77-88.

104. Moriwaki K, Chan FK. RIP3: a molecular switch for necrosis and inflammation. *Genes Dev* 2013, **27**(15)**:** 1640-1649.

105. Schon MP, Wienrich BG, Drewniok C, Bong AB, Eberle J, Geilen CC, *et al.* Death receptor-independent apoptosis in malignant melanoma induced by the small-molecule immune response modifier imiquimod. *J Invest Dermatol* 2004, **122**(5)**:** 1266-1276.

106. Chirkova T, Boyoglu-Barnum S, Gaston KA, Malik FM, Trau SP, Oomens AG, *et al.* Respiratory syncytial virus G protein CX3C motif impairs human airway epithelial and immune cell responses. *Journal of virology* 2013, **87**(24)**:** 13466-13479.

107. Stevens WW, Kim TS, Pujanauski LM, Hao X, Braciale TJ. Detection and quantitation of eosinophils in the murine respiratory tract by flow cytometry. *Journal of immunological methods* 2007, **327**(1-2)**:** 63-74.

108. Zhang JQ, Biedermann B, Nitschke L, Crocker PR. The murine inhibitory receptor mSiglec-E is expressed broadly on cells of the innate immune system whereas mSiglec-F is restricted to eosinophils. *Eur J Immunol* 2004, **34**(4)**:** 1175-1184.

109. Waris ME, Tsou C, Erdman DD, Day DB, Anderson LJ. Priming with live respiratory syncytial virus (RSV) prevents the enhanced pulmonary inflammatory response seen after RSV challenge in BALB/c mice immunized with formalin-inactivated RSV. *Journal of virology* 1997, **71**(9)**:** 6935-6939.

110. Lee S, Stokes KL, Currier MG, Sakamoto K, Lukacs NW, Celis E, *et al.* Vaccine-elicited CD8+ T cells protect against respiratory syncytial virus strain A2-line19F-induced pathogenesis in BALB/c mice. *Journal of virology* 2012, **86**(23)**:** 13016-13024.

111. McGinnes LW, Gravel KA, Finberg RW, Kurt-Jones EA, Massare MJ, Smith G, *et al.* Assembly and immunological properties of Newcastle disease virus-like particles containing the respiratory syncytial virus F and G proteins. *Journal of virology* 2011, **85**(1)**:** 366-377.

112. Kurt-Jones EA, Popova L, Kwinn L, Haynes LM, Jones LP, Tripp RA, *et al.* Pattern recognition receptors TLR4 and CD14 mediate response to respiratory syncytial virus. *Nat Immunol* 2000, **1**(5)**:** 398-401.

113. Puthothu B, Forster J, Heinzmann A, Krueger M. TLR-4 and CD14 polymorphisms in respiratory syncytial virus associated disease. *Dis Markers* 2006, **22**(5-6)**:** 303-308.

114. Klein Klouwenberg P, Tan L, Werkman W, van Bleek GM, Coenjaerts F. The role of Toll-like receptors in regulating the immune response against respiratory syncytial virus. *Crit Rev Immunol* 2009, **29**(6)**:** 531-550.

115. Johnson S, Oliver C, Prince GA, Hemming VG, Pfarr DS, Wang SC, *et al.* Development of a humanized monoclonal antibody (MEDI-493) with potent in vitro and in vivo activity against respiratory syncytial virus. *The Journal of infectious diseases* 1997, **176**(5)**:** 1215-1224.

116. Murawski MR, McGinnes LW, Finberg RW, Kurt-Jones EA, Massare MJ, Smith G, *et al.* Newcastle disease virus-like particles containing respiratory syncytial virus G protein induced protection in BALB/c mice, with no evidence of immunopathology. *Journal of virology* 2010, **84**(2)**:** 1110-1123.

117. Haynes LM, Jones LP, Barskey A, Anderson LJ, Tripp RA. Enhanced disease and pulmonary eosinophilia associated with formalin-inactivated respiratory syncytial virus vaccination are linked to G glycoprotein CX3C-CX3CR1 interaction and expression of substance P. *Journal of virology* 2003, **77**(18)**:** 9831-9844.

118. Varga SM, Wang X, Welsh RM, Braciale TJ. Immunopathology in RSV infection is mediated by a discrete oligoclonal subset of antigen-specific CD4(+) T cells. *Immunity* 2001, **15**(4)**:** 637-646.

119. Graham BS, Henderson GS, Tang YW, Lu X, Neuzil KM, Colley DG. Priming immunization determines T helper cytokine mRNA expression patterns in lungs of mice challenged with respiratory syncytial virus. *Journal of immunology* 1993, **151**(4)**:** 2032-2040.

120. Blanco JC, Boukhvalova MS, Pletneva LM, Shirey KA, Vogel SN. A recombinant anchorless respiratory syncytial virus (RSV) fusion (F) protein/monophosphoryl lipid A (MPL) vaccine protects against RSV-induced replication and lung pathology. *Vaccine* 2013.

121. Polack FP, Teng MN, Collins PL, Prince GA, Exner M, Regele H, *et al.* A role for immune complexes in enhanced respiratory syncytial virus disease. *The Journal of experimental medicine* 2002, **196**(6)**:** 859-865.

122. Boelen A, Andeweg A, Kwakkel J, Lokhorst W, Bestebroer T, Dormans J, *et al.* Both immunisation with a formalin-inactivated respiratory syncytial virus (RSV) vaccine and a mock antigen vaccine induce severe lung pathology and a Th2 cytokine profile in RSV-challenged mice. *Vaccine* 2000, **19**(7-8)**:** 982-991.

123. Waris ME, Tsou C, Erdman DD, Zaki SR, Anderson LJ. Respiratory synctial virus infection in BALB/c mice previously immunized with formalin-inactivated virus induces enhanced pulmonary inflammatory response with a predominant Th2-like cytokine pattern. *Journal of virology* 1996, **70**(5)**:** 2852-2860.

124. Prince GA, Jenson AB, Hemming VG, Murphy BR, Walsh EE, Horswood RL, *et al.* Enhancement of respiratory syncytial virus pulmonary pathology in cotton rats by prior intramuscular inoculation of formalin-inactiva ted virus. *Journal of virology* 1986, **57**(3)**:** 721-728.

125. Kamphuis T, Meijerhof T, Stegmann T, Lederhofer J, Wilschut J, de Haan A. Immunogenicity and protective capacity of a virosomal respiratory syncytial virus vaccine adjuvanted with monophosphoryl lipid A in mice. *PloS one* 2012, **7**(5)**:** e36812.

126. Johnson TR, Teng MN, Collins PL, Graham BS. Respiratory syncytial virus (RSV) G glycoprotein is not necessary for vaccine-enhanced disease induced by immunization with formalin-inactivated RSV. *Journal of virology* 2004, **78**(11)**:** 6024-6032.

127. Gelfand EW. Development of asthma is determined by the age-dependent host response to respiratory virus infection: therapeutic implications. *Current opinion in immunology* 2012, **24**(6)**:** 713-719.

128. Villenave R, Shields MD, Power UF. Respiratory syncytial virus interaction with human airway epithelium. *Trends Microbiol* 2013, **21**(5)**:** 238-244.

129. Ruotsalainen M, Hyvarinen MK, Piippo-Savolainen E, Korppi M. Adolescent asthma after rhinovirus and respiratory syncytial virus bronchiolitis. *Pediatr Pulmonol* 2013, **48**(7)**:** 633-639.

130. Connors M, Kulkarni AB, Firestone CY, Holmes KL, Morse HC, 3rd, Sotnikov AV, *et al.* Pulmonary histopathology induced by respiratory syncytial virus (RSV) challenge of formalin-inactivated RSV-immunized BALB/c mice is abrogated by depletion of CD4+ T cells. *Journal of virology* 1992, **66**(12)**:** 7444-7451.

131. Olson MR, Hartwig SM, Varga SM. The number of respiratory syncytial virus (RSV)-specific memory CD8 T cells in the lung is critical for their ability to inhibit RSV vaccine-enhanced pulmonary eosinophilia. *Journal of immunology* 2008, **181**(11)**:** 7958-7968.

132. Weinberger B, Herndler-Brandstetter D, Schwanninger A, Weiskopf D, Grubeck-Loebenstein B. Biology of immune responses to vaccines in elderly persons. *Clinical infectious diseases : an official publication of the Infectious Diseases Society of America* 2008, **46**(7)**:** 1078-1084.

133. Siegrist CA, Aspinall R. B-cell responses to vaccination at the extremes of age. *Nature reviews Immunology* 2009, **9**(3)**:** 185-194.

134. MacLennan IC, Gulbranson-Judge A, Toellner KM, Casamayor-Palleja M, Chan E, Sze DM, *et al.* The changing preference of T and B cells for partners as T-dependent antibody responses develop. *Immunol Rev* 1997, **156:** 53-66.

135. Khanolkar A, Badovinac VP, Harty JT. CD8 T cell memory development: CD4 T cell help is appreciated. *Immunol Res* 2007, **39**(1-3)**:** 94-104.

136. Galli G, Medini D, Borgogni E, Zedda L, Bardelli M, Malzone C, *et al.* Adjuvanted H5N1 vaccine induces early CD4+ T cell response that predicts long-term persistence of protective antibody levels. *Proc Natl Acad Sci U S A* 2009, **106**(10)**:** 3877-3882.

137. Sokolovska A, Hem SL, HogenEsch H. Activation of dendritic cells and induction of CD4(+) T cell differentiation by aluminum-containing adjuvants. *Vaccine* 2007, **25**(23)**:** 4575-4585.

138. Kamath AT, Rochat AF, Christensen D, Agger EM, Andersen P, Lambert PH, *et al.* A liposome-based mycobacterial vaccine induces potent adult and neonatal multifunctional T cells through the exquisite targeting of dendritic cells. *PLoS One* 2009, **4**(6)**:** e5771.

139. McAleer JP, Vella AT. Educating CD4 T cells with vaccine adjuvants: lessons from lipopolysaccharide. *Trends Immunol* 2010, **31**(11)**:** 429-435.

140. McKee AS, Munks MW, Marrack P. How do adjuvants work? Important considerations for new generation adjuvants. *Immunity* 2007, **27**(5)**:** 687-690.

141. Serre K, Mohr E, Benezech C, Bird R, Khan M, Caamano JH, *et al.* Selective effects of NF-kappaB1 deficiency in CD4(+) T cells on Th2 and TFh induction by alum-precipitated protein vaccines. *Eur J Immunol* 2011, **41**(6)**:** 1573-1582.

142. Gaspal FM, Kim MY, McConnell FM, Raykundalia C, Bekiaris V, Lane PJ. Mice deficient in OX40 and CD30 signals lack memory antibody responses because of deficient CD4 T cell memory. *J Immunol* 2005, **174**(7)**:** 3891-3896.

143. Mou Z, Liu D, Okwor I, Jia P, Orihara K, Uzonna JE. MHC class II restricted innate-like double negative T cells contribute to optimal primary and secondary immunity to Leishmania major. *PLoS pathogens* 2014, **10**(9)**:** e1004396.

144. Pearce EL, Shedlock DJ, Shen H. Functional characterization of MHC class II-restricted CD8+CD4- and CD8-CD4- T cell responses to infection in CD4-/- mice. *Journal of immunology* 2004, **173**(4)**:** 2494-2499.

145. Klein L, Kyewski B, Allen PM, Hogquist KA. Positive and negative selection of the T cell repertoire: what thymocytes see (and don't see). *Nature reviews Immunology* 2014, **14**(6)**:** 377-391.